ACTA UNIVERSITATIS SZEGEDIENSIS

ACTA MINERALOGICA-PETROGRAPHICA

Tomus XXXI

SZEGED, HUNGARIA

1990

HU ISSN 0365—8066
HU ISSN 0324—6523

SERIES NOSTRA AB INSTITUTIS MINERALOGICIS, GEOCHIMICIS PETROGRAPHICIS UNIVERSITATUM HUNGARICUM ADIUVATUR

Kiadja

a József Attila Tudományegyetem Ásványtani, Geokémiai és Kőzettani Tanszéke
H-6722 Szeged, Egyetem u. 2—6

Kiadványunk címének rövidítése
Acta Miner. Petr., Szeged

SOROZATUNK A MAGYARORSZÁGI EGYETEMEK ROKON TANSZÉKEINEK TÁMOGATÁSÁVAL JELENIK MEG

CONTENTS

Acta Mineralogica-Petrographica, Szeged, XXXI, 5—11, 1990

AN ICOSAHEDRAL SILICATE QUASICRYSTAL MODEL

G. GÉVAY*

Educational Technology Center, Attila József University

ABSTRACT

Putting silicon atoms in the corners of a regular pentagonal dodecahedron as well as oxygens in the mid-points of edges, silico-dodecahedrane units are obtained. These, in turn, linking together by face sharing, provide a "decoration" of the icosahedral PENROSE-MACKAY quasilattice. Thus, a silicate quasicrystal model is obtained. Some of the properties and relations of this hypothetical structure are discussed in the paper.

INTRODUCTION

The notion of quasilattice has been introduced by ALAN MACKAY (1981), who described it as a non-periodic space filling composed of two kinds of rhombohedra. The two different rhombohedral unit cells, by repeated juxtaposition, fill the space without gaps and overlaps in such a way that the structure exhibits icosahedral orientational symmetry (i.e. the characteristic directions are parallel to the axes of a regular icosahedron; a mathematically rigorous association of the icosahedral point group to such type of quasilattices has first been given by KRAMER and NERI 1984).

This construction arose from purely mathematical considerations, and as MACKAY (1981) admitted in his paper, "we cannot find any evidence for the actual appearance of our pentagonal structure". However, the experimental discovery of Al-Mn alloys exhibiting icosahedral diffraction symmetry (SHECHTMAN *et al.* 1984) changed the situation radically. Mackay's idea became the starting point of a series of models attempting to explain the structure of such alloys (see e.g. LEVINE and STEINHARDT 1984, 1986; JARIĆ 1986; KATZ and DUNEAU 1986; SOCOLAR and STEINHARDT 1986; GRAMLICH 1987; PRINCE 1987; YANG and KUO 1987; YAMAMOTO and HIRAGA 1988; JANOT *et al.* 1989). LEVINE and STEINHARDT (1984, 1986) coined the name "quasicrystal" (quasiperiodic crystal) for such structures. Now this term is used in a very broad sense independently of the contradictions which arise theoretically and conceptually (PAULING 1987; SENECHAL and TAYLOR 1990).

In what follows, we raise the question of what the structure of a silicate quasicrystal may be like. The question is not totally meaningless, since the plenty of quasicrystalline samples obtained in various laboratories of the world from various alloys can give the impression that quasiperiodicity is reserved by Nature for alloys only. In an earlier issue of this journal we shortly discussed a related problem (GÉVAY and SZEDERKÉNYI 1987—1988). In the present note it is shown

* H—6722 Szeged, Hungary

that, at least theoretically, such construction is possible. Our arguments are largely geometrical and the question of a possible crystal chemical or even mineralogical reality of the model is left open.

DESCRIPTION OF THE SILICATE QUASICRYSTAL MODEL

A hierarchical organization is assumed, thus we take the individual levels one after the other.

Our basic unit is the silica tetrahedron $(SiO_4)^{4-}$ which is common in almost all silicates. These tetrahedra are assumed to link together forming five-membered rings by corner sharing. Since we consider regular pentagonal rings, this point is a definite departure from classical crystal chemistry in that such rings are unknown in the world of minerals, although *irregular* pentagonal rings do occur (ZOLTAI and STOUT 1984). (This lack is clearly related to the crystallographic prohibition of pentagonal symmetry.) On the other hand, the status of our regular pentagonal ring is rather peculiar, as we shall see at once. ZOLTAI and BUERGER (1960) performed electrostatic energy calculations for rings with different numbers of tetrahedra taking into consideration several possible symmetries of the tetrahedral arrangements. They found that for the symmetry that is also relevant to our case (*Fig. 1*), five tetrahedra per rings is the energetically most favourable number. We consider this result as somewhat supporting our conception.

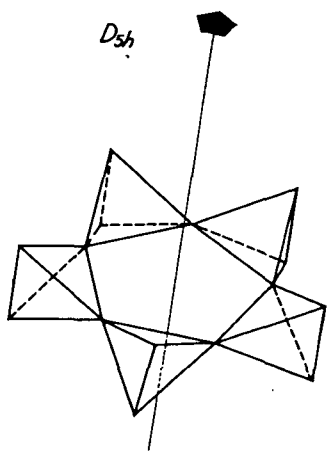

Fig. 1. The five-membered ring of silica tetrahedra. Symmetry of this arrangement is D_{5h} - $\bar{1}0m2$

At the next stage these tetrahedral pentagons are considered as faces of a regular pentagonal dodecahedron (*Fig. 2*). This idea originates from our work on a related field (GÉVAY and KEDVES 1990) where we assumed a hydrocarbon $C_{20}H_{20}$ molecule in the same manner, i.e. at the vertices of the dodecahedron carbon atoms are located. In the meantime we got to know that our hypothetical dodecahedrane was an existing compound synthesized recently and some of its properties had already been established (PAQUETTE *et al.* 1981). It seems quite natural to transmit the schema to silicates taking into account the close chemical relationship between carbon and silicon.

Thus, in our "silico-dodecahedrane" the silicon atoms are located at the vertices and three of the oxygens coordinated around a silicon atom are at the mid-points of edges and every fourth oxygen is directed outwards. The formula of the frame can be given as $(Si_{20}O_{50})^{20-}$.

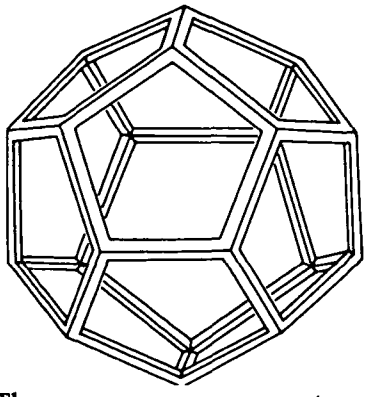

Fig. 2. Regular pentagonal dodecahedron, the geometric skeleton of the silico-dodecahedrane $(C_{20}O_{50})^{20-}$ units.

There are numerous ways to go on further. For the bio-organic case work is in progress (KEDVES 1988; GÉVAY and KEDVES in preparation.) Here we consider one way of linkage of the silico-dodecahedrane units, notably that by face sharing (this does not contradict Pauling's rules, as the dodecahedron here is not a coordination polyhedron). Even face sharing itself offers a variety of possibilities to form chains of dodecahedra having face in common. Taking into account that the interfacial angle of a regular pentagonal dodecahedron is π-arctan 2 = 116°34' (the interaxial angle of five-fold rotations is arctan 2 = 63°26'), the only values of the angle that is formed by the centers of three consecutive dodecahedra in a chain are 63°26', 116°34' and 180°. These angles are realized in a rhombic arrangement of 16 dodecahedra (*Fig. 3*) at the acute angle, obtuse angle and at the edge of the rhombus, respectively (see the dotted lines).

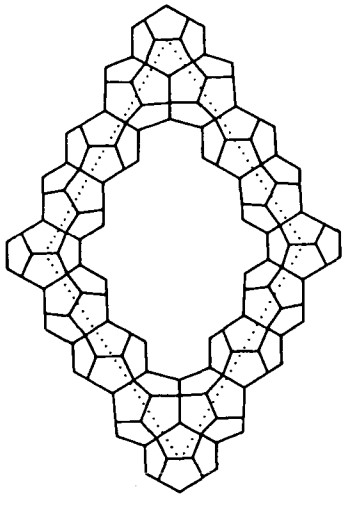

Fig. 3. The „golden rhombus" composed of 16 dodecahedral units. The dodecahedra are drawn as non-transparent solids for the sake of better visualization. The abstract rhombus skeleton is indicated by dotted lines.

We obtained a "golden rhombus" of silico-dodecahedrane units, as the ratio of its diagonals is $\tau = (1+\sqrt{5})/2 \approx 1.618$, the golden section (actually, tan 1/2 arctan2 = τ). At the acute angles of this rhombus three adjacent dodecahedra have pairwise one face in common, hence some distortion is to be presupposed: the interfacial angles at the common faces must be somewhere between 116°34' and 120°. (On the other hand, small distortions occur at the "edge-dode-

cahedra" as well, since the tetrahedral and dodecahedral geometry are not perfectly compatible, being the relevant angles 109°28' and 108°, respectively. We assume that the Si-O-Si bond chains can relax to an appropriate state so that the structure will be relatively strain-free).

Now the rhombuses can be the faces of two different rhombohedra, with acute angle or with obtuse angle meeting at the poles (*Fig. 4*). These rhombohedra correspond just to the unit cells of the Mackay quasilattice, the copies of which

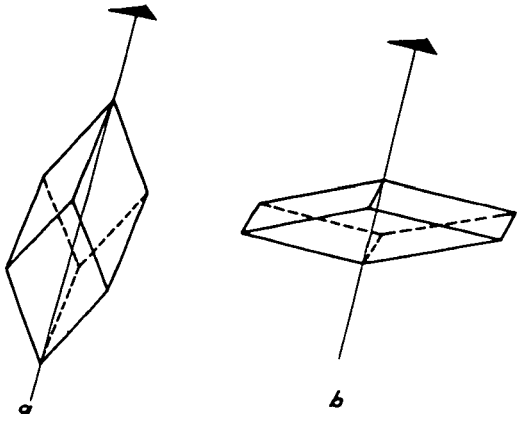

Fig. 4. The prolate (a) and oblate (b) rhombohedron composed of golden rhombuses. Their volume ratio as well as ratio of frequency in the icosahedral Mackay quasilattice is τ.

"tile" the three-dimensional space. The icosahedral orientational symmetry appears as follows. There are 10 distinct orientations (up to central inversion) for the three-fold axes of rhombohedra — these are just the directions of three-fold rotations of a regular icosahedron. On the other hand, the directions of edges of the rhombohedra are parallel to the five-fold axes of icosahedron (the axes of icosahedron are shown in *Fig. 5*). Thus the chemical bonds fit to definite directions,

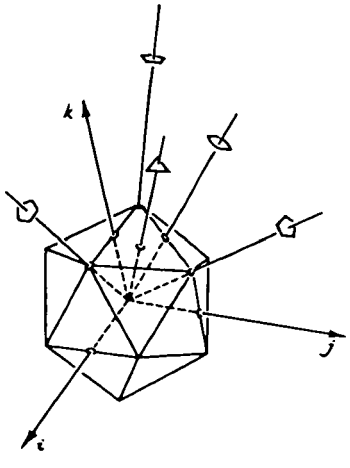

Fig. 5. Rotation axes of the icosahedron, the dual counterpart of the regular pentagonal dodecahedron.

hence the bond orientation order (declared as one of the defining properties of a quasicrystal by LEVINE and STEINHARDT 1986) is ensured.

There are a number of papers discussing various properties of abstract (icosahedral) quasilattices (see e.g. the references in this note). Here only we note that in one of the simplest cases there are altogether (up to rotations and inversion) 24 distinct arrangements of cells ("vertex neighbourhoods"), which involve from four to twenty rhombohedra (KATZ and DUNEAU 1986, GINGL 1988). At the same time, it is an interesting fact that in this case the average number of cells meeting at a vertex is 8 (cf. the classical lattices !) (GINGL 1988.)

It is somewhat difficult to illustrate packing of the rhombohedra. Here we show (*Fig. 6*) an appropriate projection of one layer of the rhombohedral packing which provides just the famous PENROSE pattern (a two-dimensional quasilattice with decagonal orientational symmetry: the prototype for MACKAY's construction that has therefore been called 3-dimensional PENROSE lattice).

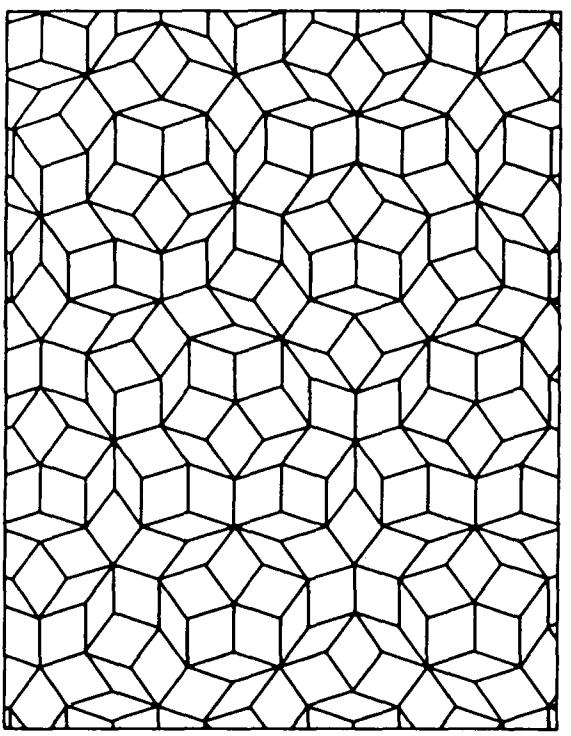

Fig. 6. The 2-dimensional Penrose quasilattice.

To sum up, the levels of the hierarchy are as follows:
(a) The silica tetrahedra $(SiO_4)^{4-}$;
(b) the regular pentagonal ring of tetrahedra;
(c) the regular pentagonal dodecahedron $(Si_{20}O_{50})^{20-}$;
(d) the "golden rhombus" composed of 16 dodecahedra;
(e) rhombohedra, prolate and oblate;
(f) the silicate quasicrystal itself.

The reverse conception (which is more usual in solid state physics) is as follows. Take an abstract quasilattice (i.e. the bare geometric skeleton) and decorate it by atoms (or clusters of atoms). In this sense our silicate quasicrystal is an icosahedral quasilattice decorated appropriately by silico-dodecahedrane units. "Appropriateness" may mean a lot of things, but let us see here some elementary geometric relations.

Observe that the symmetry elements of the lattice as well as of the decorating dodecahedra coincide (apart from small local distortions that may occur). Furthermore, the rather elementary requirement is met that the silico-dodecahedrane units have enough room within the rhombohedra (that is why the rhombohedron edges should be assumed to consist of three dodecahedra: the poles of the oblate rhombohedron are rather close to each other).

This is the point to mention the free oxygen bonds. Our quasilattice is not a pure $(SiO_2)_\infty$ structure, because not all corners of the dodecahedra are shared by other dodecahedra. Thus, one should suppose presence of cations compensating the net negative charge of the frame.

SOME FURTHER REMARKS AND CONCLUSIONS

It would be difficult to assign our silicate to any of the traditional classes of silicate structures. It is not a proper ring silicate, because a five-membered group is not an isolated unit here but part of a polyhedral cage (the difference is reflected in the distinction between the terms *ring* and *loop* (ZOLTAI and STOUT 1984); in our case *loop* would be more suitable). With the dodecahedra as repeating units, this structure is similar to, for example, the well known sodalite structure where the characteristic units are truncated octahedra. But it is not a proper network silicate either, because of the cavities within the rhombohedra (actually, as YANG and KUO (1987) observe, in an icosahedral quasilattice the prolate rhombohedra form the main skeleton and the oblate rhombohedra fill the empty space left by the former). Thus, it could perhaps be termed as a "quasi-network" silicate (or quasiperiodically polymerized silicate).

On the other hand, like in network silicates, we assume the possibility of substitution of silicon by other suitable cation (e.g. Al^{3+}) in the tetrahedral sites, with simultaneous appearance of the necessary charge compensating secondary cations.

What is more, just as we exploited the analogy between carbon and silicon, one may take into consideration the Si-Ge analogy as well. Indeed, as classification of the silicate minerals served as a pattern for classification of germanates (STRUNZ 1960), it is natural to suppose that our model can be considered a hypothetical germanate quasicrystal as well.

Some of the features of this structure, not discussed here, provides analogies to other non-classical structures. The well-known self-similarity property as well as the hierarchical organization relates it to the structure discussed e.g. by SCHNEER (1988). The unit $(Si_{20}O_{50})^{20-}$ might well be a building element of less polymerized structures, or of structure built by other construction principles (GÉVAY and KEDVES 1990), etc.

In sum, we demonstrated geometrically that a certain variant of quasicrystalline silicate structure is possible. Although we did not apply arguments that would go beyond the limits of a field which might be called a "solid state geometry", our hope is that the model will bring us closer to the reality of non-metallic quasicrystals.

REFERENCES

GÉVAY, G. and KEDVES, M. (1990): A structural model of the sporopollenin based on dodecahedrane units. Acta Biol. Szeged, **35**, 53—57

GÉVAY, G. and KEDVES, M. (in preparation): Some dodecahedrane-based quasi-crystalloid model for cell wall investigations in palynology.

GÉVAY, G. and SZEDERKÉNYI, T. (1987—1988): Quasicrystals and their spontaneous formation possibilities in the Nature. Acta Miner. Petr. Szeged, **29**, 5—12.

GINGL, Z. (1988): Local structure of quasicrystals (Hungarian). Diploma work, JATE Institute of Mineralogy, Geochemistry and Petrography, Szeged.

GRAMLICH, V. (1987): Quasikristalle: zur Kristallographie von Strukturen mit "nichtkristallographischer" Symmetrie. Fortschr. Miner. **65**, 161—171.

JANOT, C., DUBOIS, J. M., de BOISSIEU, M and PANNATIER, J. (1989): Neutron scattering studies of quasicrystals. Physica B. **156-157**, 25—30.

JARIĆ, M. V. (1986): Diffraction from quasicrystals: Geometric structure factor. Phys. Rev. B. **34**, 4685—4698.

KATZ, A. and DUNEAU, M. (1988): Quasiperiodic patterns and icosahedral symmetry. J. Physique **47**, 181—196.

KEDVES, M. (1988): Quasi-crystalloid basic molecular structure of the sporoderm. — 7th Internat. Palynol. Congr. Brisbane. Abstracts, 82.

KRAMER, P. and NERI, R. (1984): On periodic and non-periodic space fillings of E^n obtained by projection. Acta Cryst. **A40**, 580—587.

LEVINE, D. and STENHARDT, P. J. (1984): Quasicrystals: a new class of ordered structures. Phys. Rev. Lett. **53**, 2477—2480.

LEVINE, D. and STENHARDT, P. J. (1986): Quasicrystals. I. Definition and structure. Phys. Rev. B **34**, 596—616.

MACKAY, A. L. (1981): De Nive Quinquangula: On the pentagonal snowflake. Sov. Phys. Crystallogr. **26**, 517—522.

PAQUETTE, L. A., BALOGH, D. W., USHA, R., KOUNTZ, D. and CHRISTOPH, G. G. (1981): Crystal and molecular structure of a pentagonal dodecahedrane. Science, **211**, 575—576.

PAULING, L. (1987): So-called icosahedral and decagonal quasicrystals are twins of an 820-atom cubic crystal. Phys. Rev. Lett. **58**, 365—368.

PRINCE, E. (1987): Diffraction patterns from tilings with fivefold symmetry. Acta Cryst. **A43**, 393—400.

SCHNEER, C. J. (1988): Symmetry and morphology of snowflakes and related forms. Canad. Mineral. **26**, 391—406.

SENECHAL, M. and TAYLOR, J. (1990): Quasicrystals: the view from Les Houches. Math. Intelligencer **12**, 54—64.

SHECHTMAN, D., BLECH, J., GRATIAS, D. and CAHN, J. W. (1984): Metallic phase with long-range orientational order and no translational symmetry. Phys Rev. Lett. **53**, 1951—1953.

SOCOLAR, J. E. S. and STEINHARDT, P. J. (1986): Quasicrystals. II. Unit-cell configurations. Phys. Rev. B **34**. 617—646.

STRUNZ, H. (1960): Die Beziehungen der Isotypie zwischen Silikaten und Germanaten. Versuch einer Germanat-Klassifikation. Naturwiss. **47**, 154—155.

YAMAMOTO, A. and HIRAGA, K. (1988): Structure of an icosahedral Al-Mn quasicrystal. Phys. Rev. B **37**, 6207—6214.

YANG, Q. B. and KUO, K. H. (1987): A new description of pentagonal Frank-Kasper phases and a possible structure model of the icosahedral quasicrystal. Acta Cryst. A **43**, 787—795.

ZOLTAI, T. and BUERGER, M. J. (1960): The relative energies of rings of tetrahedra. Z. Kristallogr. **114**, 1—8.

ZOLTAI, T. and STOUT, J. H. (1984): Mineralogy. Concepts and Principles. Burgess Publ. Co., Minneapolis.

Manuscript received, 22 August, 1989

Acta Mineralogica-Petrographica, Szeged, XXXI, 13—23, 1990

NEW DATA ON THE GEOTHERMOMETRY AND GEOBAROMETRY OF THE SOMOGY-DRÁVA BASIN, SW TRANSDANUBIA, HUNGARY

K. TÖRÖK*

Department of Petrology and Geochemistry, Eötvös Loránd University

ABSTRACT

The mineral assemblages of the medium grade polymetamorphic rocks of the Somogy-Dráva Basin are rich in critical minerals which make it possible to expand our knowledge on the metamorphic p—T evolution of the area using mineral equilibria and different geothermo-barometric methods. Previous studies (ÁRKAI 1984; ÁRKAI *et al.* 1985) revealed three metamorphic events.

Applying four geothermo-barometric methods which provided consistent data with the mineral assemblage, the estimated p—T conditions were about 500—1030 Mpa and 539—685°C during the first metamorphic event.

The second, low pressure metamorphism produced 4 different mineral assemblages which crystallized as a result of different reactions during the prograde metamorphism.

1/ andalusite+biotite +/- staurolite relics

2/ andalusite+garnet+biotite (sometimes with sillimanite and staurolite relics)

3/ andalusite+biotite+cordierite +/- sillimanite, garnet, plagioclase, muscovite, with rare staurolite relics in the andalusite.

4/ andalusite+biotite+staurolite, where the andalusite and the staurolite crystallized simultaneously along with the biotite.

These mineral assemblages refer to a maximum temperature of about 600°C. There is only a few geothermo-barometric data on the second stage of the metamorphism which show pressures consistent with the mineral assemblages (200—350 Mpa) but the temperatures seem to be a little low (520—536 °C).

The third, retrograde metamorphism, related to milonitisation, was a very low-low grade one which usually did not exceed the biotite isograde (ÁRKAI 1984), disregarding some exceptional cases.

INTRODUCTION

The Somogy-Dráva Basin is situated in the south-western part of Transdanubia as a part of the Pannonian Basin (*Fig. 1a*). The crystalline basement of the Somogy-Dráva Basin is covered by thick neogene sediments. All the samples are exposed by hydrocarbon exploratory boreholes of the National Hydrocarbon and Gas Trust.

Detailed textural and microprobe analyses were carried out on several core samples, so as to contribute to the better understanding of the polymetamorphic history of the crystalline basement of the Somogy-Dráva Basin. The location of the studied samples with indication of the most important metamorphic minerals, and the depth of the core sample is presented in *Fig. 1b.*

* H—1088 Budapest, Múzeum krt. 4/a

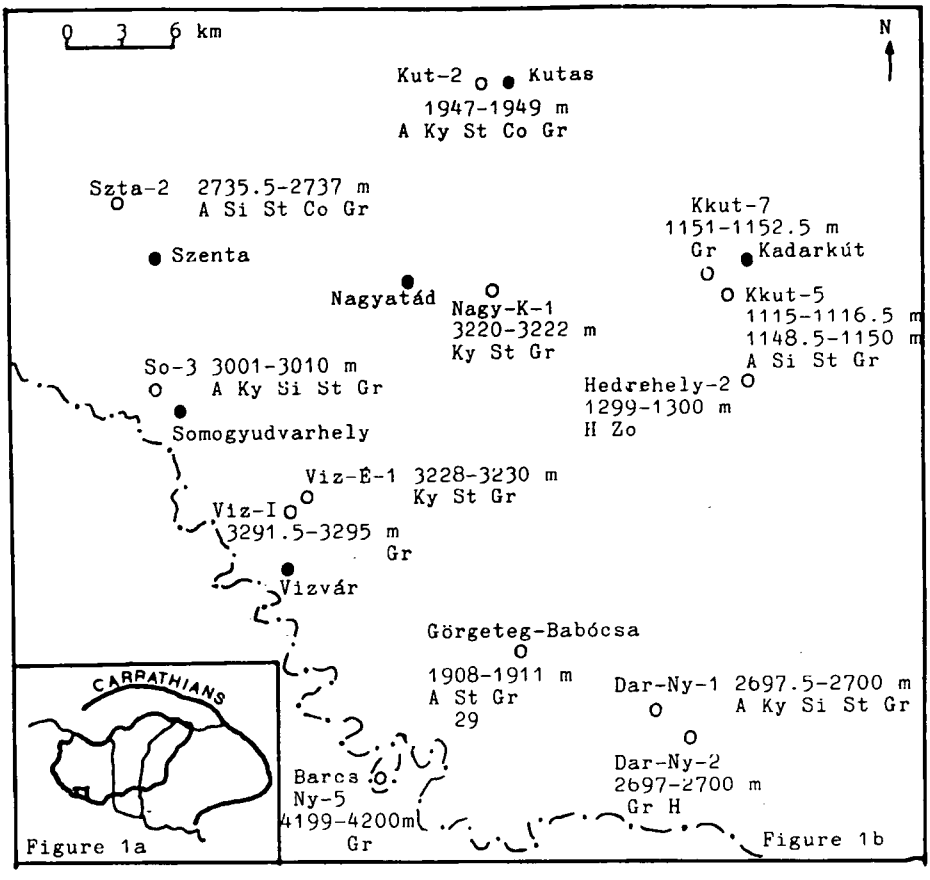

Fig. 1a. Location of the Somogy-Dráva Basin in Hungary

Fig. 1b. Location of the studied boreholes in the Somogy-Dráva Basin with indication of the most important metamorphic minerals and the depth of the studied core samples.
Legends: A—andalusite, Ky—kyanite, Si—sillimanite, Co—cordierite, St—staurolite, Gr—garnet, H—hornblende, Zo—zoisite.
o—borehole, •—village

GEOLOGY OF THE STUDIED AREA

The medium grade, mostly metasedimentary rocks of the Somogy-Dráva Basin underwent a complex, polymetamorphic history, summarized in Table 1. The main rock types of the crystalline basement are mica-schist, gneiss, and milonite. Amphibolite and amphibole gneiss was exposed only in some boreholes on the territory of the Somogy-Dráva Basin.

The age of the first metamorphic event is a topic of great discussions, because there is no reliable radiometric age data available so far. It varies from Proterozoic (pre-Baikalian) to early Hercynian depending on the geological analogies used by the author in question. The K—Ar measurements conducted by BALOGH *et al.* (1981), indicate the Hercynian age for the second stage of the metamorphism in

the neighbourhood of the Somogy-Dráva Basin. The third metamorphic event, related to milonitisation is assumed to be late Hercynian or Alpine.

TABLE 1.

Polymetamorfic evolution of the Somogy–Dráva Basin

metamorphic event	p—T conditions, critical minerals	references
1./ Barrow-type medium grade	510—600 °C 590—890 MPa kyanite, staurolite	SZEDERKÉNYI (1976) ÁRKAI (1984) ÁRKAI *et al.* (1985)
2./Abukuma-type medium grade	andalusite	LELKES-FELVÁRI-SASSI (1981)
3./very low-low grade, milonitisation		TÖRÖK (1986)

The crystalline basement of the Somogy-Dráva Basin has a close genetic connection with the surrounding metamorphic complexes of the Slavonian Mountains, the Transsylvanian Midmountains the South- and the Eastern Carpathians and the Serbo-Macedonian Massif (SZEDERKÉNYI 1976, 1984; JANTSKY 1979; ÁRKAI *et al.* 1985).

TEXTURAL ANALYSIS AND MINERAL ASSEMBLAGES

The mineral assemblages, referring to different metamorphic stages, were distinguished by textural analysis. In accordance with the previous authors (LELKES-FELVÁRI and SASSI 1981; ÁRKAI 1984; ÁRKAI *et al.* 1985) the kyanite-staurolite-garnet-plagioclase-biotite-muscovite (sillimanite?) paragenesis is thought to be the oldest one. These early micas form the S_1 schistosity, which preserved in some early porphyroblasts, or in certain places, where the development of the S_2 and S_3 schistosity was not effective enough to clear all the previous information.

Two generations of garnet can be distinguished during the first metamorphic event. The oldest one is pretectonic, the youngest is syntectonic with "S" shaped inclusion trails. Some of the garnets display compositional zoning. These porphyroblasts have cores richer in grossularite component relatively to their rims (see Table 2.), showing the effect of the prograding metamorphism. The staurolite crystallized in two stages as well. The first generation forms inclusions in syntectonic garnet, while the second generation is posttectonic along with the kyanite porphyroblasts. There is no textural evidence for the formation of sillimanite during the first metamorphism, but it cannot be excluded either.

The mineral assemblages of the second metamorphic stage preserved more information on the metamorphic reactions, therefore they were studied in more details. The most characteristic mineral is andalusite which is present in two generations. The oldest one is posttectonic regarding the S_1, but pretectonic to the S_2 schistosity. The second generation is posttectonic to the S_2 schistosity. Both generations contain abundant staurolite relics or sometimes fibrolite. The presence of the staurolite relics was also revealed by ÁRKAI (1984). Cordierite is also present, but it is quite rare. It was found together with the younger generation of the andalusite. The third generation of staurolite also formed together with the second andalusite, but never coexists with cordierite. Sillimanite is present as fibrolite along the S_2 schistosity, or unoriented.

According to the textural analysis, four different mineral assemblages could be distinguished during the second period of the metamorphism.

1/ andalusite+biotite ± staurolite relics as inclusions in andalusite. This mineral paragenesis is the most frequent of all. The probable reactions involving staurolite breakdown and formation of the paragenesis are:

$$\text{staurolite+muscovite+quartz=}Al_2SiO_5\text{+biotite+}H_2O \quad (1)$$

$$\text{Mg-chlorite+staurolite+muscovite+quartz=}Al_2SiO_5\text{+biotite+}H_2O \quad (2)$$

The reaction (2) takes place at 200 Mpa and 575 ± 15 °C according to HOSCHEK (1969) *Fig. 2.*

2/ andalusite+garnet+biotite (sometimes with sillimanite and staurolite relics). This paragenesis was also observed by LELKES-FELVÁRI *et al.* (1989) in sample originating from the Vajta-3 borehole in the northern part of South Transdanubia. In this case it is necessary to take into account the breakdown of the staurolite near the andalusite/sillimanite stability border in the following reaction:

$$\text{Fe-staurolite+quartz=}Al_2SiO_5\text{+garnet+}H_2O \quad (3)$$

(GANGULY 1972), where the Al_2SiO_5 phase can be both sillimanite and andalusite (FERRY 1980; PIGAGE and GREENWOOD 1982) *Fig. 2.*

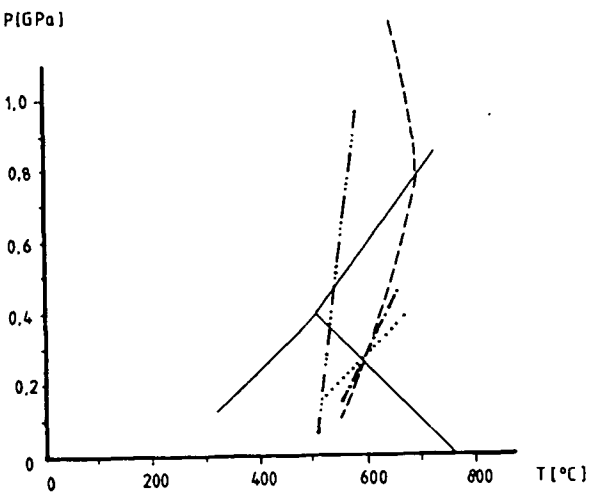

Fig. 2. Stability and reactions of the critical minerals.
Legends: —.—.— staurolite+quartz+muscovite=Al_2SiO_5+biotite+H_2O /1/ (HOSCHEK 1969).
— — — Fe-staurolite+quartz=Al_2SiO_5+almandine+H_2O /3/, (PIGAGE and GREENWOOD 1982)
. . . . . staurolite+quartz=cordierite+Al_2SiO_5+H_2O /6/ HOSCHEK (1969)
— . . . — chlorite+muscovite=staurolite+quartz+biotite+H_2O /7/ (WINKLER 1976)
The Al_2SiO_5 stability fields are after HOLDAWAY (1971)

3/ andalusite+biotite+cordierite ± sillimanite, garnet, plagioclase, muscovite, with rare staurolite relics in the andalusite. This complex mineral assemblage might

have formed in several reactions in the course of the prograding metamorphism.

$$\text{chlorite+muscovite+quartz=andalusite+cordierite+biotite+}H_2O \qquad (4)$$

reaction indicates the beginning of the medium grade. According to HIRSCHBERG and WINKLER (1968) this reaction occurs at 525 ± 10 °C and 200 Mpa, or at 555 ± 10 °C and 400 Mpa.

As the temperature rises, the old staurolite becomes unstable and brakes down in the following reaction:

$$\text{staurolite+Na-rich muscovite+quartz=}Al_2SiO_5\text{+biotite+K-rich muscovite+}$$
$$\text{+albite+almandine+}H_2O \text{ (GUIDOTTI 1970).} \qquad (5)$$

According to GANGULY (1972) the reaction

$$\text{staurolite+quartz=cordierite+}Al_2SiO_5+H_2O \qquad (6)$$

is also possible (*Fig. 2*).

The last step was in the prograde reactions, when the micas partly transformed into fine grained aggregates of fibrolite as the temperature reached the sillimanite stability field.

4/ andalusite+biotite+staurolite, where the andalusite and the staurolite crystallized simultaneously along with the biotite. This assemblage is more common than the andalusite+biotite+cordierite, which can be the alternative of the assemblage 4., because staurolite never coexists with cordierite.

The mineral assemblages of both the first and the second metamorphic event preserved only at that places, where the subsequent milonitisation and retrograde metamorphosis had no effect on the rock. In the milonitized zones the old mineral assemblages has been altered. The only indicators of the preexisting mineral assemblages are the chlorite pseudomorphs after garnet, or the sericite ± chlorite pseudomorphs after kyanite, andalusite, or staurolite. The milonites usually contain carbonate minerals, sometimes in great quantity, pirite, newly formed muscovite, sericite, in one sample new biotite, rarely anhydrite and gypsum. The newly formed micas show the S_3 schistosity, related to the milonite formation.

The P—T conditions of the first and second metamorphic stages can be estimated on the basis of the mineral reactions and mineral equilibria. The temperature conditions of the first metamorphism may have been limited between the "staurolite in" and the "sillimanite in" isograde. However there is a good amount of uncertainty in the case of the upper limit, because the presence of the sillimanite has not been proved, but there is no evidence to anticipate it either. The pressure may have a wide range variation in the common stability field of the kyanite and staurolite. The second metamorphism has the lower temperature limit where the cordierite or the staurolite appears, and the andalusite is stable as well. The upper temperature limit is over the „sillimanite in" isograd. According to the reactions, displayed on *Fig. 2.*, the temperature during the second metamorphic event may have been between 520—620 °C. The pressure is limited by the stability of andalusite. It is assumed to have been between 200—400 Mpa. The third, retrograde metamorphism, related to milonitisation, was a very low-low grade one which usually did not exceed the biotite isograde (ÁRKAI 1984), disregarding some exceptional cases.

Microprobe measurements were carried out on garnets, biotites, muscovites, plagioclases and hornblendes from selected samples. The samples are mica-schists and gneisses, except one sample, the Hedrehely—2 which is amphibole-biotite gneiss. The analytical data are displayed in Tables 2—6. The measurements were made in Novosibirsk at the Institute of Geology and Geochemistry of the Siberian Branch of the Academy of Sciences of the Sovietunion on a Cameca microprobe (E_o=20 kV, I_s=40 nA, T=10 s).

The mineral assemblages made it possible to apply several geothermometers and geobarometers:

1/ *Garnet-biotite geothermometer* (FERRY and SPEAR 1978). All of the selected samples contained garnet and biotite, except for the Hedrehely—2 (*Fig.1b*) amphibole gneiss. The geothermometer gives a temperature interval between 539 and 666 °C, but most of the temperature data fell within the range from 572—607 °C. The temperature was also calculated using the Hoinkes (1986) calibration of the garnet-biotite geothermometer which takes into account the grossularite content of the garnet. But the temperatures provided by this method are unrealistically high (600—805 °C), which is not supported by the mineral assemblage, that is why this method was not taken into account further.

2/ *Plagioclase-biotite-muscovite-garnet geothermo-barometer* (GHENT and STOUT 1981). It provided a wide pressure interval — 650—1030 Mpa — and a quite uniform temperature range between 558 and 685 °C. The geothermo-barometer gives systematically higher temperatures than the garnet-biotite geothermometer. This difference is between 17 and 30 °C.

3/ *Hornblende-plagioclase geothermo-barometer* (PLJUSNINA 1982). The hornblende-plagioclase geothermo-barometer could be applied only on one sample (Hedrehely—2), and provided 520 °C—530 °C temperature and 300 Mpa—350 Mpa pressure. The obtained temperature and pressure data (Table 7.) are comparable with those obtained by ÁRKAI *et al.* (1985) from the hornblende-plagioclase assemblage of a mafic resistite from the "Mórágy granite" rather than with the temperature and pressure conditions of the Darány—2 amphibolite from the Somogy-Dráva Basin (ÁRKAI 1984). This fact indicates, that this hornblende-plagioclase assemblage crystallized during the second metamorphism.

4/ *Plagioclase-garnet-Al_2SiO_5-quartz geobarometer* (GHENT 1976). The temperature data, needed for the geobarometer, were provided by the average value of the garnet-biotite geothermometer (FERRY and SPEAR 1978) and the plagioclase-biotite-muscovite-garnet geothermo-barometer (GHENT and STOUT 1981). The equations ($a^{gr}_{gro}=X^{3gr}_{gro}\gamma^{3gr}_{gro}$; $a^{pl}_{an}=X^{pl}_{an}\gamma^{pl}_{an}$) and the activity coefficient of the anorthite in plagioclase were used for calculation of the activity of the grossularite component in garnet and anorthite component in plagioclase, given by GHENT (1976). The activity coefficient of the grossularite in garnet was obtained from ASWORTH and EVIRGEN (1985).

The estimated pressures provided by the geobarometer, are between 500 and 915 Mpa. These values are quite close to those obtained from the plagioclase-biotite-muscovite-garnet geothermo-barometer. The difference ranges between 71 and 3 Mpa.

TABLE 2.

Garnet analyses

locality	Szenta-2					Barcs-Ny-5			Kkút-5 1115 m		Darány-Ny-1		Kadarkút-7		Kutas-2	Kadarkút-5 1148 m			Víz-É-1	
	rim	core	rim	core	rim	rim	rim	core	rim	rim	rim	rim	rim	rim	rim	rim	rim	rim	rim	rim
	1.	2.	3.	4.	5.	6.	7.	8.	9.	10.	11.	12.	13.	14.	15.	16.	17.	18.	19.	20.
SiO_2	37.50	38.02	37.42	38.10	38.36	37.57	36.48	37.67	36.23	36.29	37.13	36.88	36.04	36.31	36.96	36.80	36.13	36.73	36.42	35.92
TiO_2	0.07	0.05	0.05	0.07	0.04	0.03	0.04	0.08	0.02	0.00	0.01	0.00	0.07	0.00	0.00	0.00	0.00	0.00	0.00	0.00
Al_2O_3	21.05	21.10	20.96	21.32	21.48	21.23	20.98	21.22	20.60	20.83	21.22	20.98	20.55	20.80	20.75	20.97	20.68	21.02	20.66	20.90
FeO*	33.45	32.05	33.36	32.25	34.19	34.26	33.83	30.98	35.44	36.06	35.28	35.11	35.57	36.07	34.35	35.05	34.83	35.46	34.59	33.08
MnO	0.86	0.73	2.17	0.75	2.23	1.30	1.82	2.11	1.66	1.21	0.77	1.58	2.25	1.52	4.36	1.49	1.57	1.26	3.93	2.51
MgO	2.60	2.18	2.79	2.10	2.79	2.45	2.47	1.25	2.67	3.24	3.17	2.89	3.18	3.36	3.33	2.81	2.82	3.15	3.24	3.71
CaO	4.46	6.42	3.24	5.35	3.32	4.69	3.00	8.01	3.34	2.19	3.57	3.33	2.26	2.08	1.86	2.86	3.02	2.82	1.73	3.94
Na_2O	0.03	0.04	0.03	0.03	0.03	0.05	0.04	0.03	0.08	0.09	0.08	0.15	0.13	0.05	0.18	0.10	0.11	0.12	0.12	0.14
K_2O	0.00	0.01	0.01	0.01	0.01	0.01	0.61	0.00	0.02	0.01	0.01	0.01	0.02	0.00	0.01	0.01	0.03	0.02	0.01	0.54
total	100.02	100.60	100.03	99.98	102.45	101.59	99.63	101.30	100.06	99.92	101.26	100.93	99.87	100.46	101.80	100.09	99.19	100.58	100.70	100.75
Cation numbers on the basis of 12 oxygen																				
Si	3.005	3.021	3.006	3.037	3.008	2.981	2.987	2.991	2.945	2.945	2.958	2.958	2.936	2.933	2.954	2.971	2.952	2.954	2.944	2.896
Ti	0.004	0.002	0.003	0.004	0.002	0.001	0.002	0.004	0.001	0.000	0.000	0.000	0.004	0.000	0.000	0.000	0.000	0.000	0.000	0.000
Al	1.988	1.976	1.984	2.003	1.985	1.985	2.005	1.986	1.973	1.992	1.992	1.983	1.973	1.980	1.954	1.995	1.991	1.992	1.968	1.987
Fe	2.242	2.129	2.241	2.150	2.242	2.273	2.294	2.054	2.409	2.447	2.350	2.355	2.409	2.437	2.296	2.367	2.380	2.385	2.338	2.231
Mn	0.058	0.049	0.147	0.050	0.148	0.087	0.125	0.141	0.114	0.083	0.051	0.107	0.155	0.104	0.295	0.101	0.108	0.085	0.296	0.171
Mg	0.310	0.258	0.334	0.249	0.326	0.289	0.289	0.147	0.323	0.391	0.376	0.345	0.386	0.437	0.396	0.338	0.343	0.377	0.390	0.446
Ca	0.383	0.546	0.278	0.457	0.279	0.398	0.260	0.681	0.290	0.190	0.306	0.286	0.197	0.180	0.159	0.247	0.264	0.243	0.149	0.341
Na	0.004	0.006	0.004	0.004	0.004	0.007	0.006	0.004	0.012	0.014	0.012	0.023	0.020	0.007	0.028	0.015	0.017	0.018	0.018	0.022
K	0.000	0.001	0.001	0.001	0.001	0.001	0.063	0.000	0.002	0.001	0.001	0.001	0.002	0.000	0.001	0.001	0.003	0.002	0.001	0.056
total	7.994	7.988	7.998	7.955	7.995	8.022	8.031	8.008	8.069	8.063	8.046	8.058	8.078	8.078	8.083	8.035	8.058	8.056	8.077	8.149

TABLE 3.

Biotite analyses

locality	Szenta-2				Barcs-Ny-5				Vízvár-É-1		Kkut-5 1115		Kutas-2		Kkut-5 1148		Kkut-7		Darány-Ny-1	
	1.	2.	3.	4.	5.	6.	7.	8.	9.	10.	11.	12.	13.	14.	15.	16.	17.	18.	19.	20.
SiO_2	34.15	34.68	34.59	35.29	35.27	35.11	34.78	35.57	35.61	30.80	35.61	34.86	37.34	36.57	33.12	34.67	36.31	34.14	35.60	35.12
TiO_2	1.99	1.96	2.05	2.42	2.31	2.13	1.98	2.14	1.59	0.24	1.43	1.49	1.79	1.88	1.19	1.83	1.55	1.34	1.73	1.49
Al_2O_3	19.21	19.35	19.76	20.22	19.92	20.33	18.97	19.20	18.31	19.77	19.92	19.72	21.60	20.12	18.46	19.34	19.79	19.41	19.41	19.65
FeO*	21.60	21.04	20.96	20.35	21.70	21.52	23.93	23.40	20.65	21.84	21.31	21.35	15.57	17.75	21.68	22.79	19.57	19.40	22.02	23.40
MnO	0.13	0.11	0.13	0.13	0.20	0.19	0.25	0.23	0.13	0.17	0.05	0.04	0.12	0.11	0.14	0.12	0.14	0.12	0.09	0.10
MgO	8.99	9.06	8.68	8.55	8.33	8.45	6.91	6.95	9.95	13.20	8.90	8.85	10.04	10.56	9.34	8.65	10.01	9.49	8.33	8.48
CaO	0.04	0.03	0.04	0.03	0.00	0.00	0.00	0.01	0.00	0.93	0.04	0.03	0.02	0.01	0.07	0.03	0.02	0.01	0.04	0.05
Na_2O	0.22	0.35	0.18	0.33	0.24	0.25	0.19	0.25	0.26	0.49	0.25	0.23	0.23	0.23	0.57	0.26	0.18	0.20	0.28	0.27
K_2O	8.55	8.57	8.34	8.57	8.84	8.83	8.88	9.00	9.41	8.98	8.92	8.99	7.72	8.78	8.54	8.71	9.10	8.00	8.87	7.37
total	94.89	95.15	94.74	95.89	96.81	96.81	95.89	96.76	95.95	96.40	96.42	95.57	94.44	96.01	93.10	96.41	96.67	92.71	96.37	95.97
Cation numbers on the basis of 11 oxygen																				
Si	2.635	2.658	2.655	2.665	2.661	2.645	2.686	2.709	2.771	2.383	2.689	2.665	2.760	2.717	2.623	2.644	2.711	2.673	2.701	2.673
Ti	0.115	0.113	0.118	0.139	0.131	0.121	0.115	0.123	0.091	0.014	0.081	0.086	0.099	0.105	0.071	0.105	0.087	0.079	0.099	0.085
Al	1.747	1.747	1.787	1.800	1.771	1.805	1.726	1.723	1.643	1.803	1.773	1.777	1.882	1.762	1.723	1.741	1.742	1.791	1.735	1.762
Fe	1.394	1.348	1.346	1.285	1.369	1.365	1.545	1.491	1.315	1.413	1.346	1.365	0.962	1.103	1.436	1.454	1.22	1.270	1.397	1.490
Mn	0.009	0.007	0.009	0.009	0.013	0.012	0.017	0.015	0.009	0.011	0.003	0.003	0.008	0.007	0.009	0.008	0.009	0.008	0.006	0.007
Mg	1.034	1.034	0.993	0.963	0.936	0.949	0.795	0.790	1.129	1.522	1.002	1.009	1.107	1.169	1.102	0.984	1.114	1.108	0.942	0.962
Ca	0.003	0.002	0.003	0.003	0.000	0.000	0.000	0.000	0.003	0.077	0.003	0.002	0.002	0.001	0.006	0.002	0.002	0.008	0.004	0.004
Na	0.032	0.052	0.027	0.048	0.035	0.036	0.029	0.038	0.038	0.073	0.036	0.034	0.032	0.034	0.087	0.038	0.027	0.031	0.041	0.040
K	0.842	0.837	0.817	0.825	0.850	0.849	0.875	0.874	0.913	0.886	0.859	0.877	0.728	0.832	0.862	0.847	0.867	0.799	0.859	0.715
total	7.813	7.800	7.755	7.645	7.776	7.774	7.788	7.763	7.852	8.181	7.791	7.817	7.580	7.730	7.919	7.823	7.778	7.767	7.783	7.738

TABLE 4.

Muscovite Analyses

locality	Szenta—2				Barcs—Ny—5	Barcs—Ny—5			Viz—É—1		Kkut—5 1115		Kutas—2		Dar—Ny—1		Kkut—7		Kkut—5 1148,5	
	1.	2.	3.	4.	5.	6.	7.	8.	9.	10.	11.	12.	13.	14.	15.	16.	17.	18.	19.	20.
SiO_2	48.04	48.79	47.16	47.04	49.89	50.67	46.86	48.54	44.96	45.02	46.06	45.54	44.72	44.61	46.83	47.41	44.55	45.29	47.39	46.95
TiO_2	0.62	0.55	0.56	0.60	0.59	0.42	0.64	0.65	0.23	0.50	0.42	0.44	0.45	0.33	0.40	0.43	0.62	0.54	0.36	0.39
Al_2O_3	36.02	36.56	35.74	35.06	32.09	30.40	34.84	31.82	34.40	34.15	36.51	36.09	35.80	36.63	36.91	37.34	34.48	35.39	35.24	36.95
FeO*	0.89	0.80	0.73	0.86	1.46	1.80	1.11	1.81	1.72	2.04	1.08	1.08	0.64	0.66	0.85	0.85	1.38	0.98	1.19	0.92
MnO	0.00	0.00	0.00	0.00	0.01	0.00	0.00	0.00	0.11	0.02	0.02	0.00	0.02	0.01	0.02	0.00	0.00	0.01	0.00	0.01
MgO	0.63	0.65	0.55	0.80	1.57	2.08	0.92	1.84	0.74	1.22	0.48	0.47	0.51	0.44	0.44	0.45	0.92	0.66	0.95	0.47
CaO	0.02	0.02	0.04	0.03	0.01	0.00	0.01	0.01	0.15	0.06	0.01	0.01	0.05	0.05	0.02	0.01	0.05	0.03	0.02	0.02
Na_2O	0.83	0.86	0.98	1.01	0.62	0.673	0.80	0.62	1.08	1.05	1.42	1.37	1.48	1.40	1.13	0.85	1.13	1.13	0.64	1.12
K_2O	8.80	8.68	9.09	9.20	9.05	9.10	9.40	9.29	8.54	8.69	8.77	8.52	8.69	8.53	8.36	8.11	8.79	8.46	8.85	8.50
total	95.68	96.92	94.60	94.85	95.28	95.11	94.58	94.66	91.97	92.76	94.76	93.53	92.21	92.60	94.95	95.45	91.93	92.43	94.62	95.31
Cation numbers on the basis of 11 oxygen																				
Si	3.130	3.137	3.114	3.122	3.279	3.343	32.117	3.233	3.084	3.069	3.054	3.056	3.043	3.020	3.078	3.089	3.058	3.071	3.134	3.078
Ti	0.031	0.026	0.028	0.030	0.029	0.021	0.032	0.032	0.012	0.026	0.021	0.022	0.023	0.017	0.020	0.021	0.032	0.027	0.018	0.019
Al	2.766	2.77	2.782	2.742	2.486	2.363	2.732	2.498	2.781	2.744	2.853	2.854	2.871	2.922	2.859	2.867	2.789	2.828	2.747	2.855
Fe	0.048	0.043	0.040	0.048	0.080	0.099	0.062	0.106	0.099	0.117	0.060	0.061	0.037	0.037	0.047	0.046	0.079	0.055	0.066	0.050
Mn	0.000	0.000	0.000	0.000	0.000	0.000	0.000	0.000	0.006	0.001	0.001	0.000	0.001	0.001	0.001	0.001	0.000	0.000	0.000	0.000
Mg	0.061	0.063	0.055	0.079	0-.153	0.205	0.091	0.182	0.076	0.124	0.047	0.047	0.051	0.045	0.043	0.044	0.095	0.067	0.093	0.046
Ca	0.002	0.002	0.003	0.002	0.001	0.000	0.001	0.000	0.011	0.005	0.001	0.001	0.004	0.004	0.002	0.001	0.004	0.002	0.001	0.001
Na	0.105	0.108	0.125	0.130	0.079	0.081	0.103	0.080	0.144	0.139	0.182	0.178	0.195	0.184	0.144	0.107	0.150	0.141	0.082	0.142
K	0.732	0.712	0.765	0.779	0.759	0.766	0.798	0.789	0.748	0.756	0.741	0.729	0.741	0.731	0.701	0.674	0.769	0.732	0.747	0.711
total	6.875	6.861	6.913	6.931	6.867	6.878	6.935	6.921	6.960	6.981	6.961	6.948	6.966	6.960	6.895	6.848	6.976	6.924	6.889	6.902

TABLE 5.

Plagioclase analyses

locality	Barcs—Ny—5				Szta—2				Viz—É—1		Kkut—5 1115		Kutas—2		Dar—Ny—1			Kkut—7		Kkut—5 1148,5		Hedrehely—2			
	1.	2.	3.	4.	5.	6.	7.	8.	9.	10.	11.	12.	13.	14.	15.	16.	17.	18.	19.	20.	21.	22.	23.	24.	25.
SiO_2	65.91	65.44	65.12	65.53	63.02	62.86	64.42	63.95	64.49	62.27	63.27	63.14	60.29	63.36	63.75	61.92	61.74	63.15	63.10	62.02	61.88	61.35	60.48	67.85	68.83
TiO_2	0.02	0.02	0.01	0.01	0.02	0.02	0.02	0.02	0.02	0.04	0.01	0.00	0.01	0.00	0.01	0.00	0.01	0.01	0.01	0.01	0.00	0.01	0.01	0.01	0.00
Al_2O_3	21.46	21.25	21.24	20.54	22.71	22.80	21.84	21.77	21.91	23.91	22.03	22.00	23.68	21.98	21.73	23.56	23.07	22.08	21.66	23.68	23.12	23.07	23.39	19.61	10.21
FeO*	0.04	0.00	0.04	0.02	0.05	0.02	0.01	0.04	0.01	0.05	0.01	0.02	0.04	0.00	0.16	0.02	0.00	0.02	0.01	0.00	0.13	0.04	0.05	0.12	0-.02
MnO	0.00	0.00	0.00	0.00	0.00	0.00	0.00	0.01	0.00	0.00	0.01	0.02	0.02	0.01	0.03	0.02	0.00	0.02	0.01	0.00	0.02	0.01	0.00	0.00	0.00
MgO	0.001	0.00	0.001	0.00	0.01	0.01	0.01	0.01	0.04	0.03	0.02	0.02	0.03	0.02	0.03	0.03	0.02	0.02	0.02	0.12	0.05	0.01	0.02	0.03	0.02
CaO	2.65	2.52	2.64	1.79	4.13	4.29	3.41	3.56	3.,21	6.07	3.57	3.63	3.65	3.77	3.05	5.15	4.91	3.58	3.46	4.34	3.62	4.63	5.22	0.44	0.32
Na_2O	9.67	10.04	9.38	10.18	9.29	9.41	9.45	9.12	8.76	7.54	9.43	8.70	7.66	8.95	8.97	8.29	8.23	9.33	9.35	7.80	7.93	8.66	8.23	11.15	10.50
K_2O	0.10	0.12	0.18	0.12	0.11	0.10	0.08	0.11	0.13	0.08	0.10	0.11	1.20	0.09	0.17	0.08	0.10	0.09	0.13	0.46	0.90	0.19	0.15	0.06	0.07
total	99.85	99.39	98.63	98.20	99.35	99.51	99.24	98.58	98.68	99.99	98.46	97.63	96.57	98.18	97.86	99.05	98.10	98.28	97.76	98.55	97.64	97.96	97.57	99.27	98.98
Cation numbers on the basis of 8 oxygen																									
Si	2.895	2.893	2.896	2.924	2.804	2.796	2.857	2.855	2.868	2.755	2.834	2.844	2.762	2.841	2.862	2.765	2.781	2.833	2.845	2.776	2.797	2.772	2.748	2.985	3.022
Ti	0.001	0.001	0.000	0.000	0.001	0.001	0.001	0.001	0.001	0.001	0.000	0.000	0.000	0.000	0.000	0.000	0.000	0.000	0.000	0.000	0.000	0.000	0.000	0.000	0.000
Al	1.111	1.107	1.113	1.080	1.191	1.195	1.142	1.145	1.148	1.247	1.163	1.168	1.278	1.162	1.150	1.240	1.225	1.168	1.151	1.249	1.232	1.229	1.253	1.017	0.994
Fe	0.001	0.000	0.001	0.001	0.002	0.001	0.000	0.000	0.004	0.002	0.000	0.001	0.001	0.000	0.006	0.000	0.000	0.000	0.000	0.005	0.005	0.001	0.002	0.005	0.001
Mn	0.000	0.000	0.000	0.000	0.000	0.000	0.000	0.000	0.001	0.000	0.000	0.001	0.001	0.000	0.001	0.001	0.000	0.001	0.001	0.000	0.001	0.000	0.000	0.000	0.000
Mg	0.001	0.000	0.000	0.000	0.001	0.001	0.001	0.001	0.002	0.002	0.001	0.001	0.002	0.001	0.002	0.002	0.002	0.001	0.002	0.008	0.003	0.001	0.001	0.002	0.001
Ca	0.125	0.119	0.126	0.086	0.197	0.205	0.162	0.170	0.153	0.288	0.171	0.175	0.179	0.181	0.147	0.246	0.237	0.172	0.167	0.208	0.175	0.224	0.254	0.021	0.015
Na	0.824	0.860	0.809	0.881	0.802	0.811	0.812	0.789	0.756	0.647	0.819	0.759	0.681	0.779	0.781	0.718	0.719	0.812	0.818	0.677	0.695	0.759	0.725	0.951	0.894
K	0.006	0.007	0.100	0.007	0.006	0.006	0.005	0.006	0.007	0.004	0.006	0.006	0.070	0.005	0.008	0.005	0.006	0.005	0.007	0.026	0.052	0.011	0.009	0.004	0.004
total	4.963	4.987	4.957	4.979	5.004	5.014	4.980	4.969	4.939	4.946	4.996	4.955	4.974	4.970	4.957	4.977	4.969	4.991	4.991	4.951	4.960	4.998	4.992	4.984	4.930

TABLE 6.

Hornblende analyses

	1. /n=4/	2. /n=4/
SiO_2	46.01	46.56
TiO_2	0.61	0.66
Al_2O_3	7.76	7.96
FeO^*	17.66	17.20
MnO	0.32	0.31
MgO	11.90	11.97
CaO	11.54	11.52
Na_2O	1.30	1.32
K_2O	0.86	0.85
total	97.96	98.35
Cation numbers on the basis of 23 oxygen		
Si	6.888	6.917
Ti	0.068	0.074
Al	1.37	1.39
Fe	2.213	2.137
Mn	0.040	0.038
Mg	2.655	2.651
Ca	1.851	1.830
Na	0.377	0.379
K	0.164	0.162
total	15.626	15.578

5/ *Muscovite-biotite geothermometer* (HOISCH 1989). The pressure data, needed for the calculation of the muscovite-biotite geothermometer, were obtained from the plagioclase-biotite-muscovite-garnet geothermo-barometer (GHENT and STOUT, 1981). The data, obtained from the muscovite-biotite geothermometer give a temperature range between 542 and 675 °C. These values are mostly higher by 3—93 °C than those provided by the garnet-biotite geothermometer, with one exception in the case of the Darány-Ny-1 sample where the garnet-biotite geothermometer gives higher temperature, by 23—50 °C.

All of the temperature and pressure data, obtained from the geothermometers and geobarometers listed above are summarized in Table 7. The *Fig.3.* shows a comparison of data provided by the different geothermometers and geobarometers including those published by ÁRKAI (1984) and ÁRKAI *et al.* (1985). In the case of single geothermometers (like the garnet-biotite geothermometer and the muscovite-biotite geothermometer) and geobarometer (like the plagioclase-garnet-Al_2SiO_5-quartz geobarometer) the obtained data were plotted with pressure or temperature data calculated from other methods from the same sample. The combination of the pressure and temperature data are listed in the figure caption.

TABLE 7.

Summary of p—T data provided by different geothermo-barometers. Pressure and temperature conditions, obtained from different geothermometers and geobarometers

Locality	T_1	T_2	T_3	P_1	P_2
Kutas—2	558	539	542	650	0
Kutas—2	0	0	559	0	500
Víz—É—1	600	583	0	703	747
Víz—É—1	615	598	628	678	626
Kkút—5. 1115	595	572	611	845	817
Kkút—5. 1115	660	639	599	774	760
Szta—2	585	563	641	890	906
Szta—2	630	605	630	900	915
Szta—2	630	607	675	890	887
Kkút—7	600	579	672	757	684
Kkút—7	625	604	612	770	717
Dar—Ny—1	685	666	616	820	914
Dar—Ny—1	662	642	619	810	847
Kkút—5. 1148.5	605	587	597	740	718
Kkút—5. 1148.5	650	630	0	830	847
Barcs—Ny—5	605	575	0	1030	0
Barcs—Ny—5	620	590	0	920	0
Hedrehely—2	520	0	0	350	0
Hedrehely—2	530	0	0	300	0

O not determinable, because the composition of the determined minerals is out of the required range.

T_1, P_1—plagioclase-biotite-muscovite-garnet geothermo-barometer (GHENT and STOUT 1981).

T_2—garnet-biotite geothermometer (FERRY and SPEAR 1978).

T_3—muscovite-biotite geothermometer (HOISCH 1989).

P_2— plagioclase-garnet-Al_2SiO_5-quartz geobarometer (GHENT 1976).

The pressure (P_1) and temperature (T_1) data of the Hedrehely—2 (Hed—2) sample were provided by the hornblende-plagioclase geothermo-barometer (PLJUSNINA 1982).

SUMMARY

The pressure and temperature data provided by the different geothermometers and geobarometers mostly refer to the first metamorphic event, except for those obtained from the hornblende-plagioclase geothermo-barometer. There is no considerable difference between the datasets provided by different methods. Most of the temperature data fell within the range of 570 and 630 °C. It is a little bit higher than the interval between 510—600 °C, published by ÁRKAI (1984) and ÁRKAI *et al.* (1985), but it is still in a good agreement with the mineral assemblage. The different geothermometers had almost the same difference between the minimum and the maximum temperature values with a little shift to higher temperatures in the following order: the garnet-biotite, then the muscovite-biotite and finally the plagioclase-biotite-muscovite-garnet geothermometer. The relatively great difference between the minimum (539 °C) and maximum (685 °C) temperature can be

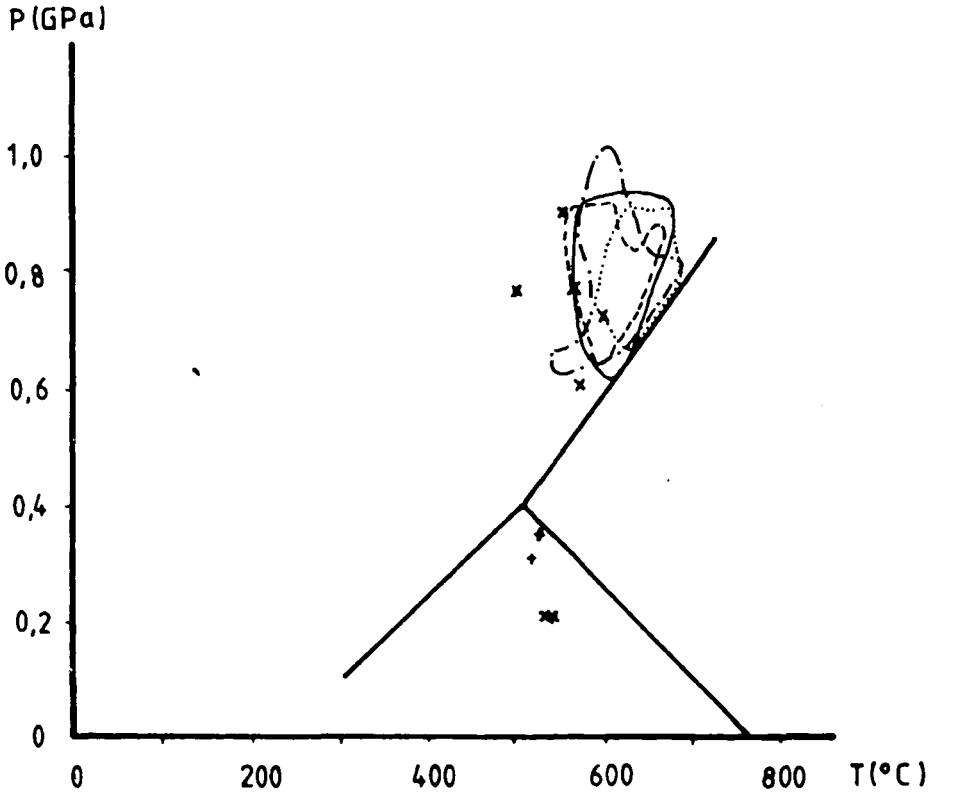

Fig. 3. Summary and comparison of p—T data provided by different geothermometers and geobarometers. See text for details, and Table 7. for more legends.

——— p—T interval, plotted from $P_2 - \frac{T_1 + T_2}{2}$

—.—.— p—T range, obtained from the plagioclase-biotite-muscovite-garnet geothermo-barometer (GHENT and STOUT 1981).

. . . . . p—T field provided by T_3-P_1

— — — p—T field drawn from $T_2 - \frac{P_1 + P_2}{2}$

\+ data obtained from hornblende-plagioclase geothermo-barometer (PLJUSNINA 1982)

x geothermo-barometric data published by ÁRKAI (1984) and ÁRKAI *et al.* (1985).

The Al_2SiO_5 stability fields are after HOLDAWAY (1971)

explained as original differences in the metamorphic grade, though there is no systematic change either in the pressure or in the temperature of the first metamorphic event. The pressure seems to be less uniform than the temperature. It varies highly from 500 Mpa to 1030 Mpa. ÁRKAI *et al.* (1985) had the same observation with a range between 590 and 890 Mpa, both in the Somogy-Dráva Basin and in the other parts of the crystalline basement of the Pannonian Basin.

The mineral equilibria and the available geothermo-barometric data give support to two possible conclusions:

1/ The temperature of the first metamorphic stage was quite uniform (mainly between 570 and 630 °C), and it was the pressure which had greater variation.
2/ The different samples with different recorded pressures represent equilibrium under different pressure conditions during either the top or the retrograde stage of the first metamorphism. In this case the p—T path may have been quite steep.

The pressure and temperature data of the first metamorphism do not seem to support the possibility of the formation of the sillimanite during this time, because neither of the p—T data was plotted within the stability field of the sillimanite.

The pressure and temperature conditions of the second metamorphic event is determined mainly by mineral equilibria. There are only two geothermo-barometric data determined by ÁRKAI *et al.* (1985), for the metamorphic terrain near the Somogy-Dráva Basin (534—536 °C, and about 200 Mpa), and two provided by this study for the Somogy-Dráva Basin (520—530 °C and 300—350 Mpa). These data indicate low pressure and temperature near the beginning of the medium grade. The pressure data are consistent with the observed andalusite-staurolite-sillimanite, and the andalusite-cordierite-sillimanite critical mineral assemblage, but the temperature was probably higher than those obtained from the hornblende-plagioclase geothermo-barometer. In compliance with the appearance of the sillimanite in the mineral assemblage, the temperature may have been about 600 °C (*Fig. 2*).

ACKNOWLEDGEMENTS

The author is wishes to thank N. POSPELOVA (Institute of Geology and Geochemistry of the Siberian Branch of the Academy of Sciences of the Soviet-union, Novosibirsk) for her kind help with the microprobe analyses, J. KÓKAI (Chief geologist of National Hydrocarbon and Gas Trust) for providing the samples. Thanks are also due to Prof. I. KUBOVICS, CS. SZABÓ (Department of Petrology and Geochemistry, Eötvös University) and to GY. BUDA (Department of Mineralogy, Eötvös University) for critical review of the manuscript, to ZS. KOVÁCS (National Hydrocarbon and Gas Trust) for providing the map with the localities of the boreholes and to Mrs. A. SZILÁGYI for drawing the figures.

REFERENCES

ÁRKAI, P. (1984): Polymetamorphism of the crystalline basement of the Somogy-Dráva Basin (Southwestern Transdanubia, Hungary) Acta Miner. Petr. Szeged, **XXVI/2**, pp. 129—153.

ÁRKAI, P., G. NAGY, G. DOBOSI (1985): Polymetamorphic evolution of the South-Hungarian crystalline basement, Pannonian Basin: Geothermometric and geobarometric data. Acta. Geol. Hung. **28**, 165—190.

ASHWORTH, J. R., M. M. EVIRGEN (1985): Plagioclase relations in pelites, central Menderes Massif, Turkey. II.Perturbation of garnet-plagioclase geobarometers. Jour. Metam. Geol. **3**. pp. 219—229.

BALOGH, K., E. ÁRVA-SÓS, GY. BUDA (1981): Chronology of granitoid and metamorphic rocks of Transdanubia (Hungary). Anuarul Inst. Geol. Geophys. **61**. pp. 359—364. Bucuresti.

FERRY, J. M. (1980): Comparative study of geothermometers and geobarometers in pelitic schists from south central Maine. Amer. Miner. **65**. pp. 720—732.

FERRY, J. M., F. S. SPEAR (1978): Experimental calibration of the partitioning of Fe and Mg between biotite and garnet. Contrib. Miner. Petrol. **66**, 113—117.

GANGULY, J. (1972): Staurolite stability and related parageneses: theory, experiments and applications. Journ. of Petrol. **13** part **62**, pp. 335—365.

GHENT, E. D. (1976): Plagioclase-garnet-Al_2SiO_5-quartz: a potential geobarometer-geothermometer. Amer. Miner. **61**, pp. 710—714.
GHENT, E. D., M. Z. STOUT (1981): Geobarometry and geothermometry of plagioclase-biotite-garnet-muscovite assemblages. Contrib. Miner. Petrol. **76**, pp. 92—97.
GUIDOTTI, C. V. (1970): The mineralogy and petrology of the transition from the lower to upper sillimanite zone in the Oquossoc area, Maine. Jour. Petrol. **11.**, pp. 277—338.
HIRSCHBERG, A., H. G. F. WINKLER, (1968): Stabilität-beziehungen zwischen chlorit, cordierit und almandin bei der metamorphose, Contrib. Miner. Petrol. **18.**, pp. 17—42.
HOINKES, G. (1986): Effect of grossular-content in garnet on the partitioning of Fe and Mg between garnet and biotite. Contrib. Miner. Petrol. **92.** pp. 393—399.
HOISCH T. D. (1989): A muscovite-biotite geothermometer. Amer. Miner. **74.** pp. 565—572.
HOLDAWAY, M. J. (1971): Stability of andalusite and the aluminium silicate phase diagram. Amer. J. Sci. **271**, pp. 97—131.
HOSCEK, G. (1969): The stability of staurolite and chloritoid and their significance in metamorphism of pelitic rocks. Contrib. Miner. Petrol. **22.**, pp. 208—232.
JANTSKY, B. (1979): Geology of the granitized crystalline basement of the Mecsek mountains (in Hungarian and in French). Annual report of the Hungarian Geological Institute. **60**, pp. 1—385.
LELKES-FELVÁRY, GY., F. P. SASSI (1981): Outlines of pre-Alpine metamorphism in Hungary. IGCP Project No. 5 Newsletter. **3**, pp. 89—99.
LELKES-FELVÁRI, C. MAZZOLI, D. VISONA (1989): Contrasting mineral assemblages in polymetamorphic rocks from South Transdanubia (Hungary) Eur. Jour. Mineral. **1** - No 1., pp. 143—146.
PIGAGE, L. C., H. J. GREENWOOD (1982): Internally consistent estimates of pressure and temperature: The staurolite problem. Amer. Jour. of Sci. **282**, Summer, pp. 943—969.
PLJUSNINA, L. P. (1982): Geothermometry and geobarometry of plagioclase-hornblende bearing assemblages. Contrib. Miner. Petrol. **80**, pp. 140—146.
SZEDERKÉNYI, T. (1976): Barrow type metamorphism in the crystalline basement of South-east Transdanubia, Hungary. Acta Geol. Acad. Sci. Hung. **20.** pp. 47—61.
SZEDERKÉNYI, T. (1984): The crystalline basement of the Alföld and its geologic connections. DSc. Theses, Szeged (in Hungarian).
TÖRÖK, K. (1986): Contribution to the geology of the crystalline basement of South Transdanubia. Diploma work, unpublished, Eötvös University Budapest (in Hungarian).
WINKLER, H.G.F. (1976): Petrogenesis of metamorphic rocks. 4. edition Springer, New York, Heidelberg, Berlin.

Manuscript received, 21 October, 1990

Acta Mineralogica-Petrographica, Szeged, XXXI, 25—42, 1990

MIDDLE TRIASSIC MAGMATIC SEQUENCES FROM DIFFERENT TECTONIC SETTINGS IN THE BÜKK MTS. NE HUNGARY

ZS. SZOLDÁN*

Department of Petrology and Geochemistry,
Eötvös Loránd University

ABSTRACT

In the Bükk Mts. (NE Hungary) two Middle Triassic magmatic event can be detected. In the first phase of the magmatism (Upper Anisian — Lower Lanidian) lava flows and pyroclastics with andesitic-rhyolitic composition were produced, while the younger magmatic horizon (Upper Lanidian — Lower Carnian) is represented by basaltic lava flows and subvolcanic intrusions, as well as some basic tuffs. On the basis of the major and trace element characteristics and the chemical composition of the clinopyroxenes, the first phase shows calc-alkaline orogenic, while the second has within-plate alkaline affinity.

INTRODUCTION

The whole Middle Triassic Eastern Bükk magmatic complex were considered by BALLA (1984,1987) as a single sequence and product of a shoshonitic-latitic type magmatism relating to subduction based on major elements chemistry published in the preceeding years (SZENTPÉTERY 1923—29, 1931—39,1950; BALOGH 1964).

DOBOSI (1986) in opposition to BALLA (1984,1987) suggested a slightly alkalinity and within-plate affinity of the Carnian Eastern Bükk metabasalts by chemical compositions of the pyroxenes appearing only in one sample. In this suggestion this alkaline volcanism may have been connected with the initial rifting of the continental shelf of Apulia (BALOGH *et al.* 1984).

The aim of this paper is to determine the geochemical affinity and the magmatectonic setting of the Middle Triassic Eastern Bükk magmatic sequence using new data and to solve the ambivalence of tectonic setting rised by previous examinations.

REGIONAL GEOLOGICAL SETTING, MODE OF OCCURRENCE, METAMORPHISM AND AGE

The Bükk Mts. located in the Igal—Torna—Bükk tectonic unit of the Pannonian region can be found in NE Hungary (*Fig. 1*). Numerous authors (BALOGH 1964; KÁZMÉR and KOVÁCS 1985; KOVÁCS 1982,1984,1989) suggested the relationship of this tectonic unit to the Dinarides and Southern Alps by stratigra

* H—1088 Budapest, Múzeum krt. 4/a, Hungary

phical and geodynamical investigations, which is also supported by the occurrence of the Middle Triassic "porphyrites and diabases" in the Bükk Mts. (e.g.: DERCOURT *et al.* 1984; CROS & SZABÓ 1984; KUBOVICS *et al.* 1990).

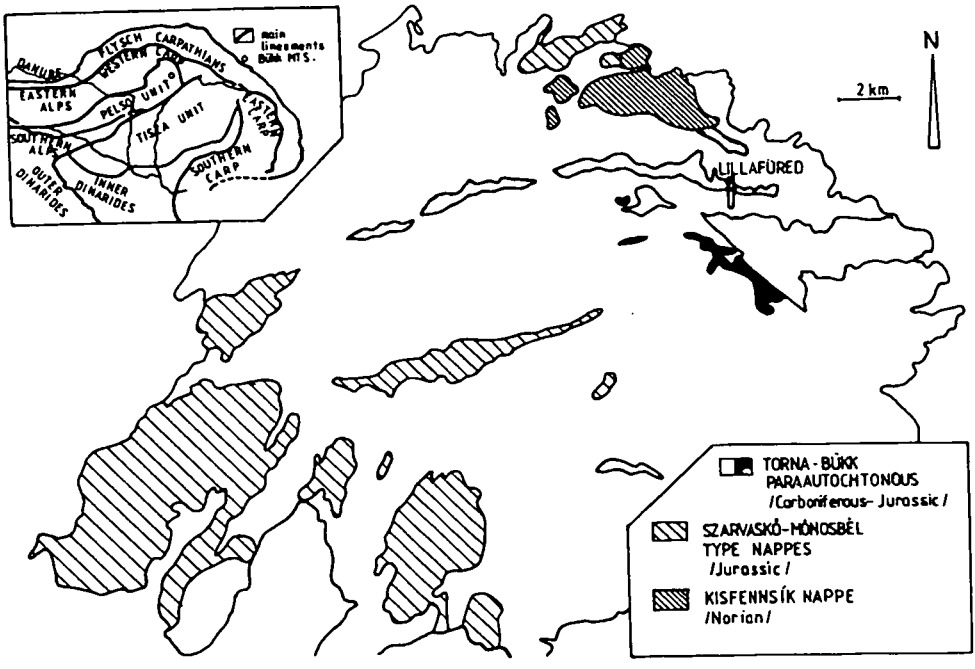

Fig. 1. Geological sketch of Bükk Mts. with the areal distribution of the Middle Triassic magmatites. — grey: Upper Anisian-Lower Ladinian intermediate-acidic metavolcanics; black: Upper Ladinian-Carnian metabasalts.

Triassic igneous rocks occur in three horizons of the largest tectonic unit (Bükk—Torna Paraautochtonous) of the Bükk Mts. (*Fig. 1*—2) (CSONTOS 1988). The Upper Anisian — Lower Lanidian, about 200 m thick, stratovolcanic sequence (Szentistvánhegy Fm.) formed partly at subareal and partly at submarine conditions consists of metaandesites, metarhyolites and its tuffs (SZENTPÉTERY 1923—29, 1931—39; PANTÓ 1951, 1961; BALOGH 1964).

The rocks of the following magmatic horizon (crop out in the surroundings of the Szinva Spring) Upper Lanidian — Lower Carnian age formed by submarine magmatic processes and consist of tuffits, basic tuffs and some basaltic lava flows (CSONTOS 1988).

The youngest magmatic event represented by a few, small subvolcanic, basaltic intrusions emplaced in cherty limestone (Lusta Valley) and in equivalent of the Raiblian shale (Létrástető) (BALOGH 1964; CSONTOS 1988).

This temporal evolution of the Eastern Bükk Middle Triassic magmatism is very similar to the Triassic volcanic activity in the Southern Alps (CASTELLARIN *et al.* 1980; PISA *et al.* 1980), i.e. a mainly subareal volcanism producing "acidic" lava flows and pyroclastic deposits changes into submarine basaltic magmatism.

Based on the secondary mineral assemblages of the magmatites, the composition ratio of the coexisting pumpellyite-chlorite-actinolite-epidote and the com-

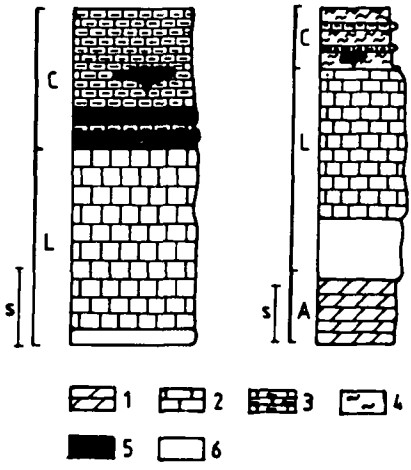

Fig. 2. Stratigraphical position of the Middle Triassic Eastern Bükk magmatites (after CSONTOS 1988) — 1. dolomite (deposited on outer shelf carbonate platform); 2. limestone (like at the dolomite); 3. cherty limestone (deposited in intraplatform basins); 4. shale (equivalent of the Raiblian shale); 5. U. Anisian-L. Ladinian intermediate-acidic volcanics; 6. U. Ladinian-Carnian basaltic volcanics and subvolcanic intrusions. s: 200 m.

position of pumpellyite ÁRKAI (1973, 1983) pointed out, that the Eastern Bükk magmatites were affected by an Alpine regional, high temperature pumpellyite-prehnite-quartz facies (WINKLER 1965) showing transition towards the greenschist facies metamorphism. This is why the attempts to determinate the magmatectonic setting of Eastern Bükk magmatites based on major-element geochemistry did not yield unequivocal results.

ÁRVA—SÓS *et al.* (1987) have determined the K/Ar age of some Eastern Bükk basic metatuffs and metarhyolites (quartz-porphyry) (Table 1). By reason of the recent petrographical investigations monomineralic phases (plagioclase and pyroxene-rich fractions) of the main metabasalt type were measured. As shown by the

TABLE 1.

K—Ar ages of the Eastern Bükk metamagmatites (measured by ÁRVA-SÓS).

		Phase measured	Potassium content	$^{40}Ar_{rad}$ (ncm^3/cm)	$^{40}Ar_{rad}$ (%)	K—Ar age (million years)
1.	Bag	w.r.	5.165	2.153 *E-5	97.0	104.0± 5
2.	Bag	w.r.	6.63	2.590 *E-5	87.0	98.0± 5
3.	Bag	w.r.	4.51	1.704 *E-5	98.0	95.0± 5
4.	Lil	w.r.	2.49	8.287 *E-6	93.0	84.4± 4
5.	Luv	py.	0.558	2.5627*E-6	66.4	114.0± 4.5
6.		pl.	21.029	8.9418*E-6	87.2	110.0± 4.2
7.	Szis	py.	0.115	7.1473*E-7	31.4	153.0±10.2
8.		s.m.	1.803	8.7824*E-6	86.5	121.0± 4.6
9.	Lét	py.	1.006	3.6689*E-6	73.1	91.5± 3.6
10.		pl.	2.479	7.3516*E-6	89.5	74.8± 2.8

w.r. — whole rock samples; pl. — phase abundant in plagioclase; py.— phase abundant in pyroxene; s.m. — phase abundant in secondary minerals — Bag—metarhyolite; Lil—metaandesite tuff; Luv—intrusion of Lusta Valley; Szis—lava flows at the Szinva Spring; Lét—intrustion of Létrástetõ

1.—4. ÁRVÁNÉ SÓS *et al.*, 1987.

5.—10. new data.

data (Table 1) obtained from whole-rock samples and monomineralic phases the radiometric ages indicate the Alpine regional metamorphic event (ÁRKAI 1973, 1983) probably connected to the Austrian (Upper Cretaceous) orogeny (ÁRVA—SÓS *et al.* 1987).

PETROGRAPHY

1. The older "andesitic-rhyolitic" sequence

The detailed petrographical descriptions were reported in works of SZENTPÉTERY (1923—29, 1931—1939), PANTÓ (1951, 1961), BALOGH (1964) and ÁRKAI (1973), therefore only the most relevant features of the fresh lava-types selected to the determination of the magmatectonic setting are briefly summarized here.

The metaandesites are strongly porphyritic and can be divided into two types. The first is characterized by plagioclase (An 10—30) phenocrysts and chlorite pseudomorphs after pyroxene microphenocrysts. The groundmass is strongly altered and made up of plagioclase, apatite, zircon, leucoxene and opaque minerals. The second type has chloritic-nontronitic-seladonitic pseudomorphs after orthorombic and monoclinic pyroxene phenocrysts and andesinic (rare labradoritic) plagioclase phenocrysts. The groundmass is composed of plagioclase and mafic mineral relics, leucoxene and opaques.

Fig. 3. Ignimbrite with flow texture — Flow structure formed around sanidine crystals.| II N, M:32x.

The studied metarhyolites are represented by a porphyritic and an ignimbritic type. In the first type weakly resorbed quartz and strongly resorbed alkali feldspar phenocrysts occur. The groundmass is totally recrystallized and consists of quartz and sericite. The ignimbritic type with flow texture contains crystalloclasts and lithoclasts, as well as some vitroclasts (*Fig. 3*). The crystalloclasts are sanidine, plagioclase, quartz, zircon and chloritic-hematitic pseudomorphs after amphibole (?); the lithoclasts are rhyolites-dacites with porphyritic texture and glassy or slightly crystallized groundmass. The matrix is strongly hematitized and devitrified glass.

2. The younger "basalts"

SZENTPÉTERY (1950a, b), PANTÓ (1951) and ÁRKAI (1973) published the petrography of the metabasalts from the Eastern Bükk, but the spatial distribution

1/ The temperature of the first metamorphic stage was quite uniform (mainly between 570 and 630 °C), and it was the pressure which had greater variation.
2/ The different samples with different recorded pressures represent equilibrium under different pressure conditions during either the top or the retrograde stage of the first metamorphism. In this case the p—T path may have been quite steep.

The pressure and temperature data of the first metamorphism do not seem to support the possibility of the formation of the sillimanite during this time, because neither of the p—T data was plotted within the stability field of the sillimanite.

The pressure and temperature conditions of the second metamorphic event is determined mainly by mineral equilibria. There are only two geothermo-barometric data determined by ÁRKAI *et al.* (1985), for the metamorphic terrain near the Somogy-Dráva Basin (534—536 °C, and about 200 Mpa), and two provided by this study for the Somogy-Dráva Basin (520—530 °C and 300—350 Mpa). These data indicate low pressure and temperature near the beginning of the medium grade. The pressure data are consistent with the observed andalusite-staurolite-sillimanite, and the andalusite-cordierite-sillimanite critical mineral assemblage, but the temperature was probably higher than those obtained from the hornblende-plagioclase geothermo-barometer. In compliance with the appearance of the sillimanite in the mineral assemblage, the temperature may have been about 600 °C (*Fig. 2*).

ACKNOWLEDGEMENTS

The author is wishes to thank N. POSPELOVA (Institute of Geology and Geochemistry of the Siberian Branch of the Academy of Sciences of the Soviet-union, Novosibirsk) for her kind help with the microprobe analyses, J. KÓKAI (Chief geologist of National Hydrocarbon and Gas Trust) for providing the samples. Thanks are also due to Prof. I. KUBOVICS, CS. SZABÓ (Department of Petrology and Geochemistry, Eötvös University) and to GY. BUDA (Department of Mineralogy, Eötvös University) for critical review of the manuscript, to ZS. KOVÁCS (National Hydrocarbon and Gas Trust) for providing the map with the localities of the boreholes and to Mrs. A. SZILÁGYI for drawing the figures.

REFERENCES

ÁRKAI, P. (1984): Polymetamorphism of the crystalline basement of the Somogy-Dráva Basin (Southwestern Transdanubia, Hungary) Acta Miner. Petr. Szeged, **XXVI/2**, pp. 129—153.

ÁRKAI, P., G. NAGY, G. DOBOSI (1985): Polymetamorphic evolution of the South-Hungarian crystalline basement, Pannonian Basin: Geothermometric and geobarometric data. Acta. Geol. Hung. **28**, 165—190.

ASHWORTH, J. R., M. M. EVIRGEN (1985): Plagioclase relations in pelites, central Menderes Massif, Turkey. II.Perturbation of garnet-plagioclase geobarometers. Jour. Metam. Geol. **3**. pp. 219—229.

BALOGH, K., E. ÁRVA-SÓS, GY. BUDA (1981): Chronology of granitoid and metamorphic rocks of Transdanubia (Hungary). Anuarul Inst. Geol. Geophys. **61**. pp. 359—364. Bucuresti.

FERRY, J. M. (1980): Comparative study of geothermometers and geobarometers in pelitic schists from south central Maine. Amer. Miner. **65**. pp. 720—732.

FERRY, J. M., F. S. SPEAR (1978): Experimental calibration of the partitioning of Fe and Mg between biotite and garnet. Contrib. Miner. Petrol. **66**, 113—117.

GANGULY, J. (1972): Staurolite stability and related parageneses: theory, experiments and applications. Journ. of Petrol. **13** part **62**, pp. 335—365.

and the significant features of the main lava-types they described was not quite clear.

A. Lava flows at the Szinva Spring. This rock has schistose structure and mildly to strongly porphyritic texture (max 40%). The former is abundant in vesicles, but the latter does not have them. The deformed phenocrysts are: colourless augite and sericitic pseudomorphs after plagioclase (*Fig. 4*). The groundmass is totally altered and makes up of augite relicts, actinolite, chlorite, sericite and leucoxene.

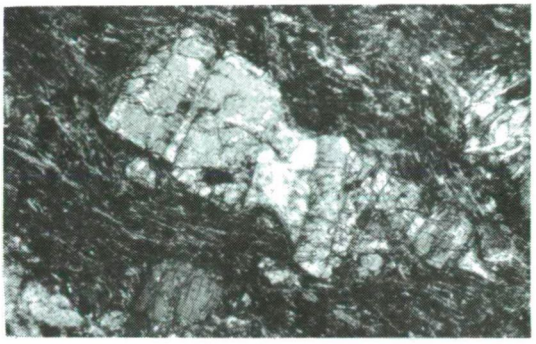

Fig. 4. Metabasalt with schistose structure and porphyritic texture (lava flow from Szinva Spring). — Aparted augite phenocrystal. x N, M:32x.

B. Intrusions emplaced in cherty limestone. This metabasalt has subophitic texture. The strongly coloured clinopyroxene phenocrysts have brownish pink to reddish brown dichroism, zoned and hour-glass structure. The clinopyroxenes partly enclose the plagioclase phenocrysts (they have completely sericitized) indicating that the crystallization of the plagioclases preceeded the formation of the clinopyroxenes. The totally destroyed groundmass consists of secondary minerals (chlorite, epidote, actinolite, opaques, leucoxene and albite).

C. Intrusions in the Raiblian shale — type formation. This is the most fresh Eastern Bükk metabasalt type, which has subaphyric texture. The very rare microphenocrysts (olivine) appear as replaced by calcite and chlorite. The groundmass consists of abundant augite and andesinic/labradoritic plagioclase (An 58—46), subordinate biotite, leucoxenized opaques and scarce apatite. Clinopyroxenes are weakly coloured (pale brownish yellow) and their zoned structure can be observed rarely as well.

GEOCHEMISTRY

The major elements determined by wet chemical analysis using atomic absorption method for Al, Mn, Mg, Ca, Na, K, flame-photometric method for Ti, P, and thermometric method for Si, Fe; Ni, Rb, Sr and Ba were determined by atomic absorption method (analyzed by L. HOFFMANN, Dept. of Petr. and Geochem., Eötvös University, Budapest). Y, Zr, and Nb were measured by quantitative spectrographic analysis (analyzed by J. NAGY-BALOGH, Dept. of Petr. and Geochem., Eötvös University, Budapest). Rare-earth elements, Hf, Ta, Th, Cr, Co and Sc were determined by INAA in the Nuclear Technical Institute of the Technical University, Budapest (analyzed by ZS. MOLNÁR).

1. Major-element geochemistry

A. Metaandesites and metarhyolites. Among the intermediate-acidic volcanics five groups were distinguished using Q-mode cluster analyses on major element chemical compositions (Table 2). As shown in the total alkalia-silica diagram (*Fig. 5*) the transition is continuous between the rock types, especially in the intermediate range. Due to the subsequent alkali enrichment the data-points trend to move towards the trachitic field. The AFM diagram (*Fig. 6*) indicates calc-alkaline trend to this volcanic sequence.

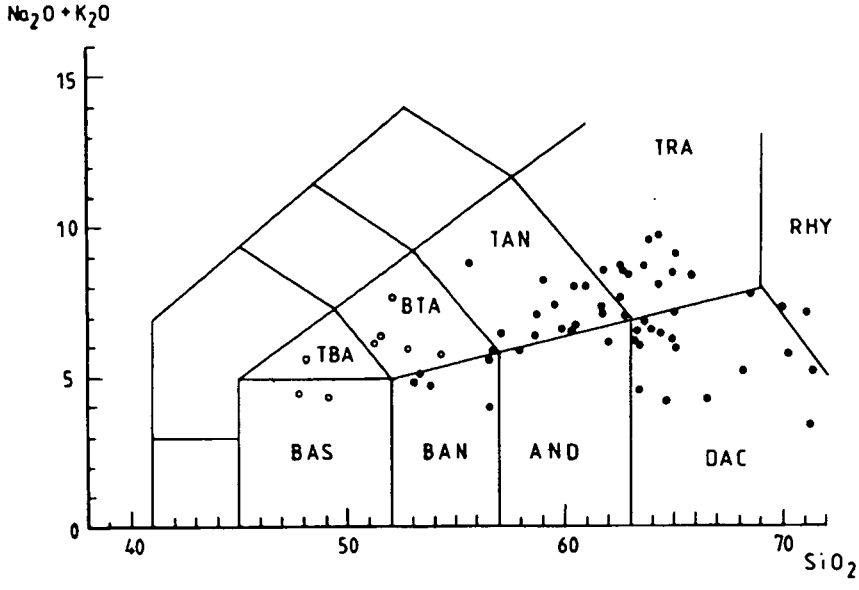

Fig. 5. TAS diagram for the Middle Triassic Eastern Bükk volcanic and subvolcanic rocks (open circles: "younger" metabasalts; solid circles "older" intermediate-acidic rocks).

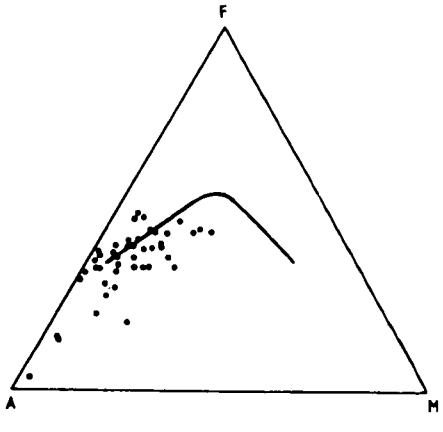

Fig. 6. AFM diagram for the Middle Triassic Eastern Bükk intermediate-acidic volcanics ("older" sequence).

TABLE 2.

The average major element and normative compositions of the Eastern Bükk intermediate–acidic volcanic groups ("older" sequence) distringuished by Q–mode cluster analyses.

	I		II		III		IV		V	
	a	b	a	b	a	b	a	b	a	b
SiO_2	76.33	76.78	72.53	72.69	63.75	65.36	58.73	60.41	54.12	55.84
TiO_2	0.08	0.08	0.12	0.12	1.43	1.47	1.50	1.54	1.52	1.57
Al_2O_3	11.85	11.92	13.75	13.78	16.32	16.73	19.19	19.74	17.71	18.27
Fe_2O_3	0.63	0.63	0.87	0.87	3.06	3.14	2.81	2.89	3.95	4.08
FeO	0.51	0.51	0.87	0.87	1.71	1.75	2.89	2.97	4.29	4.43
MnO	0.00	0.00	0.00	0.00	0.10	0.10	0.12	0.12	0.08	0.08
MgO	0.42	0.42	0.39	0.39	1.23	1.26	1.49	1.53	3.27	3.37
CaO	1.02	1.03	0.77	0.77	3.40	2.77	4.09	3.17	7.29	6.97
Na_2O	2.46	2.47	1.82	1.82	4.46	4.57	5.43	5.59	3.53	3.64
K_2O	5.77	5.80	8.44	8.46	2.41	2.47	1.82	1.87	1.57	1.62
P_2O_5	0.35	0.35	0.22	0.22	0.37	0.38	0.16	0.16	0.13	0.13
CO_2	0.00		0.00		0.55		0.79		0.42	
$+H_2O$	0.71		0.67		1.70		1.53		1.93	
$-H_2O$	0.10		0.11		0.14		0.09		0.44	
Sum	100.23	100.00	100.56	100.00	100.63	100.00	100.64	100.00	100.25	100.00
q	38.21		27.79		22.57		11.80		8.89	
c	0.54		0.75		2.41		3.15		—	
or	34.30		49.99		14.60		11.06		9.57	
ab	20.94		15.44		38.69		47.26		30.82	
an	2.79		2.39		11.25		14.66		28.73	
cpx	—		—		—		—		3.97	
di	—		—		—		—		3.20	
hd	—		—		—		—		0.77	
opx	1.34		1.66		3.14		4.57		8.83	
en	1.05		0.97		3.14		3.82		6.92	
fs	0.29		0.68		—		0.75		1.91	
mt	0.92		1.26		1.74		4.19		5.91	
il	0.15		0.23		2.78		2.93		2.98	
hm	—		—		1.94		—		—	
ap	0.83		0.52		0.90		0.39		0.32	
M	59.48		44.41		56.18		47.89		57.60	
DI	93.45		93.22		75.86		70.12		49.28	
SI	4.29		3.15		9.56		10.32		19.69	

Data are from SZENTPÉTERY (1923—39) and BALOGH (1964), partly analyzed by L. HOFFMANN (ELTE Dept. of Petr. and Geochem.). I—II.: metarhyolite, III.: metadacite, IV.: metaandesite, V.: basaltic andesite; a: raw data, b: volatile-corrected data.

Comparing the Eastern Bükk rock types with the volcanics of some orogenic areas (EWART and LE MAITRE 1980), the following substantial differences appear: the Eastern Bükk rhyolites have higher K_2O-contents (high normative orthoclase values) than the references, while the Eastern Bükk andesites and the basaltic andesites have higher TiO_2-, Al_2O_3-, Na_2O- (high normative corund values) and lower MgO-contents than the orogenic intermediate rocks.

B. The younger metabasalts. The analyses of the representative metabasalts samples are given in the Table 3. On the total alkalia-silica diagram (*Fig. 5*) data-points of the samples containing 4-5% volatiles concentrate in the field of trachybasalts and basaltic andesites. Based on the normative compositions of the metabasalts calculated from the volatile-free and Fe-corrected data, the lava flows occurring at the Szinva Spring may be considered as tholeiitic basalts (normative opx appears), while the intrusions of Lusta Valley and Létrástető, which have the highest S. I. and D. I. values show alkaline olivine basalt affinity (normative ne and ol in the norms) (Table 3).

2. *Trace-element geochemistry*

Analyses of the representative rock samples are given in the Table 4.

A. Metaandesites and metarhyolites. On the spiderdiagrams proposed by PEARCE (1982) some throughs and spikes appear (*Fig. 7*). In the case of primary

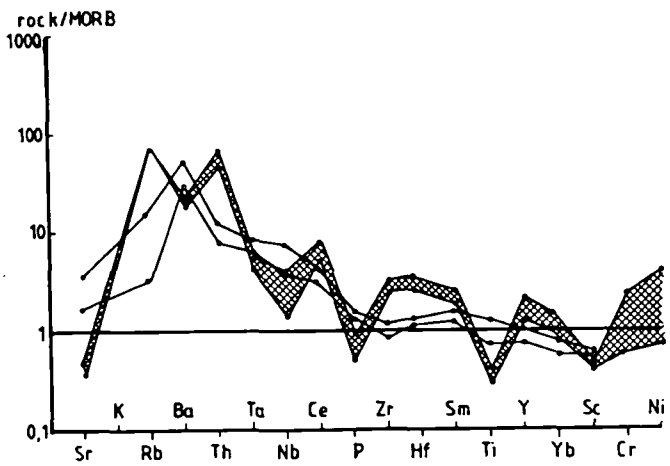

Fig. 7. Spiderdiagrams (PEARCE, 1982) of the Middle Triassic Eastern Bükk volcanic and subvolcanic rocks. (solid circles and dashed area: the "older" intermediate-acidic volcanics; area bordered by open circles: the "younger" basaltic volcanic and subvolcanic rocks).

basalts this phenomenon shows the nature of the source material and the partial melting process. Some of these geochemical features appearing in the basalt patterns can be extended to more evolved compositions, whereas others can be explained as the effect of fractional crystallization, volatile loss or crustal contamination (PEARCE 1982). For this reason trace element patterns of Eastern Bükk intermediate and acidic rocks are less suitable to determine the magmatectonic position of the older sequence. However, since the Nb and Ta behave as incompatible elements, the displayed low abundances of these elements in the Eastern Bükk metaandesithes-metarhyolites may reflect Nb-Ta depleted source indicating a

TABLE 3.

Major element and normative compositons of the representative metabasalt samples (SZENTPÉTERY 1950/a; BALOGH 1964; analyzed by L. HOFFMANN).

	LUV		SZIS		LÉT	
	a	b	a	b	a	b
SiO_2	47.90	51.66	48.00	51.39	48.00	50.42
TiO_2	1.46	1.57	0.90	0.96	1.93	2.03
Al_2O_3	13.07	14.10	14.18	15.18	18.40	19.33
Fe_2O_3	4.59	1.57	7.84	1.66	3.39	1.67
FeO	4.17	7.87	1.48	8.32	6.13	8.33
MnO	0.10	0.11	0.11	0.12	0.17	0.18
MgO	8.68	9.36	9.57	10.25	4.90	5.15
CaO	7.35	7.18	6.74	5.85	5.58	5.66
Na_2O	2.93	3.16	2.68	2.87	4.86	5.11
K_2O	2.95	3.18	2.98	3.19	1.27	1.33
P_2O_5	0.21	0.23	0.20	0.21	0.76	0.80
CO_2	0.54		1.00		0.15	
$+H_2O$	4.44		3.81		3.44	
$-H_2O$	0.60		1.00		0.20	
Sum	98.99	100.00	100.49	100.00	99.18	100.00
c	—		—		1.10	
or	18.80		18.85		7.88	
ab	24.57		24.28		41.94	
an	14.88		19.12		22.87	
ne	1.18		—		0.68	
cpx	15.58		6.89		—	
di	11.11		4.82		—	
hd	4.47		2.06		—	
opx	—		3.58		—	
en	—		2.40		—	
fs	—		1.18		—	
ol	19.20		22.54		17.41	
fo	12.73		14.63		8.98	
fa	6.47		7.91		8.43	
mt	2.28		2.41		2.42	
il	2.99		1.83		3.85	
ap	0.54		0.51		1.89	
M	67.94		68.71		52.40	
DI	44.55		43.13		50.50	
SI	37.22		38.98		23.84	

a: raw data, b: volatile- and Fe^{+2} / Fe^{+3} corrected data. **SZIS**: Szinva Spring; **LUV**: Lusta Valley; **LÉT**: : Létrástető.

TABLE 4.

Trace element contents of the representative Eastern Bükk Middle Triassic volcanic and subvolcanic rocks.

	LÉT	LUV	SZIS	LIL	NIE	BÁN
La	35.00	18.50	19.00	28.50	36.00	39.50
Ce	62.00	40.00	42.00	57.00	62.00	85.00
Sm	5.00	4.87	4.25	6.54	7.04	8.75
Eu	1.10	1.61	1.63	1.00	1.00	1.10
Yb	2.20	2.20	2.04	3.10	2.40	4.60
Lu	0.35	0.28	0.30	0.48	0.45	0.72
Hf	3.80	3.20	2.80	6.30	7.00	9.00
Ta	3.10	1.40	1.20	0.80	1.10	1.00
Th	5.40	2.10	1.60	9.50	12.60	13.20
Cr	113.00	100.00	244.00	89.00	170.00	220.00
Co	16.00	38.10	36.00	9.70	10.30	5.60
Sc	16.00	22.50	25.00	16.60	9.60	19.20
Nb	51.00	27.00	13.00	5.00	5.00	14.00
Y	27.00	29.00	24.00	39.00	41.00	67.00
Zr	116.00	99.00	76.00	227.00	220.00	297.00
Ba	781.90	637.30	640.80	378.40	223.20	n.d.
Rb	27.30	12.70	6.60	154.20	10.10	n.d.
Sr	265.10	433.40	199.80	44.00	166.10	n.d.
Ni	179.80	242.50	224.10	69.10	125.50	n.d.

REE-elements and Hf, Ta, Cr, Co, Sc analyzed by ZS.MOLNÁR (Technical University, Budapest); Nb, Y, Zr analyzed by J. NAGY-BALOGH (ELTE Dept. of Petr. and Geochem.); Ba, Rb, Sr, Ni analyzed by L. HOFFMANN (ELTE Dept. of Petr. and Geochem.)
LÉT, LUV, SZIS: metabasalt (Létrástető, Lusta Valley, Szinva Spring).
LIL, NIE: metaandesite (Lillafüred, Nagy István erőse Hill).
BÁN: metarhyolite (Bánkút).

destructive plate margin origin (WILSON 1989) for these rocks. This suggestions seems to be supported by the La/Th (GILL, 1981) and by the Th-Hf/3-Ta (WOOD 1980) discrimination diagrams. In the former plot the Eastern Bükk metaandesites correspond the criteria of orogenic andesites (2<La /Th<7), while in the latter diagram (*Fig. 8*) data-points locate in the fields of the destructive plate margin-type basalts and their differentiates.

The chondrite-normalized rare-earth element (REE) patterns of the metaandesites-metarhyolites show strong negative Eu anomalies (Eu/Sm = 0.12-0.15), which reflect the fractionation of Eu into the feldspars in an earlier stage of the magma evolution (*Fig.* 9). (This fact corresponds to the low Sr abundances displayed on the spiderdiagram, although it had partly decreased by the metamorphism as well.)

B. The younger metabasalts. As shown on the spiderdiagrams (*Fig. 7*), the style of enrichment of some elements normalized to the MORB composition (PEARCE 1982) is highly similar to the trace element patterns of the transitional basalts formed in the within-plate areas.

In opposition to the older and more acidic sequence the data-points of the metabasalts fall in the field of within-plate basalts on the WOOD (1982) diagram

(*Fig. 8*), and they plot range along the **P**-type **MORB—WPA** boundary, which is also supported by their transitional to slightly alkaline character.

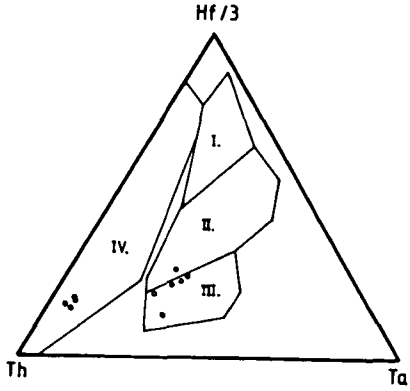

Fig. 8. Th-Hf/3-Ta discrimination diagram (WOOD 1980) for the Middle Triassic Eastern Bükk volcanic and subvolcanic rocks. (solid circles: the "older" intermediate-acidic volcanics; open circles: the "younger" basaltic volcanic and subvolcanic rocks).
I. **N-MORB**.: normal mid-ocean ridge basalts - II. **P-MORB**.: plume-MORB - III. **WPA**: within-plate alkaline basalts - IV. **DPMB**: destructive plate margin basalts and their differentiates.

The chondrite-normalized REE patterns of the Eastern Bükk metabasalts (*Fig. 9*) are only slightly light-REE enriched and have no Eu-anomaly except only those of the Létrástető intrusive rock (Eu/Sm = 0.22). With the strong enrichment displayed in the Ba-Pa range on its trace element patterns, this phenomenon indicates more evolved nature of the Létrástető intrusion compared to the other Eastern Bükk metabasalts.

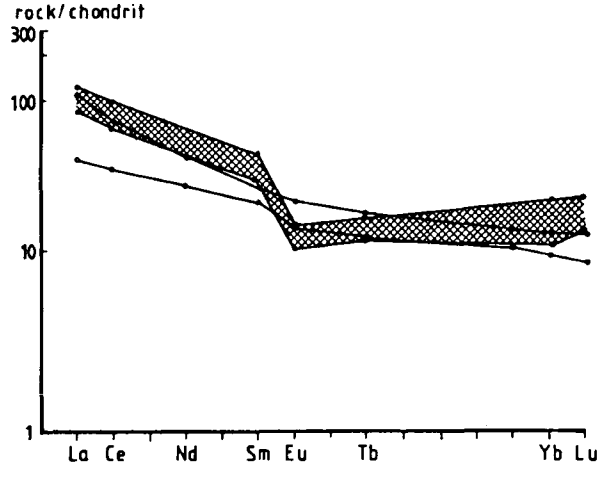

Fig. 9. Chondrite-normalized (NAKAMURA 1974) REE patterns of the Middle Triassic Eastern Bükk volcanic and subvolcanic rocks (solid circles and dashed area: the "older" intermediate-acidic volcanics; area bordered by open circles: the "younger" basaltic volcanic and subvolcanic rocks).

3. The chemical composition of pyroxenes

The chemical analyses of clinopyroxenes were performed with an AMRAY 1830I electron microprobe by M. JÁNOSI (Dept. of Petr. and Geochem. Eötvös University, Budapest) using 20 kV accelerating voltage and 20 nA beam current. Raw data were corrected by the on-line ZAF correction program.

The average compositions of the clinopyroxenes are given in the Table 5. *Fig. 10* illustrates the distribution of data-points on the Ca-Mg-Fe ternary. The LUV-pyroxenes (from the intrusions in the Lusta Valley) and LÉT-pyroxenes (from the Létrástető intrusion) can be classified partly as diopsides, but mainly as salites, while the SZIS-pyroxenes (from the lava flows occurring at Szinva Spring) proved to be salites, a part of them wollastonit-reach clinopyroxenes.

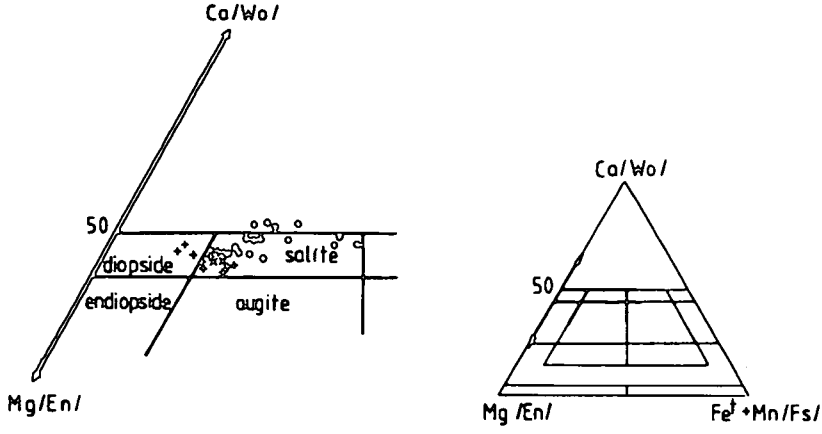

Fig. 10. Ca-Mg-Fe ternary for the clinopyroxenes from Middle Triassic Eastern Bükk metabasalts ("younger" sequence).
x: Létrástető; solid circles : Lusta Valley; +: Szinva Spring.

In the triangular diagram proposed by NISBET and PEARCE (1977) all pyroxene types show within-plate alkaline basalt (WPA) affinity.

On the plot of the discrimination functions F_1 against F_2 (NISBET and PEARCE, 1977) the data-points of the pyroxenes mostly fall on the boundary of the WPA-VAB-OFB fields, while the LUV-pyroxenes show an alkaline trend characterized by enrichment of TiO_2, Al_2O_3 and FeO from the core to the rim (*Figs. 11, 12*).

In the discrimination diagram based on Ti and Ca+Na content of clinopyroxenes (LETERRIER *et al.* 1982) (*Fig. 13*) the SZIS-pyroxenes show the less and the LUV-pyroxenes the most alkaline character, while the LÉT-pyroxenes have transitional position.

If we accept the assumption, that the two younger magmatic events (i.e. Upper Lanidian — Lower Carnian /Szinva Spring/; in the upper part of the Carnian /Lusta Valley, Létrástető/) producing the basaltic rocks form a single cogenetic sequence, we have to concede the slightly alkaline character indicating by SZIS-pyroxenes, i.e. they were formed from an evolved liquid with modified composition compared to the initial magma.

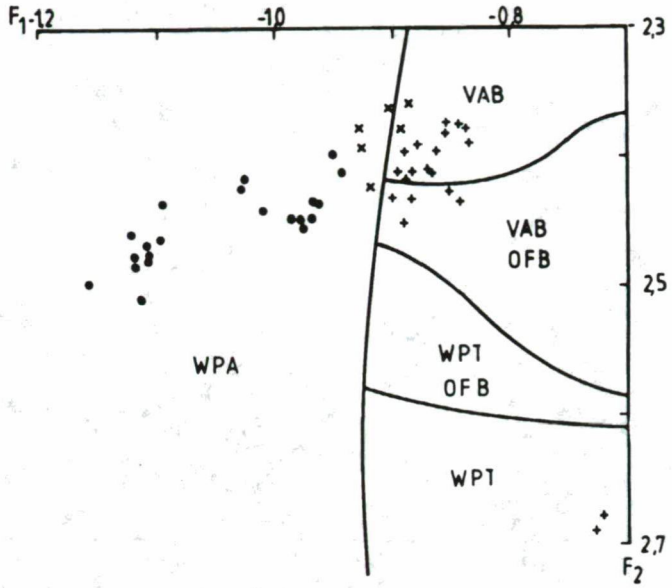

Fig. 11. Plots of discriminant function F_1 vs. F_2 (NISBET and PEARCE 1977) for the clinopyroxenes from Middle Triassic Eastern Bükk metabasalts ("younger" sequence).
VAB: volcanic arc basalts; **OFB**: ocean-floor basalts; **WPA**: within-plate alkaline basalts; **WPT**: within-plate tholeiitic basalts; x: Létrástetõ; solid circles : Lusta Valley; +: Szinva Spring.

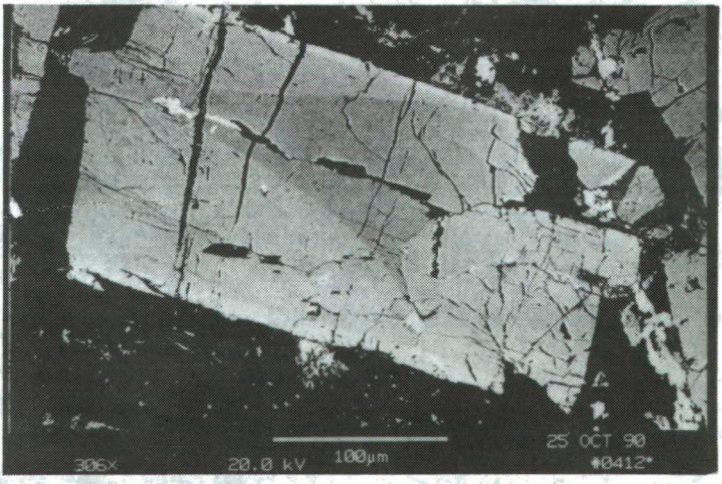

Fig. 12. Backscattered electron image of LUV-pyroxenes with hour-glass structure.

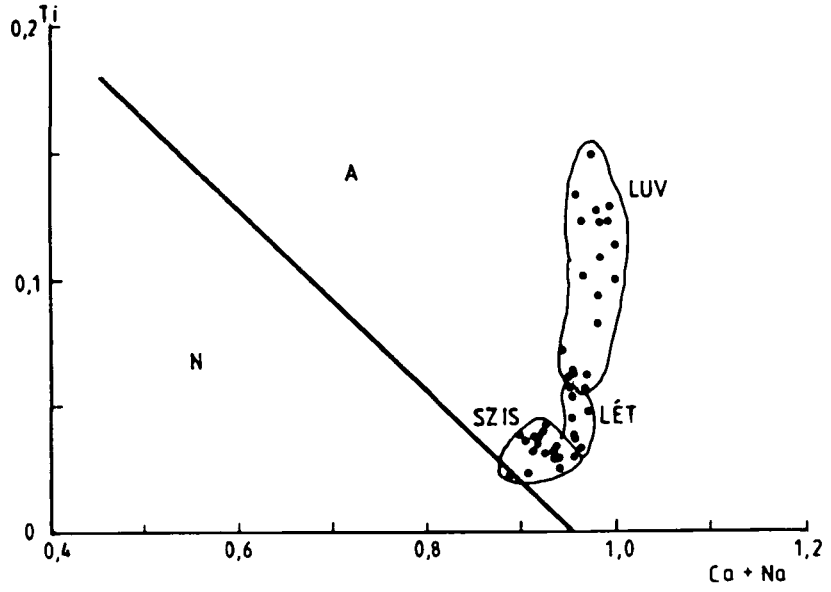

Fig. 13. Ti vs. Ca+Na discriminant diagrams (LETERRIER *et al.* 1982) for the clinopyroxenes from Middle Triassic Eastern Bükk metabasalts ("younger" sequence).
A: field of the alkaline basalts.
B: field of the non-alkaline basalts.
LÉT: Létrástető; **LUV:** Lusta Valley; **SZIS:** Szinva Spring.

SUMMARY

All geochemical patterns show, that the andesitic-rhyolitic lavaflows, tuffs and ignimbrites in the Upper Anisian - Lower Lanidian volcanic horizon erupted at a convergent plate margin and they have calc-alkaline character (*Fig. 14*).

In contrast with the former volcanism, the Upper Lanidian - Carnian volcanic (Szinva Spring) and subvolcanic (Létrástető, Szinva Valley) basalts formed by within-plate magmatic processes (*Fig. 14*). The lava flows in the volcanoclastic sequence at Szinva Spring erupted in the initial stage of the basic volcanism and have slightly alkaline or rather transitional character, while the subvolcanic intrusions (Létrástető, Szinva Valley) consist of alkaline basalt types according to their more differenciated nature.Although the Triassic igneous rocks in the Dinarides have been found by PAMIĆ (1984) as the products of a rifting episode, the magmatism also shows the geochemical ambivalence detected in the magmatic sequence of the Bükk Mts. as well. On the basis of the major-element geochemistry, the basic and some intermediate rocks in the Dinarides show tholeiitic nature, whereas some intermediate- and all acidic rocks show calc-alkaline affinity. Since the trace element patterns of the basic volcanics indicate within-plate character (like in the Bükk Mts.),therefore in the suggestion of PAMIĆ (1984) the whole Triassic magmatic sequence of the Dinarides is genetically related to the rifting of a stable continental realms.

TABLE 5.

Average compositions of clynopyroxenes from Middle Triassic Eastern Bükk metabasalts ("younger sequence").

	LÉT (n=6)		LUV (n=3) a		LUV (n=3) b		SZIS (n=4) a		SZIS (n=12) b	
SiO_2	49.15	(0.88)	48.40	(0.53)	44.32	(1.06)	51.53	(0.46)	49.22	(0.41)
TiO_2	1.45	(0.26)	2.18	(0.02)	4.37	(0.20)	0.73	(0.07)	1.18	(0.14)
Al_2O_3	3.69	(0.62)	4.40	(0.14)	7.93	(0.85)	3.45	(0.05)	5.24	(0.52)
Cr_2O_3	0.09	(0.19)	0.02	(0.02)	0.05	(0.04)	0.16	(0.12)	0.14	(0.09)
FeO_t	6.67	(0.57)	8.19	(0.15)	9.25	(0.46)	6.24	(0.36)	6.98	(0.92)
MnO	0.11	(0.07)	0.12	(0.03)	0.14	(0.03)	0.12	(0.03)	0.11	(0.07)
MgO	14.19	(0.40)	13.36	(0.07)	10.81	(0.23)	16.21	(0.55)	14.16	(0.54)
CaO	22.32	(0.07)	22.73	(0.29)	22.66	(0.60)	21.42	(0.40)	21.91	(0.32)
Na_2O	0.76	(0.11)	0.64	(0.16)	0.81	(0.11)	0.55	(0.07)	0.61	(0.,14)
Cation numbers on the basis of 6 oxygens										
Si	1.859		1.818		1.680		1.892		1.837	
Al_4	0.141		0.182		0.320		0.108		0.163	
Al_6	0.024		0.013		0.034		0.041		0.068	
Ti	0.041		0.062		0.125		0.020		0.033	
Gr	0.003		0.001		0.001		0.005		0.004	
Fe^{3+}	0.127		0.133		0.141		0.090		0.102	
Fe^{2+}	0.084		0.124		0.153		0.101		0.116	
Mn	0.004		0.004		0.004		0.004		0.004	
Mg	0.800		0.748		0.611		0.887		0.788	
Ca	0.905		0.915		0.920		0.843		0.876	
Na	0.056		0.046		0.060		0.039		0.044	
K	0.000		0.000		0.000		0.000		0.000	
Ac	5.57		4.63		5.97		3.93		4.44	
Jd	0.00		0.00		0.00		0.00		0.00	
TiTs	4.12		6.15		12.46		2.00		3.32	
CrTs	0.26		0.05		0.13		0.47		0.41	
CaTs	2.41		1.29		3.36		4.14		6.76	
FATs	7.13		8.72		8.08		5.06		5.73	
Wo	38.27		37.64		33.99		36.30		35.68	
En	40.00		37.40		30.53		44.36		39.38	
Fs	4.38		6.38		7.84		5.25		5.98	
mg	0.79		0.74		0.68		0.82		0.78	

n=number of analysis; standard deviations are given in the parenthesis; analyzed by M. JÁNOSI (ELTE Dept. of Petr. and Geochem.)

LÉT: Létrástető - The average of all analysis.

LUV: Lusta Valley - Composition of the core (a) and the rim (b) of a representative grain presented on the *Fig. 12*.

SZIS: Szinva Spring - a: Average core-composition of some clinopyroxenes. — b: Average composition of the non-zoned clinopyroxenes and the rim of the grains listed in file a.

	Variation plot	Spider	Th—Hf—Ta	Chem comps of clinopyroxenes
metabasalts				
		WPA—WPT	**WPA**	**ALKALINE**
Szinva Spring	———		slightly	slightly
Lusta Valley		TRANSITIONAL	slightly	slightly
Létrástető			stronger	stronger
metaandesites	OROGENIC	CONVERGENT	CONVERGENT	
metarhyolites	(La—Th)	PLATE MARGIN	PLATE MARGIN **CA**	———

Fig. 14. Summary of the magmatectonic setting determination for the Middle Triassic Eastern Bükk metamagmatites
WPA: within-plate alkaline, **WPT**: within-plate tholeiitic, **CA**: calc-alkaline character.

Despite the within-plate affinity of the Eastern Bükk metabasalts, they may have been formed even at a convergent plate margin following the formation of the calc-alkaline andesite-rhyolite magmatism, like in the volcanic assemblages found in Japan and in the Andes. However an independent continental rift-type formation for the Eastern Bükk metabasalts cannot be unambiguously excluded.

The study of genetical relationship between the older intermediate-acidic and the younger basaltic formations as well as the magma-generation in the Middle Triassic convergent plate area (Southern Alps—Outer Dinarides—Bükk Mts.) (e.g. BÉBIEN *et al.*, 1978) is in progress using further geochemical and geodynamical investigations.

ACKNOWLEDGEMENTS

The author wish to thank: SZ. HARANGI and CS. SZABÓ (Eötvös University) for fruitful discussions on the chemical and petrological data; Á. SZILÁGYI—PRITZ for the figures; M. JÁNOSI, J. NAGY BALOGH, L. HOFFMANN (Eötvös University), E. ÁRVA SÓS (ATOMKI, Debrecen) and ZS. MOLNÁR (Technical University, Budapest) for their readiness to help.

This work was supported by OTKA Nº3390313, a grant of Hungarian Academy of Sciences to prof. I. KUBOVICS.

REFERENCES

ÁRKAI P. (1973): Pumpellyite-prehnite-quartz facies Alpine metamorphism in the Middle Triassic volcanogenic-sedimentary sequence of the Bükk Mountains, Northeast Hungary. — Acta Geol. Acad. Sci. Hung. **17**, 67—83.

ÁRKAI P. (1983): Very low- and low grade Alpine regional metamorphism of the Paleozoic and Mesozoic formations of the Bükkium. — Acta Geol. Hung. **26(1—2)**, 83—101.

ÁRVÁNÉ SÓS E., BALOGH K., RAVASZNÉ BARANYAI L., RAVASZ CS. (1987): K/Ar dates of Mesozoic igneous rocks in some areas of Hungary. — (in Hungarian with English abstract) Annual Report of Hung. Geol. Inst. from 1985, pp. 295—307.

BALLA Z. (1984): The North Hungarian Mesozoic mafics and ultramafics. — Acta Geol. Hung. **27**, 341—357.

BALLA Z. (1987): Mesozoic tectonics of the Bükk Mountains (N Hungary) and relations to the West Carpathians and Dinarides. — (in Hungarian with English abstract) General Geological Review **22**, 13—54.

BALOGH K. (1964): Die geologischen Bildungen des Bükk-Gebirges. — Ann. Hung. Geol. Inst. **48(2)**, 555—705.
BALOGH K., KOZUR H., PELIKÁN P. (1984): Die Deckenstruktur des Bükk-Gebirges. — Geol. Paleont. Mitt. **13**, 89—96.
BÉBIEN J., BLANCHET R., CADET J. P., CHARVET J., CHOROWITZ J., LAPIERRE H., RAMPNOUX J. (1978): Le volcanisme Triasique des Dinarides en Yougoslavie: sa place dans l'evolution geotectonique Peri-Mediterraneenne. — Tectonophysics **47**, 159—176.
CASTELLARIN A., LUCCHINI F., ROSSI P. L., SIMBOLI G., BOSSELINI A., SOMMAVILLA E. (1980): Middle Triassic magmatism in Southern Alps, II. A geodynamic model. — Riv. Ital. Paleont. **85 (3-4)**, 1111—1124.
CROS P. and SZABÓ I. (1984): Comparison of the Triassic volcanogenic formations in Hungary and in the Alps — Paleogeographic criteria. — Acta Geol Hung. **27**, 256—276.
CSONTOS L. (1988): Étude géologique d'une portion des Carpathes internes: le massif du Bükk (NE de la Hongrie) (Stratigraphie, structures, métamorphisme et géodynamique) — Manuscript, PhD Thesis, Lille.
DERCOURT J., BIGNOT G., CROS P., DE WEVER P., GUERNET G., LACHKAR G., GEYSSANT J., LEPVRIER C., GÉCZY B. (1984): Hungarian Mountains in Alpine framework — Acta. Geol. Hung. **27(3-4)**, 213—221.
DOBOSI G. (1986): Clinopyroxene composition of some Mesozoic igneous rocks of Hungary: The possibility of identification of their magma type and tectonic setting. — Ofioliti, **11(1)**, 19—34.
EWART A. and LE MAITRE R. W: (1980): Some regional compositional differences within Tertiary-Recent orogenic magmas. — Chem Geol. **30**, 257—283.
GILL J. B. (1981): Orogenic Andesites and Plate Tectonics, Springer.
KÁZMÉR M. and KOVÁCS S. (1985): Permian-Paleogene paleogeography along the eastern part of the Insubric-Periadriatic lineament system: evidence for continental escape of the Bakony-Drauzug unit. — Acta Geol. Hung. **28(1-2)**, 71—84.
KOVÁCS S. (1982): Problems of the 'Pannonian Median Massif' and the plate tectonic concept. Contributions based on the distribution of Late Paleozoic — Early Mesozoic isopic zones. — Geol. Rundschau **71(2)**, 617—640.
KOVÁCS S. (1984): North Hungarian Triassic facies types: a review. — Acta Geol Hung. **27(3-4)**, 251—264.
KOVÁCS S. (1989): Major events of the tectono-sedimentary evolution of the North Hungarian Paleo-Mesozoic: History of the Northwestern termination of the Late Paleozoic - Early Mesozoic Thetys. — in.: SENGÖR A. M. C. (ed.): Tectonic evolution of the Tethyan Region. pp. 93—108. Amsterdam, Kluwer Acad. Publ.
KUBOVICS I., SZABÓ CS., HARANGI SZ., JÓZSA S. (1990): Petrology and petrochemistry of Mesozoic magmatic suites in Hungary and adjacent areas — an overview. — Acta Geod. Geoph. Mont. Hung. **25(3-4)**, 345—371.
LETERRIER J., MAURY R. C., THONON P., GIRARD D., MARCHAL M. (1982) Clinopyroxenes composition as a method of identification of the magmatic affinities of paleo-volcanic series. — Earth Planet. Sci. Let. **59**, 139—154.
NISBET E. G. and PEARCE J. A. (1977) Clinopyroxenes compositions in mafic lavas in different tectonic settings. — Contrib. Mineral. Petrol. **63**, 139—160
PAMIĆ J. (1984): Triassic Magmatism of the Dinarides in Yugoslavia — Tectonophysics, **109**, 273—307.
PANTÓ G. (1951): Geology of the southern igneous belt in the Eastern Part of the Bükk Mountains. — (in Hungarian with English Abstract) Bull. Hung. Geol. Soc. **81**, 137—145.
PANTÓ G. (1961): Le magmatisme mésozoique en Hongrie. — Ann. Hung. Geol. Inst. **49**, 979—995.
PISA G., CASTELLARIN A., LUCCHINI F., ROSSI P. L., SIMBOLI G., BOSSELINI A., SOMMAVILLA E. (1980): Middle Triassic magmatism in Southern Alps. — Riv. Ital. Paleont. **85 (3-4)**, 1093—1110.
SZENTPÉTERY ZS. (1923): Diósgyőr és Szarvaskő vidéke paleo és mezo-eruptívumainak földtani viszonyai. — (The Paleozoic and Mesozoic volcanics at Diósgyőr and Szarvaskő — in Hungarian) Annual Report of Hung. Royal Geol. Inst. from 1917-19, pp. 75—88.
SZENTPÉTERY ZS. (1929a): Gesteinstypen aus der Umgebung von Lillafüred. — Acta Chem. Min. Phys. Szeged, **1**, 10—43.
SZENTPÉTERY ZS. (1929b): Eruptivserie im Savóstale bei Lillafüred. — Acta Chem. Min. Phys. Szeged, **1**, 72—128.
SZENTPÉTERY ZS. (1931): A Bagoly-hegy quarzporphyrja Lillafürednél. — (Quartzpophyry of Bagoly Mt. at Lillafüred — in Hungarian) — Acta Chem. Min. Phys. Szeged, **II/2**, 81—150.
SZENTPÉTERY ZS. (1932): Neuere Beiträge zur Petrologie des Lillafüreder Savóstales. — Acta Chem. Min. Phys. Szeged, **2**, 24—46.
SZENTPÉTERY ZS. (1934a): Porphyritserie ober Hámor in der Bükkgebirge — Acta Chem. Min. Phys. Szeged, **3**, 149—181.

SZENTPÉTERY ZS. (1934b): Petrologische Verhältnisse des Fehérkőberges und die detaillierte Phsysiographie seiner Eruptivgesteine — Acta Chem. Min. Phys. Szeged, **4**, 18—123.
SZENTPÉTERY ZS. (1935a): A Fehérkő aljának eruptiv része Lillafürednél — (The volcanic part of Fehérkő Mt. at Lillafüred — in Hungarian) — Mat. Term. Tud. Ért. **52**, 253—286.
SZENTPÉTERY ZS. (1935b): Alkaliplagiophyrit aus dem Bükkgebirge — Acta Chem. Min. Phys. Szeged, **4**, 171—194.
SZENTPÉTERY ZS. (1936): A lillafüredi Szentistván-hegy eruptivumainak általános kőzettani viszonyairól. — (The petrography of Szentistván Mt. volcanics at Lillafüred — in Hungarian) — Mat. Term. Tud. Ért. **54**, 279—308.
SZENTPÉTERY ZS. (1937): Stratovulkanischer Teil des Szentistvánberges im Bükkgebirge — Acta Chem. Min. Phys. Szeged, **5**, 26—134.
SZENTPÉTERY ZS. (1939): Savanyú telérkőzetek a Bükkhegységből (Acidic dyke rocks in the Bükk Mts. — in Hungarian) — Acta Chem. Min. Phys. Szeged, **7**, 47—63.
SZENTPÉTERY ZS. (1950a): Adatok a bükkhegységi diabáz ismertetéséhez. — (New data to the knowledge of the Bükk diabases — in Hungarian) Bull. Hung. Geol. Soc. **LXXX/4—6**, 168—183.
SZENTPÉTERY ZS. (1950b): Az újhutai Lőrinc-hegy diabázfajtái a Bükk-hegységben. (The diabase types of the Lőrinc Mt. at Újhuta — in Hungarian) Bull. Hung. Geol. Soc. **LXXX/7—9**, 316—323.
WILSON M. (1989): Igneous petrogenesis. London, Hyman, 1989.
WOOD D. A. (1980): The application of a Th-Hf-Ta diagram to problems of tectonomagmatic classification and to establishing the nature of basaltic lavas of the British Tertiary volcanic province. — Earth Planet. Sci. Lett. **50**, 11—30.

Manuscript received, 15 November, 1990

Acta Mineralogica-Petrographica, Szeged, XXXI, 43—55, 1990

THE GENETICS (FORMATION) OF RHYOLITE OCCURRING IN THE RUDABÁNYA MTS. (NE HUNGARY) ON THE BASIS OF REE AND OTHER TRACE ELEMENTS

Z. MÁTHÉ*

Mecsek Ore Mining Co.

Gy. SZAKMÁNY**

Department of Petrology and Geochemistry, Eötvös Loránd University

ABSTRACT

The authors performed a genetical investigation on the rhyolite occurring in the Rudabánya Mts., previously studied from a mineralogical-petrographical aspect using data on rare earth element composition as well as other trace elements. Measurements were performed using neutron activation analysis completed by — in case of some elements — quantitative spectroscopical analysis. Based on the result of the measurements the rocks were assigned to four groups by the help of cluster analysis. On the basis of the relations of incompatible and less incompatible elements they could observe that the rhyolite was formed partly by a partial melting of the crust and partly by differentiation processes within the magma chamber. The considerable negative anomaly of Eu encountered is explained by fractionation of the plagioclase, i.e., this fact would equally support that the rock was formed from differentiated remnants of the melted rocks. The triangular diagram of Th-Ta-Hf/3 (which can be effectively used for acidic rocks as well) indicates that the formation of the rhyolite can be connected to the volcanism of a plate margin being consumed (subduction). The authors could observe in one sample an essential enrichment in U, Y and lanthanids caused by, according to their investigation, a considerably high fluor-apatite content.

INTRODUCTION

The regional distribution, mineralogical composition of the rhyolite occurring in the Rudabánya Mts. as well as its relation with the embedding rocks were studied in details by SZAKMÁNY *et al.* (1989). This rock can be traced on the surface as well as in several boreholes at a relatively small area in several spots. Its mineralogical composition includes dominantly resorbed — originally idiomorphic — quartz grains and albitized sanidine due to subsequent Na-metasomatism, as well as some plagioclase of albite-oligoclase composition. The mafic constituents are baueritized and/or chloritized biotite. As accessories we can find some zircon, apatite, magnetite and ilmenite in the rock. As secondary minerals we can find calcite, chlorite, sericite, clay minerals and haematite formed from the primary constituents. The original matrix of the rock must have been mainly vitreous, that subsequently crystallized and silicified.

* H—7633 Pécs, Esztárgár L. út 19, Hungary
** H—1088 Budapest, Múzeum krt. 4/a, Hungary

The rhyolite bodies are situated in slate dated by Radiolaria stratigraphy to Middle Jurassic period (GRILL and KOZUR 1986). In course of the analysis of the contact between the rhyolite and the slate it was proved that the rhyolite intruded the loose hardly consolidated sediments in the form of half-quenched lava, and it was — to some extent — mixed with the former.

In the present paper the results of a detailed genetical analyses of the rhyolite on the basis of REE and other trace elements distribution are discussed.

DETERMINATION OF THE REE AND SOME OTHER TRACE ELEMENT CONTENT

Rare earth elements (La, Ce, Nd, Sm, Eu, Tb, Tm, Yb, Lu) as well as the majority of other trace elements (U, Th, Hf, Ta, Sc, Rb, Cs) were measured by neutron activation analysis. The measurements were performed in the Nuclear Technical Institute of the Budapest Politechnical University by J. BÉRCZI. The irradiation of the samples took 2 hours and a GeLi detector was used for detection. Quantitative evaluation of the results was performed using Ru standard.

For the determination of the trace elements Zr, Nb, Y and Be a quantitative spectroscopical method was used. The measurements were performed in the Spectroscopical Laboratory of the Department of Petrology and Geochemistry of the Eötvös Loránd University by Mrs. NAGY. Experimental conditions for the measurements were: graphite electrodes, 1:1 mixture of the powder of the sample and powdered graphite, P alfa interior standard, direct arch current (8 A) for 1.5 minutes (till complete evaporation), detection by PGS-2 lattice spectrograph, 2nd order of spectra.

DISTRIBUTION OF REE AND OTHER TRACE ELEMENTS IN THE RHYOLITE

The REE and trace element composition of the rock samples analysed are presented in Table 1. REE data, normalized for chondrite are presented (in a grouping) on *Fig. 1.* using the most generally accepted norm values for chondrite proposed by HASKIN *et al.* (1968). The 17 samples analysed can be assigned into four groups and the average values of these four groups are presented on *Fig. 1.* Within the individual groups the measured values are very close to each other thus it is not necessary to present all the 17 individual measurements.

We can see on the diagram that the run-off curves for 3 groups are fairly similar, only group IV (comprising one sample only, marked 4R) shows different concentration values and the run-off for the curve is also different from the rest of the groups. The separation of sample 4R of group IV is also evident in case of cluster analysis and non-linear mapping procedures performed for 11 trace elements (La, Ce, Sm, Eu, Tb, Tm, Yb, Lu, U, Th, Sc) in 17 samples too (*Figs. 2, 3, 4* and Table 2). The cluster analysis and the nonlinear mapping was performed in the Hungarian Geological Survey by the help of L. O. KOVÁCS and P. G. KOVÁCS. Cluster analysis was made in two versions according to a weighted-pair group average and an unweighted average. The aim of applying different methods was to separate types within the rhyolite on the basis of trace element composition. As a result of the statistical analysis, four well separated units could be established on *Figs. 2, 3* and *4.* Especially remarkable here the unique character of sample 4R, representing group IV.

Table 2 gives a comprehensive account on the location of the samples. It is observable that all outcrops yielded samples for each groups proving that the rock

TABLE 1.

REE and other trace element content of the rhyolyte samples in the Rudabánya Mts (ppm).
For location of the samples, see Table 2.

	La	Ce	Nd	Sm	Eu	Tb	Tm	Yb	Lu	U	Th	Hf	Ta	Rb	Cs	Sc	Y	Nb	Be	Zr
2R	18	38	33	10	0.24	2.0	1.0	4.5	n.a.	6.7	20	4.3	2.2	166	n.a.	3.3	50	16	6	130
3R	19	43	n.a.	9.0	0.23	1.5	0.8	3.6	0.54	2.9	19	3.8	1.8	120	n.a.	3.0	60	20	10	160
4R	83	215	n.a.	39	0.93	9.4	5.5	33	6.5	155	4.7	1.1	0.7	n.a.	n.a.	1.0	600	40	5	150
5R	27	64	40	13	0.55	2.3	1.3	5.8	0.85	6.6	25	4.7	1.8	153	n.a.	2.7	100	20	10	200
6R	37	76	48	21	0.66	3.0	1.2	5.8	0.91	4.4	24	4.9	1.8	176	n.a.	4.0	60	<16	6	160
7R	21	41	n.a.	9.5	0.20	1.5	0.9	3.2	0.5	3.3	19	4.1	1.7	n.a.	n.a.	2.8	60	16	4	160
8R	11	27	n.a.	6.1	0.15	1.3	0.8	3.2	0.51	2.3	15	3.4	1.2	n.a.	n.a.	2.6	n.a.	n.a.	n.a.	n.a.
10R	29	63	41	12	0.29	1.8	0.6	3.6	0.61	4.2	24	5.1	2.1	n.a.	n.a.	3.5	40	<16	10	160
11R	10	23	n.a.	5.1	0.08	1.0	0.6	2.7	0.47	6.6	13	2.5	1.3	80	n.a.	1.9	60	<16	4	130
13R	16	28	n.a.	6.9	0.15	1.2	0.8	3.0	0.44	3.2	26	2.6	1.4	2.7	66	n.a.	60	16	7	160
14R	9.8	22	n.a.	6.4	0.07	1.1	0.9	3.2	0.49	9.5	13	2.7	1.7	2.3	103	n.a.	25	<16	n.a.	100
15R	14	26	n.a.	6.8	0.11	1.6	1.1	4.9	0.82	13	13	2.6	n.a.	2.3	205	n.a.	40	<16	n.a.	100
16R	35	76	68	14	0.37	2.6	1.4	3.8	0.6	3.8	26	6.0	1.6	3.8	88	3.4	25	<16	10	250
18R	10	31	22	6.0	0.08	1.4	1.0	3.0	0.44	1.8	14	2.7	1.5	2.1	53	4.4	60	20	14	160
19R	10	23	n.a.	5.9	n.a.	1.4	0.9	2.5	0.37	1.8	14	3.0	1.6	2.4	66	4.1	25	<16	10	100
20R	15	34	n.a.	14	0.21	1.4	1.4	5.4	1.0	15	11	2.1	1.1	1.7	41	2.8	60	16	8	100
21R	8.8	22	n.a.	5.7	n.a.	1.1	1.1	2.7	0.42	2.5	14	3.2	1.6	2.2	81	4.5	10	<16	n.a.	60
22R	15	33	37	9.5	0.32	1.6	1.6	4.4	0.42	2.5	18	3.7	1.7	2.6	119	5.2	40	16	10	160
23R	23	47	51	11	0.46	1.9	1.3	3.1	0.48	4.8	19	4.0	1.6	62	2.5	2.5	n.a.	n.a.	n.a.	n.a.

n.a.: not analysed
Analysis performed by J. BÉRCZI at the Nuclear Technical Laboratory of the Budapest Polytechnical Institute
(REE, Th, U, Ta, Hf, Sc, Rb, Cs) by NAA, and Mrs. B. NAGY, Petrological-Geochemical Department (Nb, Z, Be, Zr) by OES

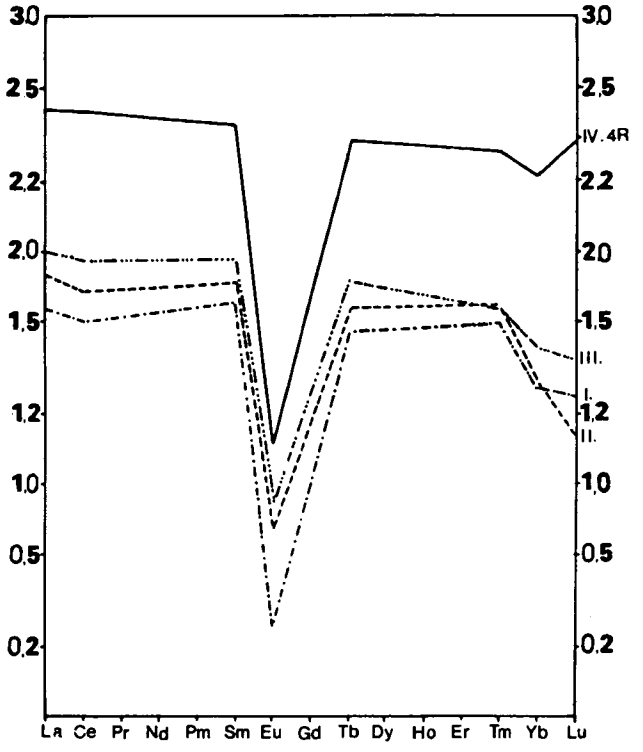

Fig. 1. Mean values normed to chondrite (after HASKIN *et al.* 1968) for the four groups formed on the basis of the REE content of rhyolites occurring in the Rudabánya Mts. For the location of the samples, see Table 2.

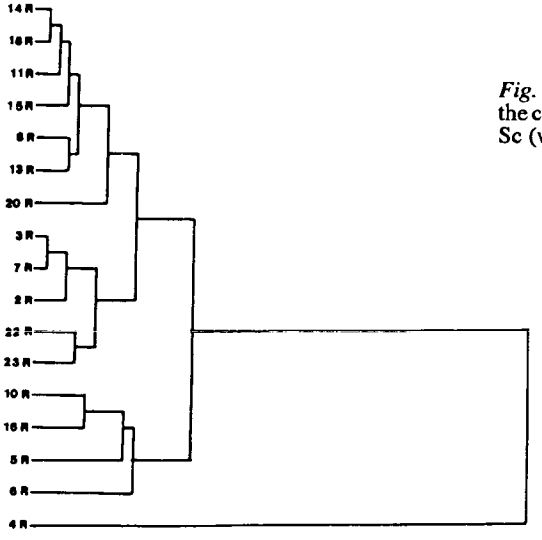

Fig. 2. Result of the cluster analysis using the concentration values of REE, U, Th and Sc (weighted-pair group average).

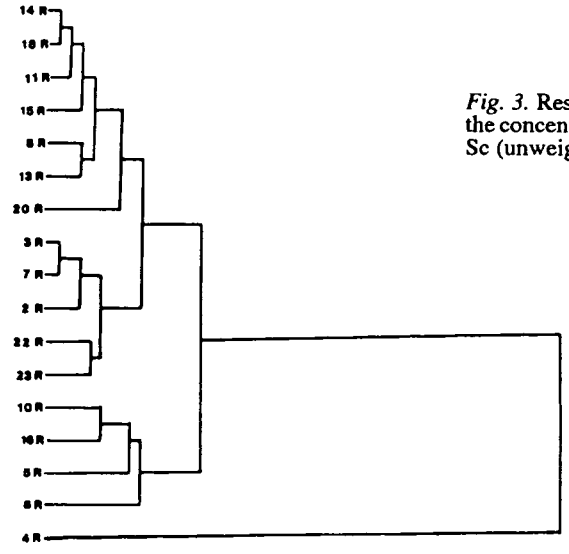

Fig. 3. Result of the cluster analysis using the concentration values of REE, U, Th and Sc (unweighted average).

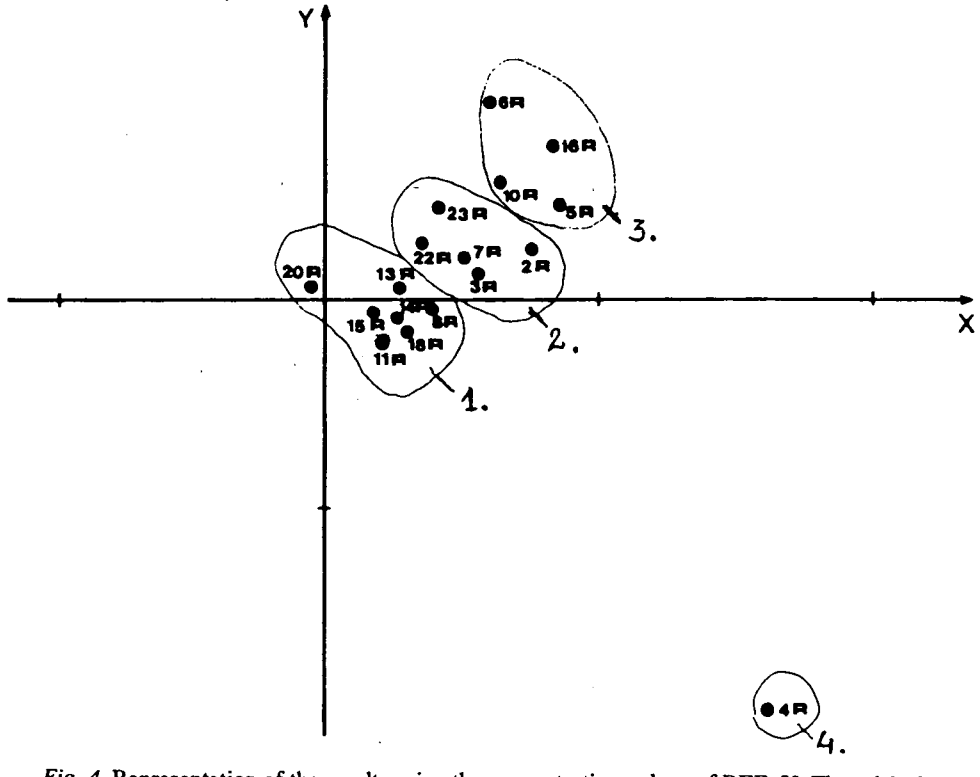

Fig. 4. Representation of the results using the concentration values of REE, U, Th and Sc by non-linear mapping method

bodies separated on the area belong for one lithological unit and reached their recent position due to posterior tectonic events. Vertically, we can observe some differences within the rhyolite; the trace element composition can help us to separate different levels within the rhyolite body. Sample 4R assigned to group IV is distinctly different from the samples of the other three groups, therefore it was analyzed in details at a later stage.

TABLE 2.

Groups formed by cluster analysis and the location of the samples

Group 1.	14R — hill slope to the NW of Vadászháza
	18R — S foothills of the plateau Balázstető
	11R — Borehole Sz-10 at 31.8 m
	15R — hill slope to the NW of Vadászháza
	8R — SW side of the outcrop lying to the SE of Vadászháza
	13R — outcrop lying to the SE of Vadászháza
	20R — Dunnatető
Group 2.	3R — Borehole Sz-10 at 55.8 m
	7R — NE side of the outcrop lying to the SE of Vadászháza, close to the contact with the slate
	2R — Borehole Sz-10 at 66.0 m, on the rhyolitic side of the contact zone
	22R — Borehole Sz-10 at 121.7 m, on the rhyolitic side of the contact
	23R — on the rhyolitic side of the contact zone at the outcrop to the SE of Vadászháza
Group 3.	10R — silicified rhyolite, outcrop lying to the SE of Vadászháza
	16R — hill slope to the NW of Vadászháza
	5R — Borehole Sz-10 at 121.8 m, on the rhyolitic side of the contact
	6R — outcrop lying to the SE of Vadászháza
Group 4.	4R — Borehole Sz-10 at 44.5 m

GENETICAL CONCLUSIONS

The groups separated on the basis of analytical data are genetically related as proved by the stable ratio of incompatible elements (*Fig. 5.*, see TREUIL *et al.* 1977). The separation of the genetically related groups can be explained by means of another diagram (*Fig. 6.*), following the data on a considerably incompatible (Th) and a less incompatible (Tb) element within the rock sequence. On one axis, the ratio of the two elements are plotted against the concentration of the more incompatible element on the other axis. We can observe on the diagram that members of the sequence formed by partial melting are dispersed along a line of general position, while those of fractional crystallization along a line described by the following equation:

$$\frac{Th}{Tb} = \text{constant}$$

We can see on *Fig. 6.* that one part of the rhyolite in the Rudabánya Mts. was formed by partial melting of the crust (groups 1., 2. on Table 2 except for samples

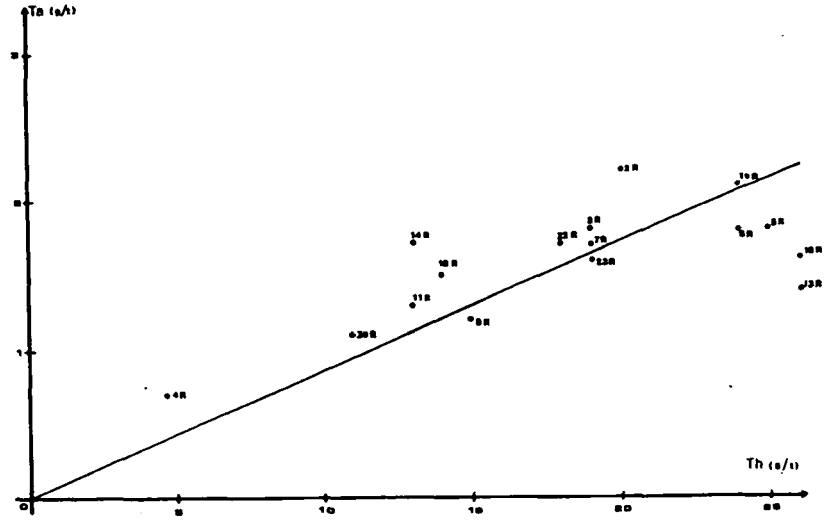

Fig. 5. The Th-Ta diagram of the rhyolites occurring in the Rudabánya Mts, (based on the method of TREUIL *et al.* 1977)

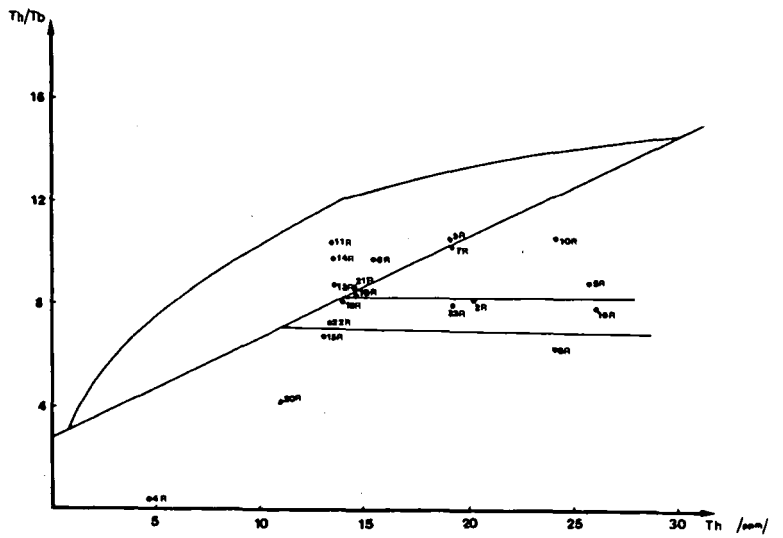

Fig. 6. The Th/Tb-Ta diagram of the rhyolites occurring in the Rudabánya Mts. (based on the method of TREUIL *et al.* 1977)

2R and 23R). Trace element concentration in these samples is generally very low. In case of another part of the samples (group 3. in Table 2), the values are scattered along the line Th/Tb = constant, that is these rocks were formed as a result of differentiation processes within the magma chamber. Highest concentration of trace element (REE, Sc, Ta, Th, Hf) were found in these samples, (see Table 1).

In course of the evaluation of the REE analytical results, we found a considerable Eu-anomaly in the rock (*Fig. 1*).

Europium can occur in the rock in two forms, namely as Eu^{2+} and Eu^{3+}. Data published by WEIL and DRAKE (1973) as well as GERASIMOVSKY *et al.* (1976) suggest that in course of the cryistallization of magmatic melts, REE are seemingly accumulated in minerals rich in Ca (mainly, plagioclase) where they can subsitute Ca in an isomorphic way. This can even be furthered by Na occurring in the melt, by following way:

$$REE^{3+}\ Na^{+} \xrightarrow{\text{Isomorphic substitution}} 2\ Ca^{2+}$$

It is generally stressed that the formation of Eu-anomaly is basically related to crystallization of plagioclase. According to WEIL and DRAKE (1973) the distribution of Eu^{2+} and Eu^{3+} between the plagioclase (S) and the melt (L) can take place according to the following reaction:

$$Eu^{2+}O\ (L) + SiO_2\ (L) + Eu^{3+}Al_3SiO_8\ (S) \rightleftharpoons Eu^{2+}Al_2Si_2O_8\ (S) + Eu^{3+}O_{1.5}\ (L)$$

$$+ AlO_{1.5}\ (S)$$

This is one of the possible ways describing the Eu^{2+}—Eu^{3+} distribution behaviour in the plagioclase — melt system. On the basis of crystal chemistry of feldspars it is presumable that Eu^{2+} is preferred in place of large cations in the feldspar structure than Eu^{3+}. That is, Eu^{2+} can substitute Ca in the plagioclase. The model propesed by WEIL and DRAKE (1973) as well as practical observations show that negative Eu anomaly tends to increase in the plagioclase by the increase of Na or the decrease of Ca concentration, that is, we have a strong positive correlation between the negative Eu anomaly and the albite content of the plagioclase.

WEIL and DRAKE (1973) emphasized that the extent of Eu-anomaly is considerably related to the oxidation potentials of the magma during crystallization. For the formation of a substantial amount of Eu^{2+}, a suitable reductive medium is needed, i.e., the Eu-anomaly hints at the oxidation-reduction relations of the environment during rock formation. In other words, the greater the negative Eu-anomaly, the crystallizing medium was possibly more reductive.

The presence of a negative or positive Eu-anomaly as well as the lack of this phenomenon has a litho-genetical significance. Basaltic magmas of primary /mantle/ origin have no Eu-anomaly, therefore wherever we find this phenomenon in a rock we can suppose certain differentiation processes in course of it's formation. FREY *et al.* (1984) and GERASIMOVSKY *et al.* (1976) considered — on the basis of rock sequences ranging from basalt to rhyolite — a negative Eu-anomaly of rhyolites as a sign of plagioclase fractionation. While plagioclase is present as a fractionating phase, it has a distinguished (favourable) position, in respect of the uptake of Eu compared to other REE. In the plagioclase feldspars of early crystallization Eu is selectively enriched, therefore its relative quantity is essentially decreased in the residual melt.

The extremely high negative Eu-anomaly of rhyolites in the Rudabánya Mts. proves that the rock must have originated by the crystallization of a residual melt. Plagioclase as the dominant mineral for the enrichment of Eu was already separated from the system (that is, the fraction rich in plagioclase had already been crystallized previously). During the crystallization of the rhyolite the environment was reductive, marked by the relatively larger quantity of Eu^{2+} substituting the Ca in the crystal lattice of the plagioclase.

Previous studies SZAKMÁNY *et al.* (1989) demonstrated that there is only a very small amount of primary plagioclase (albite, oligoclase) present in the rock. This has been corroborated by chemical analyses as well. Secondary albitization is basically proved by the very low CaO content and the relatively high amount of Na_2O. CaO is more abundant in those rocks only, where a considerable amount of calcite appeared due to secondary processes.

Another apparent feature of the REE analyses is the small enrichment of heavy lanthanids (*Fig. 1*). According to FLEISCHER (1965) these elements are mainly enriched in granate, zircon, apatite and xenotim. WATSON (1980) investigated the role of zircon in the enrichment of lanthanids by means of crystallization experiments from melts. He could determine experimentally a distribution coefficient (D) for zircon / melt for the different rare earth elements and found that for the heavy lanthanids, the value of D was higher; that is, zircon enriched heavy REE more that the light ones. Zircon is relatively frequently found in the rhyolite of the Rudabánya Mts. At the same time the samples contained a considerable amount of fluor-apatite as well (in some samples, especially in 4R, in essential quantities as treated in details below). Consequently, the heavy REE encountered are concentrated mainly in these two minerals.

The triangular diagram containing the values Th-Ta-Hf/3 was applied first by WOOD *et al.* (1979). The basic advantage of the diagram compared to previous similar ones is, that — apart from the distinction of basic rocks — it can be effectively used for the separation of acidic rocks of different genesis as well. More precisely, acidic rocks of calc-alkaline and crustal origin can be separated from pure (uncontaminated) acid rocks produced as a result of fractional crystallinization (as well as from E-type ridge basalts and intra-plate basalts, too). Another advantage of the diagram, and the reason of its applicability to acidic rocks is based on the fact that the points representing the individual acidic magmas are situated near to the relevant points of those basic melts from that they were derived through differentiation processes.

During fractional crystallization the Th content of the residual melt is relatively enriched, i.e, points tend to shift within the triangular diagram towards the apex of Th. The reason for this can be found in the fact that oxides of Fe and Ti, notably clinopyroxene and other minerals (where Hf and Ta are accumulated typically better that Th) appear among the first solid phases in acidic and intermediate magmas. The increase of the ratios of Th/Hf, Th/Ta etc. in the residual melts, however, do not obscure their relation with the original basaltic melt.

Presenting the analytical data on the rhyolites of the Rudabánya Mts. in a Th-Ta-Hf/3 diagram (*Fig. 7*), the points range into field D and its immediate

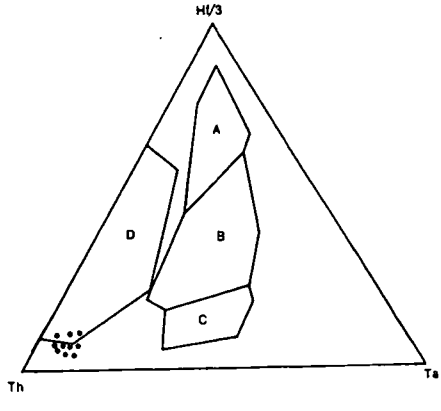

Fig. 7. The Th-Ta-Hf/3 triangular diagram of the rhyolites occurring in the Rudabánya Mts. (based on the method of TREUIL *et al.* 1977):
A: N-type ridge basalt
B: E-type ridge basalt
C: intra-plate basalt
D: consummated plate margin (subduction)

surroundings. Accordingly, the rhyolite can be connected to the volcanism of a consummated plate margin (subduction), that is a typical calc-alkaline formation.The points are very far from field C, which represents intra-plate basalts and their derivatives.

The results obtained agree well with the geological model set on the formation of the mountains and its geohistory by GRILL *et al.* (1984). RÉTI (1987) could prove the presence of an ophiolite sequence within the mountain. According to the geological model the oceanic crust was formed here in the Middle Triassic. The most active phase of the spreading could be supposed for the Ladinian-Karnian period. By the Norian stage spreading got much slower (possibly stopped) because the Hallstatt and Pötschen type limestones — denoting a sedimentary basin in state of equilibrium — are found in large areas. The authors suppose the subduction of the oceanic crust, proceeding from South to North, by the Jurassic as well as the consequent volcanic activity along the consummated plate margin.

The age of the slate embedding the rhyolite was determined by the help of Radiolaria analyses as Middle Jurassic (GRILL and KOZUR 1986). Analysing the contact zone between the rhyolite and the slate SZAKMÁNY *et al.* (1989) could detect a thermal contact, thus the age of the rhyolite can be fixed to Middle Jurassic as well, corroborating the evolution scheme outlined above.

EVALUATION OF THE ANOMALIC TRACE-ELEMENT CONTENT OF SAMPLE 4R

Studying Table 1 as well as *Figs. 1—4* carefully, we are immediately faced with the different character of the rhyolite sample marked 4R (borehole Szalonna—10, sample taken at 44.5 m). In this sample, the concentration of light lanthanids is 3—4 times, and that of heavy lanthanids as well as Y about 10 times more than in the rest of the samples. Enrichment of U in the sample is also considerable (155 g/t) while the concentration of Th and Hf is decreased to third-quarter of the quantity observed in the other samples. It is worth to note that the quantity of Zr is not considerably decreased, that is, the geochemically strongly related Zr and Hf are detached from each other. This is possibly rooted in the fact that the bulk of zirconium in this sample is stored not in the zircon but other minerals (this was supported by microscopic analysis of the sample where zircon was found in very small quantities).

For tracing the reason of the essential enrichment of REE, Y and U, we performed a more detailed analysis using X-ray diffraction and electron microprobe analysis as well. In course of evaluating the thin section obtained from the sample it was found that the sample contains an essential amount of apatite, present as accessory mineral, in the other rhyolite samples as well (*Fig. 8*).

For a more detailed analysis, the apatite was enriched by separating heavy minerals and the remnants were used for X-ray diffraction analysis. The evaluation of the X-ray diffractogram could unambiguously prove that this mineral is fluorapatite. This is also supported by the chemical analysis of the sample (high phosphorous and fluorine content, Table 3). (The result of the chemical analysis was rendered to our disposal by Prof. J. KISS). We can suppose that this mineral is the host for the great amount of REE, Y, and U found by trace element analysis. The role of apatite in REE enrichment is uniformly stressed by literature as well (FLEISCHER 1965, HENDERSON 1984). Rare eart elements seemingly show special affinity to fluorine as proved by BALASOV (1976) (in PANTO 1980). REE-fluorides, -phospates and -carbonates are relatively ill-soluble compounds, and this fact can also explain the role of apatite in the enrichment of REE.

TABLE 3.

Chemical composition of the rhyolite sample marked 4R.

SiO_2	52.40 %
TiO_2	0.05 %
Al_2O_3	4.40 %
Fe_2O_3	0.77 %
FeO	0.78 %
MnO	0.04 %
MgO	1.60 %
CaO	19.30 %
Na_2O	1.30 %
K_2O	0.27 %
P_2O_5	12.40 %
$-H_2O$	1.20 %
$+H_2O$	2.40 %
CO_2	2.30 %
F	0.96 %
$(RFF)_2O_3$	0.08 %
	100.45 %

The analysis was performed at the analytical laboratory of the MÉV.

Electron probe microanalysis of the sample has shown — apart from apatite — some traces of monacite as well which is also well known as a mineral important in the accumulation of REE, Y and U (*Figs. 9—12*).

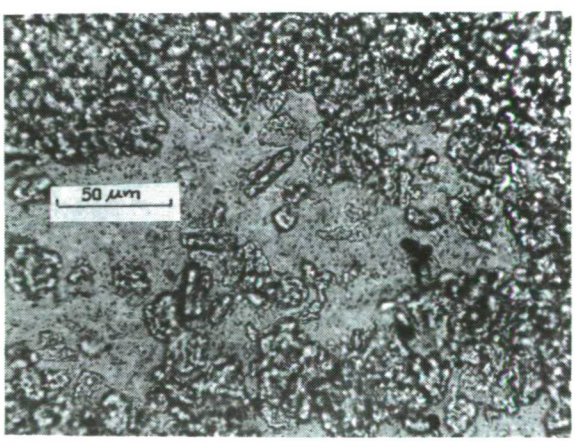

Fig. 8. Crystals of apatite in the rhyolite sample 4R (borehole Sz—10 at 44.5 m, 1N, scale 300x)

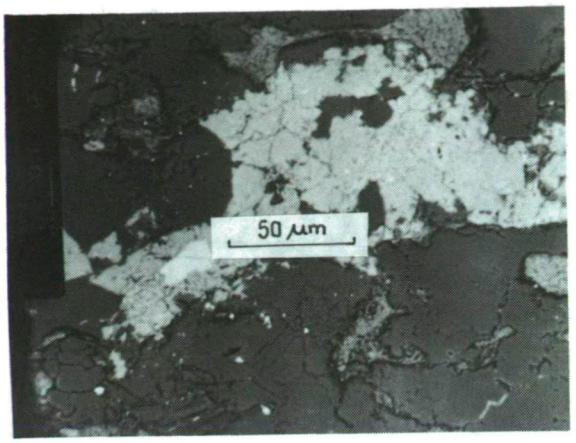

Fig. 9. Composition electron micrograph on apatite (a) and monacite (b) from sample 4R, scale 315x

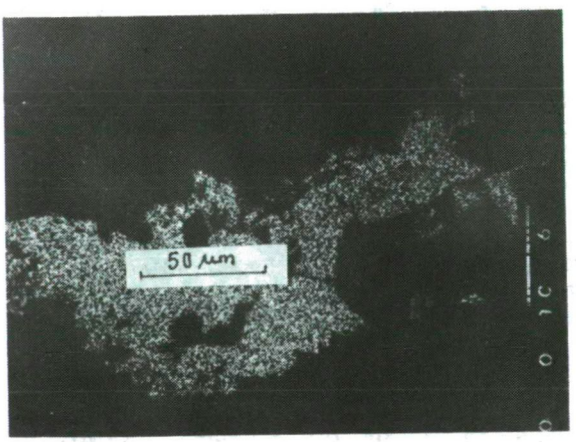

Fig. 10. P distribution on the area presented on *Fig. 9.* K_α (scale 315x)

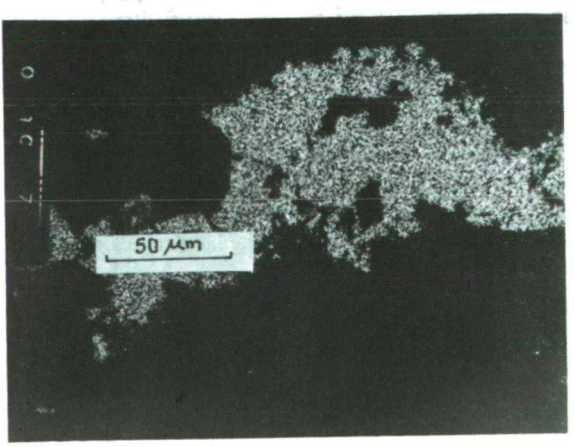

Fig. 11. Ca distribution on the area presented on *Fig 9.* K_α (scale 315x)

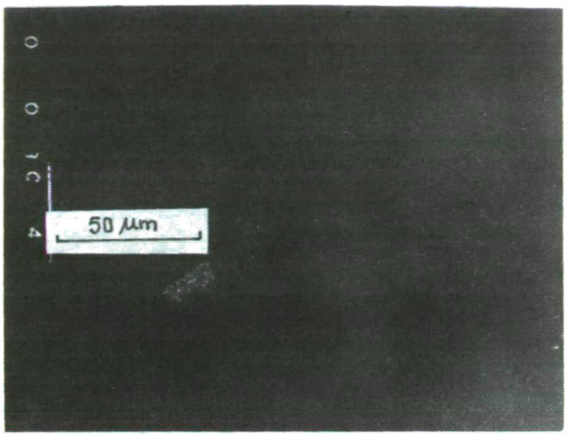

Fig. 12. Ce distribution on the area presented on *Fig. 9.* K_α (scale 315x)

SUMMARY

On the basis of trace element analysis of the rhyolite occurring in the Rudabánya Mts. we can deduce the following genetical conclusions:

— According to the diagram introduced by WOOD *et al.* (1979) the rock can be considered as the product of a volcanism in consummated plate margin (subduction zone).
— The rhyolite was formed, following the partial melting of the crust during differentiation processes. This fact is corroborated by the points fitting to relevant places on the diagrams presented by TREUIL *et al.* (1977) as well as by the considerable Eu-anomaly.
— At a certain level of the rock, a considerable enrichement of REE, Y and U was encountered.
— Results of the geochemical interpretation seem to fit well to the geological model and evolutionary scheme proposed by GRILL *et al.* (1984).

A more detailed view on the genetics of the rock, notably, the original composition of the primary melt and its evolution can be expected from further detailed studies. First of all other differentiation products of the melt (basic-neutral rocks) should be spotted within the mountain as well as its surroundings. Considering the nappe structure of the region this may not be an easy task because these units can now be several hundred kilometres far from each other due to considerable lateral movements.

REFERENCES

FLEISCHER, M. (1965): Some aspects of the geochemistry of yttrium and the lanthanides. Geochim. Cosmochim. Acta. **29,** 755—772.

FREY, F. A., GERLACH, D. C., HICKEY, R. L., LOPEZ-ESCOBAR, L., MUNIZAGA-VILLAVICENCIO, F. (1984): Petrogenesis of the Laguna del Maule volcanic complex Chile (36°S)— Contrib. Miner. Petrol. **88,** 133—149.

GERASIMOVSKY, V. I., BALASHOV, Ju. A., KARPUSHINA, V. A., SHEVALEESKY, I. D. (1976): Geochemistry of rare earths in effusive rocks of Iceland. Geokhimija. **8,** 1176—1188. (in Russian with English abstract)

GRILL, J. KOVÁCS, S., LESS, GY., RÉTI, ZS., RÓTH, L., SZENTPÉTERI, L. (1984): Az Aggtelek-Rudabányai-hegység földtani felépítése és fejlődéstörténete.(Geological constitution and history of evolution of the Aggtelek-Rudabánya Range). Földt. Kutatás. **XXVII. 4**, 49—56. (in Hungarian with English abstract).

GRILL, J., KOZUR, H. (1986): The first evidence of the Unuma echinatus Radiolarian zone in the Rudabánya Mts. (Northern Hungary). Geol. Paläont. Mitt. Innsbruck. **13**, 239—275.

HASKIN, L. A., HASKIN, M. A., FREY, F. A., WILDEMAN, T. R. (1968): Relative and absolute terrestrial abundances of the Rare Earths. In: Origin and Distribution of the Elements. L. AHRENS, ed., Pergamon Press Oxford. Int. Ser. Mon. Earth Sci. **30**, 889—912.

HENDERSON, P. (ed) (1984): Rare Earth element geochemistry. Elsevier Amsterdam, Oxford, New York, Tokyo.

PANTÓ, GY. (1980): Ritkaföldfémek geokémiája és néhány alkalmazási területe (The geochemsitry of Rare Earth Elements and the field of it's application). Thesis of D. Sc degree. Budapest (in Hungarian)

RÉTI, ZS. (1987): A Bódva-völgy bázisos-ultrabázisos kőzeteinek eredete és hegyszerkezeti helyzete /Ophiolite fragment is an evaporitic melange near Bódva valley (North Hungary) Földt. Közl. **117**, 47—59. (in Hungarian with English abstract)

SZAKMÁNY, GY., MÁTHÉ, Z., RÉTI, ZS. (1989): The position and petrochemistry of the rhyolite in the Rudabánya Mts. (NE Hungary). Acta Mineralogica-Petrographica, Szeged, XXX, 81—92.

TREUIL, M., JORON, J. L., JAFFREZIC, H. (1977): Trace element geochemistry of magmatic rock series of converning and diverging plate boundaries. Journal of Radioanalytical Chemistry. **38**, 351—362.

WATSON, E. B. (1980): Some experimentally determined zircon/liquid partition coefficients for the Rare Earth Elements. Geochim. Cosmochim Acta. **44**, 895—897.

WEILL, D. F., DRAKE, M. J. (1973): European anomaly in plagioclase felspar: experimental results and semiquantitative model. Science. **180**, 1059—1060.

WOOD, D. A., JORON, J. L., TREUIL, M. (1979): A RE-appraisal of the use of trace elements to classify and discriminate between magma series erupted in different tectonic settings. Earth Planet. Sci. Lett. **43**, 326—336.

Manuscript received, 2 August, 1990

Acta Mineralogica-Petrographica, Szeged, XXXI, 57—65, 1990

AN APPARATUS FOR SIMULTANEOUS THERMAL ANALYSIS AND ITS APPLICATION IN GEOLOGICAL RESEARCH

G. SZÖŐR*

L. Kossuth University, Department of Mineralogy and Geology

ABSTRACT

Combination of a home-made thermoanalytical device (Derivatograph, MOM) and a quadrupole mass spectrometer (QMS-D, ATOMKI) is presented, and the simultaneous thermoanalytical method (DTA, DTG, TG, QMS-EGA) has been successfully applied in many fields of mineralogy, petrology, geochemistry and chemostratigraphy.

In Hungary, positive experience has been obtained in the following fields:

— determination of rare mineral in the Carpathian Basin.
— Diagenetic and hydrothermal processes and facies were characterized by distinguished mineral associations in Hungary and Cuba.
— Geological dating by investigations of sporadic finds (bones) of Neogene vertebrates.

INTRODUCTION

The most important information on various evolved gas analytic methods, such as mass spectrometry, gas chromatography, infra-red absorption, selective sorption and thermogas titrimetry will be found in the books and in the well-known journals and monographs. The Proceedings of the ICTA and ESTA provide an up-to-date picture of the stage of development of MS and GC-MS coupling system and their applications (e.g. BRACEWELL and ROBERTSON 1980; FRIPIAT 1982; MORGAN 1977; MÜLLER—VONMOOS and MÜLLER 1974; PAULIK and PAULIK 1981; SZÉKELY *et al.* 1980; WARNE *et al.* 1985).

The new method was used parallelly with thermogas titrimetry (TGT) and IR, GC, X-ray analyses to determine composition of the inorganic and organic compounds, minerals, rocks, building and raw materials, and has been successfully applied in many fields of chemistry and geochemistry (DÉVAI *et al.* 1984; KOZÁK *et al.* 1985; SZÖŐR *et al.* 1984; SZÖŐR and BOHÁTKA 1985; SZÖŐR and BALÁZS 1988).

A few examples demonstrate that simultaneous technique is very helpful and it is basic method for wide area of experience.

* H—4010 Debrecen, P.O.Box. 4. Hungary

A home-made quadrupole mass spectometer (BERECZ *et al.* 1983) has been coupled to the Derivatograph and got a versatile instrument promising the possibility of a fast, sensitive evolved gas analysis (*Fig. 1.*).

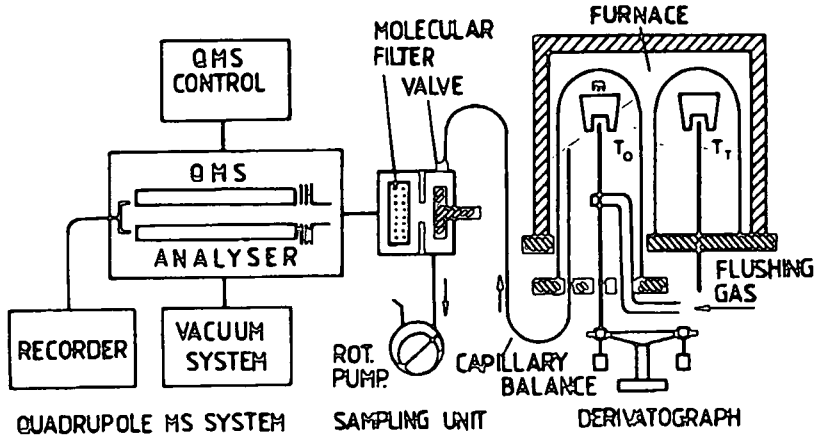

Fig. 1. Schematic drawing of the Derivatograph (MOM) and QMS-D (ATOMKI) system

The quadrupole mass spectrometer has a mass range of 1-300 a.m.u. and a sensitivity of $4 \cdot 10^{-4}$ A/mbar with Faraday cup. It is mounted on a bakeable high vacuum system consisting of a liquid nitrogen cooled refrigerator, water cooled oil trap and oil diffusion pump. Ultimate pressure is less than $1 \cdot 10^{-8}$ mbar without baking. Gases are pumped from the reaction chamber through a 1.2 m long capillary and a small portion of the sample is introduced into the quadrupole via a molecular filter at the low-pressure end of the capillary. The tip of capillary is 2 cm below the sample holder. The coupling unit can be heated up to 200 °C, its gas consumption is about 0.5 cm^3/s, response time is 50 ms but this latter is not exploited because of the large volume of the reaction chamber (~50 cm^3).

The response time of the whole coupled system is 20 s at 3 cm^3/s air flow rate. This is satisfactory as the fastest heating program of the Derivatograph is 20 °C/min. Sensitivity: during the thermoanalysis is 1 mg $Ca(COO)_2 \cdot H_2O$, the signal at the output of the quadrupole is 50 times higher than the noise amplitude. The volatile components are identified on the basis of the complete mass-spectra, while the changes in each component of given mass are monitored as a function of temperature with the aid if a peak selector.

The measurements were performed under the following conditions: temperature range 1000 °C; rate of heating: 10 °C /minute in helium or air current; sample holder: platinum or ceramic crucibles.

The interpretation of calcium oxalate monohydrate (whewellite) an example of our first investigations (*Fig. 2*).

The decomposition processes take places as follow in helium atmosphere.

$$Ca(COO)_2 \cdot H_2O = Ca(COO)_2 + H_2O \quad 210\ °C \quad (1)$$

$$Ca(COO)_2 = CaCO_3 + CO \quad 510\ °C \quad (2)$$

$$2CO = CO_2 + C$$
$$CaCO_3 = CaO + CO_2 \qquad 820\ ^\circ C \qquad (3)$$
$$CaCO_3 + C = CaO + 2\ CO$$

The processes are different in air atmosphere.

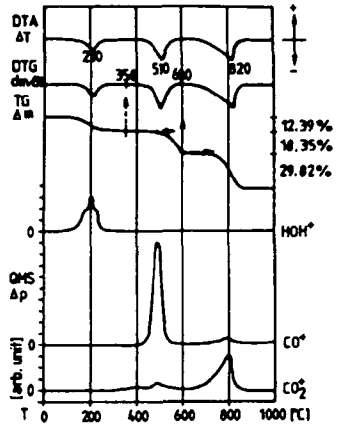

Fig. 2. The thermal decomposition of whewellite

RESULTS AND DISCUSSIONS

The examples reported in this paper demonstrate that simultaneous technique is a very helpful means in the characterization of geological materials.

Mellite, hydrate aluminium mellate, $Al_2[C_{12}O_{12}] \cdot 18$ or 16 (?) H_2O is a very rare mineral, it is unique in the Carpathian Basin (Csordakút, Hungary). The crystal water content of mellite was controversial up to the present. The *Fig. 3.* shows the loss of water in the first endothermic process, it is 39.73 %, ~16 moles in the formula (SZÖÖR and BOHÁTKA 1985).

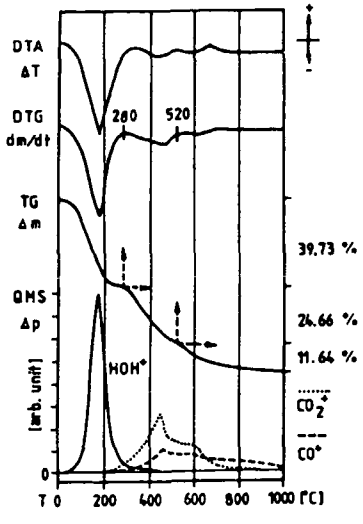

Fig. 3. The thermal decomposition of mellite

A Lower Pannonian (Miocene) gravel complex is cemented by marcasite deposited by low temperature hydrothermal activity (VICZIÁN *et al.* 1986). In this locality the light yellow incrustration on the weathered rock surface were hydrous iron sulphate minerals. The X-ray diffraction indicated the minerals as copiapite, $(Fe^{2+},Mg)Fe_4^{3+}[(OH)(SO_4)_3]_2 \cdot 20H_2O$ and rhomboclase, $Fe^{3+}H[SO_4]_2 \cdot 4H_2O$. The combined thermoanalytical investigations showed H_2O and SO_2 as main components, minor amounts of S and CO_2 indicated impurities in the evolved gases (*Fig. 4.*).

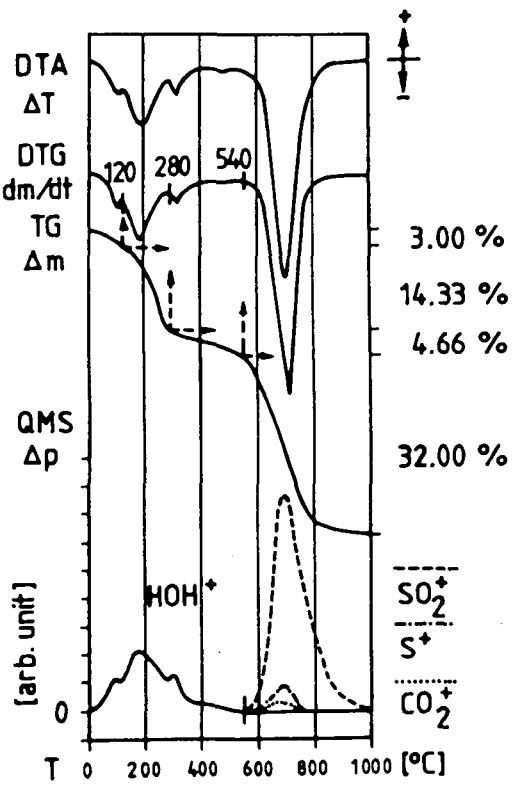

Fig. 4. The thermal decomposition of mixture copiapite and rhomboclase

The percentages of the hydrous sulphate minerals are copiapite: 54 percent, rhomboclase: 23 percent as computed considering the weight loss of H_2O and SO_3 from the total sample. The remaining 23 percent is mainly amorphous SiO_2.

This method was used to determine silicate, carbonate, hydroxide mineral paragenesis of ultramafic rocks (peridotite, serpentinite). According to the water and carbon dioxide detected to antigorite, chrysotile, brucite and magnezito-calcite were identified (*Fig. 5.*).

The mass spectrometry combined with Derivatograph can reveal the presence of various carbonates, sulphates, clay minerals in raw and building materials. *Fig. 6.* shows two typical examples.

At the foreground of North Borsod Karst, Hungary, there are some shallow boreholes, which have organic material bearing layers in the Upper Pannonian ingression lagoon sediments. Two characteristic diagenetic processes and facies

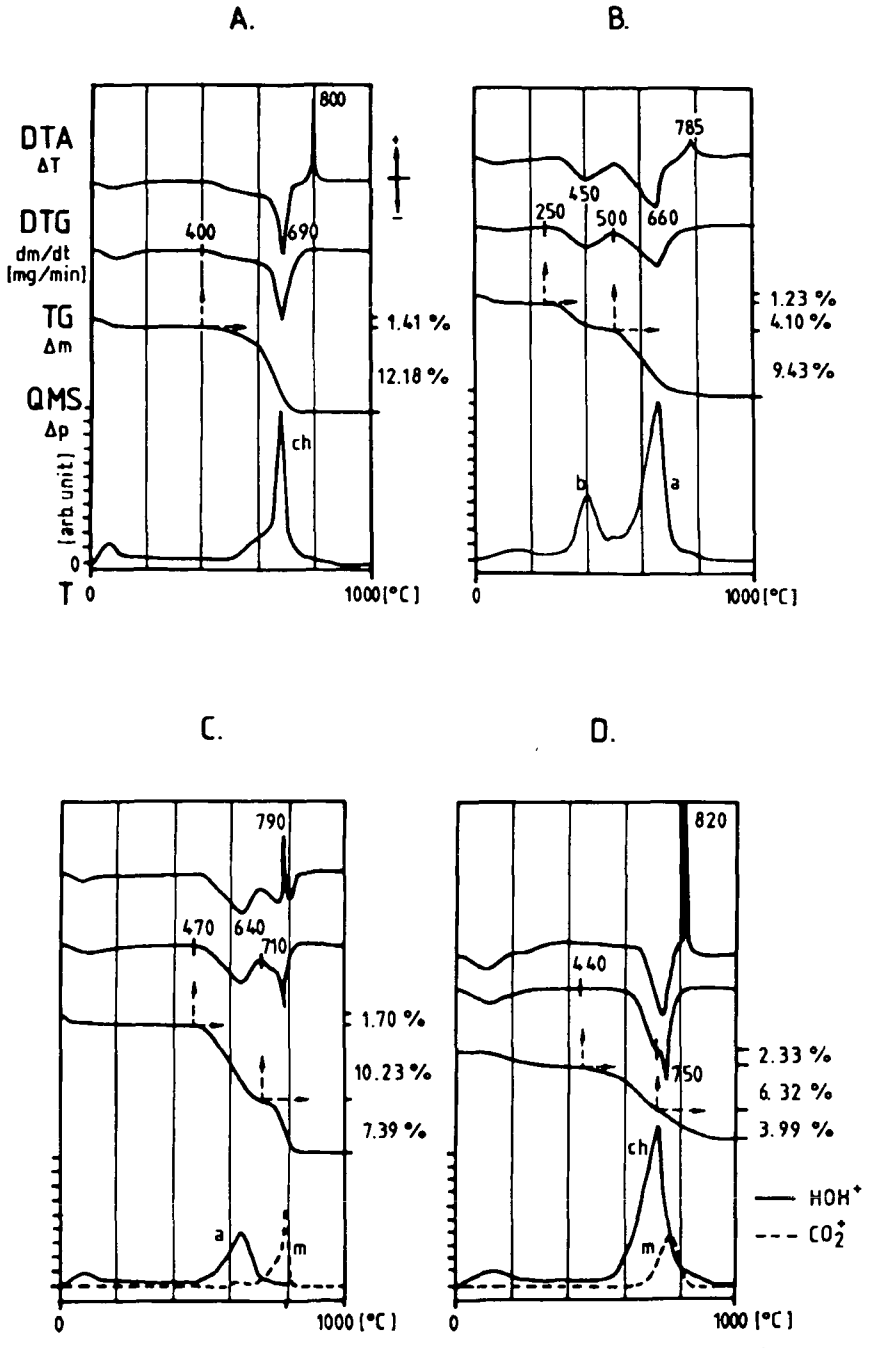

Fig. 5. Mineral paragenesis of serpentinite, from Bogoslovac, Yugoslavia (A), Trodos, Cyprus (B), Bódvarakó, Hungary (C) and Tacajo, Cuba (D)
a=antigorite, ch=chrysotile, b=brucite, m=magnesito-calcite

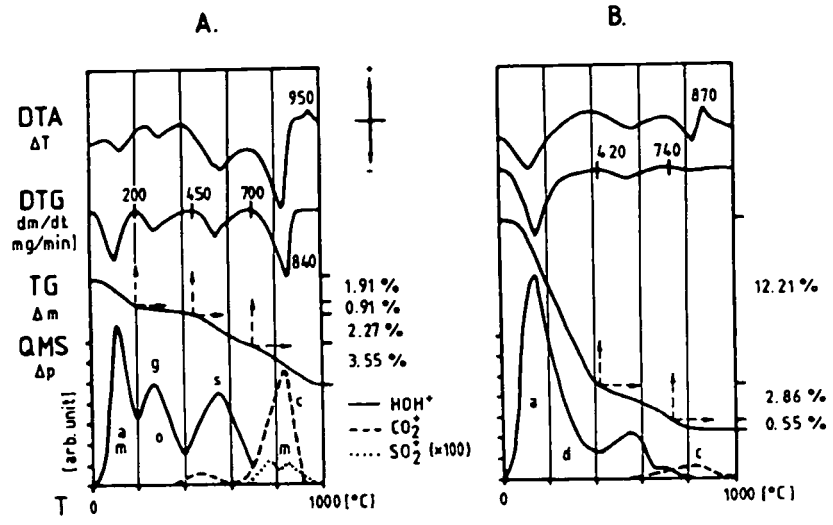

Fig. 6. Mineral paragenesis of a brick clay from Great Hungarian Plain (A) and an important tuffigene raw material, beidellite from Banes, Cuba (B)
a=amorphous material, c=calcite, d=dioctahedral smectite, g=goethite, m=mirabilite, s=interstratified mica-smectite, o=organic material

were distinguished by DTA, DTG, TG, QMS-EGA, GC, IR and Rock Eval pyrolysis methods (SZÖÖR *et al.* 1986). In the siderite facies, the organic materials was disintegrated under oxidative circumstances, while in the case of calcite and gel pyrite facies, typical aliphatic protobitumens accumulated in a reductive environment (*Fig. 7.*).

A new geochronological method has been developed by the authors (SZÖÖR, 1982a,b; SZÖÖR *et al.* 1987). The evaluation of the DTA, DTG, TG curves of Quaternary vertebrate fossil materials produced characteristic parameters closely related to geological age. Using this statement as a means for dating carried out a chronostratigraphic evaluation.

In this paper we demonstrate the mass spectrometric thermal analysis which provided the required information to explain the difference in the composition of fossil bones by measuring the evolved gases.

In the course of our work this chronological well-defined sporadic find was evaluated. The first data is 20100 years, the other one is 100000 years. *Fig. 8.* shows the results of examinations. Water as basic constituent was released up to 220 °C from the organic and inorganic structures (A process). In this range carbon dioxide relates to the beginning of the decomposition of fossile collagen. The main process B takes place between 220 and 600 °C. The quantity and MS-pattern of organic gas components are different in samples of different ages. The carbonate of apatite and calcite secondarily built into the structure dissociated in the range of 600—1000 °C (C process).

In the future it will be completed to reveal the regularities of collagene with check by GC-MS analyses.

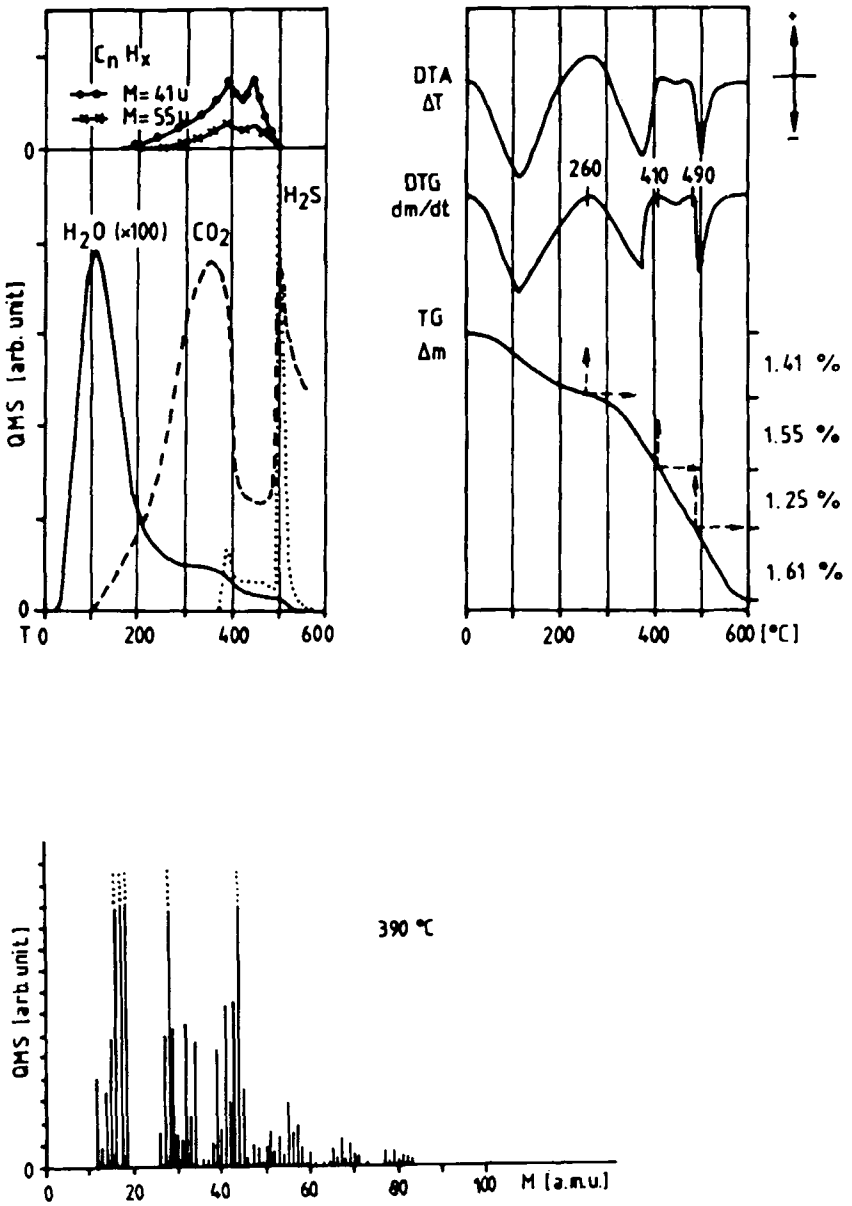

Fig. 7. DTA, DTG, TG, QMS-EGA analysis of argillaceous aleurite ("oil shale")from Teresztenye, Hungary. H_2O, CO_2, H_2S, mass number (M) 41 and 55 were continuously detected, complete mass spectrum at 390 °C (in He-atmosphere with some air-contamination)

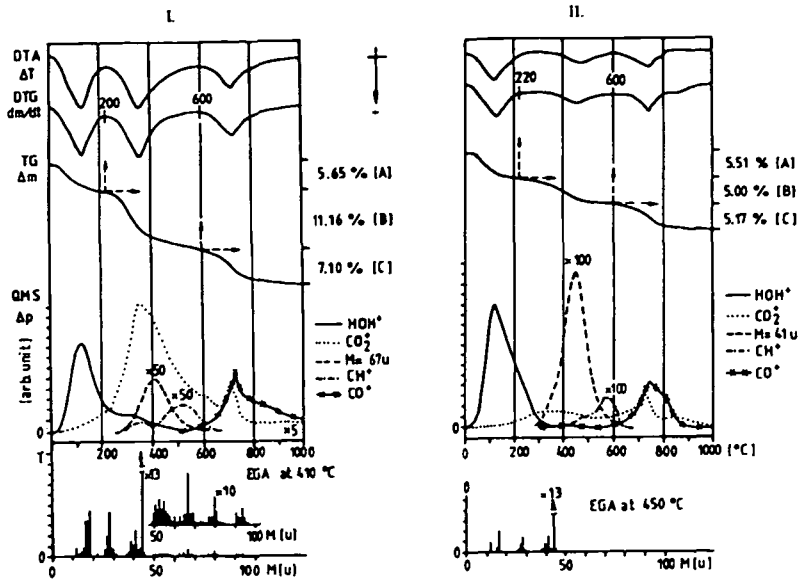

Fig. 8. DTA, DTG, TG, QMS-EGA analysis of sporadic finds (bones) I.=20000 and II.=100000 years old (B.P.)

REFERENCES

BERECZ, I., S. BOHÁTKA, G. LANGER and G. SZÖÖR, 1983: Quadrupole mass spectrometer coupled to derivatograph. — International Journal of Mass Spectrometry and Ion Physics. **47**, pp. 273—276.

BRACEWELL, J. M. and G. W. ROBERTSON, 1980: Pyrolysis-mass spectrometry studies of humification in a peat and a peaty podzol. — J. Anal. Appl. Pyrol. **2**, pp. 53—62.

DÉVAI, I., C. HEIM, I. WITTNER, G. DÉVAI, Z. DINYA, J. HARANGI, G. SZÖÖR and F. MÁTÉ, 1984: Detection of Elementary Sulphur in Freshwater Sediments. — Environmental Pollution (Ser. B) **8. 2**, pp. 155—160.

FRIPIAT, J. J., 1982: Advanced Techniques for Clay Minerals Analysis. — Elsevier

KOZÁK, M., I. BARTA, G. SZÖÖR, 1985: Mineralogical and geochemical investigation of the halloysite from Kővágóörs (Keszthely Mountain, W-Hungary) and its genetics. — Földtani Közlöny, **115**, 3. pp. 281—292.

MORGAN, D. J., 1977: Simultaneous DTA-EGA of minerals and natural mineral mixtures. — J. Therm. Anal. **12**, pp. 245—263.

MÜLLER-VONMOOS, M., R. MÜLLER, 1974: Application of DTA-TG-MS in the Investigation of Clays. — Thermal Analysis, 4th ICTA (Edited by I. Buzás) **2**, p. 521.

PAULIK, J. and F. PAULIK, 1981: Simultaneous Thermoanalytical Examination by means of the Derivatograph. — Elsevier

SZÉKELY, T., F. TILL and G. VÁRHEGYI, 1980: Characterization of Fossil Fuels by Computer Aided Thermobalance-Mass-Spectrometer System. — Thermal Analysis, 6th ICTA (Edited by W. Hemminger) **2**, pp. 365—371.

SZÖÖR G., 1982a: Fossil age determination by thermal analysis. — J. Therm. Anal. **23**, pp. 81—83.

SZÖÖR G., 1982b: Geological dating by thermal analysis. — Thermal Analysis, 7th ICTA (Edited by B. Miller) **2**, pp. 1463—1469.

SZÖÖR G., E. BALÁZS, S. BOHÁTKA, 1984: Joint Determination of Clay Minerals, Carbonates and Sulphates by complex Thermoanalytical Method. — Építőanyag. **9**, pp. 274—277. (in Hungarian)

SZÖÖR G., M. HETÉNYI, É. BALÁZS, S. BOHÁTKA, 1986: Geochemical facies analysis of the typical organic material bearing Pannonian layers at the foreground of North Borsod Karst (Hungary). Földtani Közlöny. **116–2**. pp. 137—146. (in Hungarian)

SZÖÖR, G. and S. BOHÁTKA, 1985: Derivatograph-QMS system in Geochemical Research. — Thermochim. Acta. **92**, pp. 395—398.

SZÖÖR, G., S. BOHÁTKA, L. KORDOS, 1987: Investigation of quaternary sporadic finds (Vertebrata) by DTA, DTG, TG, QMS-EGA method. — Pleistocene Environment in Hungary (Edited by M. Pécsi). Hungarian Academy of Sciences. Budapest. pp. 227—231.

SZÖÖR, G., É. BALÁZS, 1988: Mineral Efflorescence on the Surface of Walling Bricks from the Mezőtúr Factory. Építőanyag. **6**, pp. 217—222. (in Hungarian)

VICZIÁN, I., M. KOZÁK, G. SZÖÖR, 1986: Marcasite, copiapite and rhomboclase in Lower Pannonian gravels at Uzsa (Central Transdanubia). — MÁFI Évi Jelentése, pp. 377—387. (in Hungarian)

WARNE, S. S. J., A. J. BLOODWORTH, D. J. MORGAN, 1985: Thermomagnetometry and evolved gas analysis in the identification of organic and pyritic sulphur in coal and oil shale. — Thermal Analysis, 8th ICTA (Edited by A. Blažek) 2, pp. 745–748.

Manuscript received, 13 November, 1990

Acta Mineralogica-Petrographica, Szeged, XXXI, 67—75, 1990

MAJOR ELEMENT GEOCHEMISTRY OF THE LATE PALAEOZOIC-EARLY MESOZOIC GRANITOIDS IN VIETNAM

BUI MINH TAM*

Institute of Geology and Ore-research

HARANGI SZ.**

Department of Petrology and Geochemistry,
Eötvös Loránd University

ABSTRACT

In this paper authors present the preliminary results of the geochemical-petrological study of the granitoid rocks (Dienbiemphu- and Queson-complex) in Vietnam. Several petrochemical diagrams and parameters have been used to recognize the nature and the tectonic affinity of these intrusive rock assemblages. Majority of them show calc-alkaline character, however, the evolved formations display higher alkaline-content. Both granitoids are characterized by a transitional affinity, they show both compressional and extensional features as well as S- and I-type nature. The plutonic rocks of these two complexes exhibit similar petrological and geochemical characters indicating that they were formed in the same tectonic position: in the inner part of the continental margin.

INTRODUCTION

In this paper we present the preliminary results of a detailed petrological and geochemical study on the granitoid rocks of Vietnam. Our conclusions are based on the major element geochemical compositions, therefore we note that the further investigations (rare-earth element chemistry, study of the main mineral phases, i.e. feldspars, biotite, opaques etc. in these rocks) will give more exact results and may slightly modify of these conclusions. Results of this major element geochemical study, which is the first one on the Vietnam granitoids using modern petrochemical tools, can be regarded as a working hypothesis for the following investigations.

The Late Palaeozoic-Early Mesozoic granitoids of Vietnam have been divided into two complexes: the Dienbiemphu (DBP)-complex and the Queson (QS)-complex (DOPJIKOP 1965; TRAN VAN TRI and NGUYEN XUAN TUNG 1977; HUYNH TRUNG 1980).

The DBP granitoids occur in the northwestern part of Vietnam, while the QS-granitoids can be found in the northern, western and southwestern margin of the Kontum area (Middle part of Vietnam; *Fig. 1*). Both magmatites were formed during the Late Permian-Early Triassic based on the following geological evidences:

* Hanoi, Vietnam
**H—1088 Budapest, Múzeum krt. 4/a, Hungary

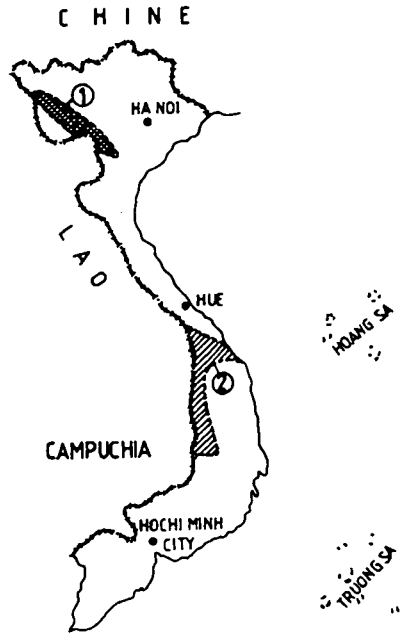

Fig. 1. Areal distribution of the granitoid rocks of the DBP- and QS-complexes.

a.) The granitoid rocks of the Nampo- and Nammung Massif belonging to the DBP-complex intruded into the Lower Permian sedimentary formations and they are overlain by Upper Triassic coal-bearing deposits (*Fig.* 2).

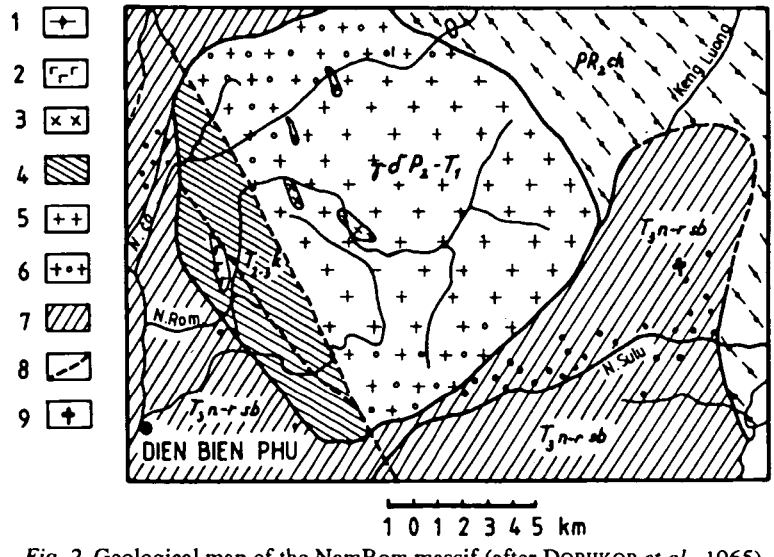

Fig. 2. Geological map of the NamRom massif (after DOPJIKOP *et al.*, 1965).
Legend: 1: Palaeozoic mica-schists, quartzite, amphibolite and marble (PZnc, PZch); 2: Late Permian gabbrodiorite; 3: Late Permian-Early Triassic diorite, quartzdiorite, granodiorite and granite; 4: Triassic Conglomerate, sandstone, argilite, rhyolite and basalt (T_2-$_3$lc); 5: Triassic biotite-granite and two-micas granite; 6: Muscovite-granite; 7: Sandstone, aleurolite and conglomerate.

b.) The granitoids of Queson Massif intruded into the Ordovician-Lower Silurian volcano-sedimentary sequence resulted in a contact metamorphic zone characterized by epidote-amphibole hornfels. The intrusive formation is overlain also by the Upper Triassic coal-bearing deposits (*Fig. 3*).

c.) K/Ar radiometric data measured on separated biotite fractions show 235—266 Ma for the DBP granites (DOPJIKOV 1965; TRAUVANTRI 1977) and 234—302 Ma for the QS granites (HUYNH TRUNG 1980).

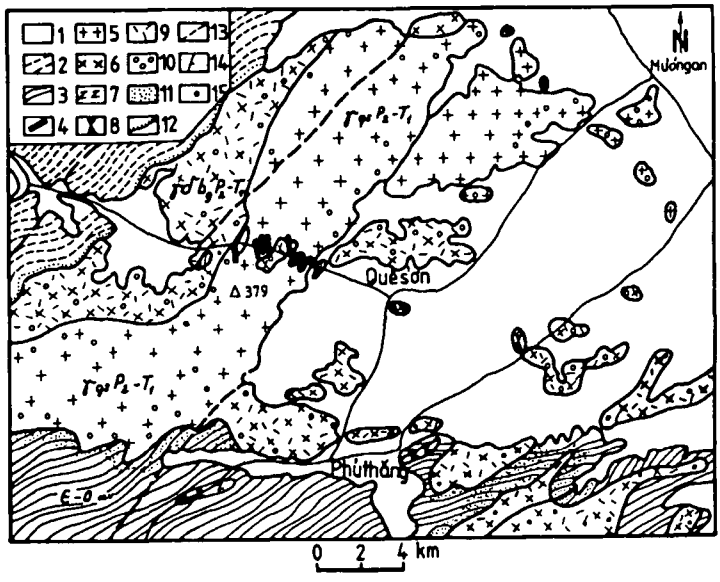

Fig. 3. Geological map of the Queson massif.

Legend: 1: Quaternary sediments; 2: Triassic coal-bearing conglomerate, sandstone and aleurolite; 3: Early Palaeozoic chlorite-quartz schists and greenschists; 4: Pegmatoids, aplite, graniteporpyre (III. phase); 5: Granite and granodiorite (II. phase); 6: Quartz-diorite, apodiorite and granodiorite (I. phase); 7: serpentinite and various ultramafics (Hiep Diu Complex); 8: diorite; 9: magmatic microclinitic rocks; 10: submagmatic microclinitic rocks; 11: Contact metamorphic rocks; 12: Geological boundary; 13: Faults; 14: Tectonic lines; 15: Locations of the samples collected for radiometric age-analyses.

PETROGRAPHY

The studied granitoid-complexes are considered to belong to a gabbrodiorite-quartzdiorite-granite-granosyenite differentiation sequence. The intrusive magmatism can be divided into three main phases resulted in the following formations:

/1/ *Gabbrodiorite and quartzdiorite (tonalite).* Mineral composition: plagioclase (50—60%), amphibole (10—15%), biotite (10—15%), clinopyroxene (3—5%), quartz (5—10%) and alkali feldspar (0—3%).

/2/ *Granite.* Mineral composition: plagioclase (30—35%), biotite (10—15%), amphibole (5—10%), alkali feldspar (25—30%), quartz (30—35%).

/3/ *Aplite, microgranite and graniteporphyre.* Mineral composition: alkali feldspar (35—40%), quartz (35—40%), plagioclase (20—25%), biotite (0—5%).

Accessory minerals of the formations are magnetite, ortite, sphene and ilmenite appearing with varying amount in the gabbrodiorite-granite assemblage.

Geological and petrological data indicate that the granitic magma resulted only in the large granodiorite and granite bodies (2. phase) and it did not differentiated further forming volatile-rich, granitophile rare-earth element-bearing phases. Aplites, microgranites and graniteporphyres may have been formed from an independent granitic magma (3. phase)

PETROCHEMISTRY

DBP Complex. Majority of data points of the DBP granites fall into the calc-alkaline field on the SiO_2 vs. alkali ratio diagram and only the late stage leucogranites show alkali nature (*Fig.4*). The petrochemical trend shows a continuous alkali-enrichment during the differentiation. The Na/K ratio in the DBP granites is predominantly larger than 1 (*Fig. 5*). The distribution of data points in the Na-K-Ca triangular diagram indicates that the first phase separated from the granitic magma was the Ca-rich plagioclase followed by the crystallization of alkali feldspar and Ab-rich plagioclase. The Na/K ratio decreases with the fractional crystallization, however, Na_2O always exceeds the potassium-content. This characteristics can be explained as the sodium-rich sequence derived from the partial melting of the oceanic slab subducted below the continental crust, then this acidic magma intruded into the upper levels and suffered crustal contamination resulted in a light potassium-enrichment.

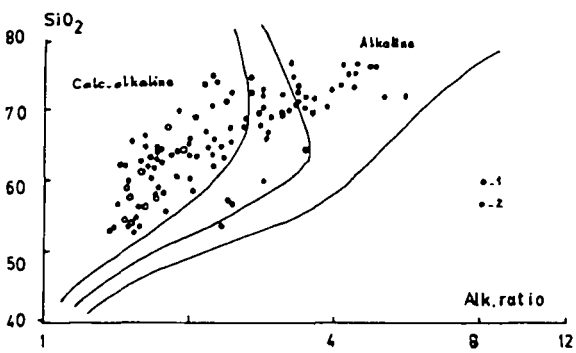

Fig. 4. Distribution of data-points of the DBP- and QS-granitoids on the WRIGHT-alkalinity ratio vs. SiO_2 plot.

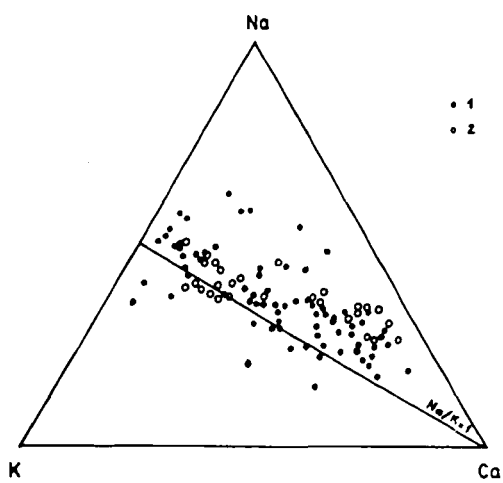

Fig. 5. Na-K-Ca triangular diagram for the DBP- and QS-granitoids.

The F/M ratio of the DBP granites is always larger than 1 *(Fig. 6)*, the MgO-content is moderate, while the total FeO is low as compared to the high alkali abundances. The petrochemical trend presented on the AFM diagram (*Fig. 6*) starts from the iron-rich composition and shows a continuous alkali-enrichment and a depletion in the mafic elements during the differentiation process. This evolution suggests that the Fe/Mg ratio remained more or less constant during the crystallization of the granitic magma.

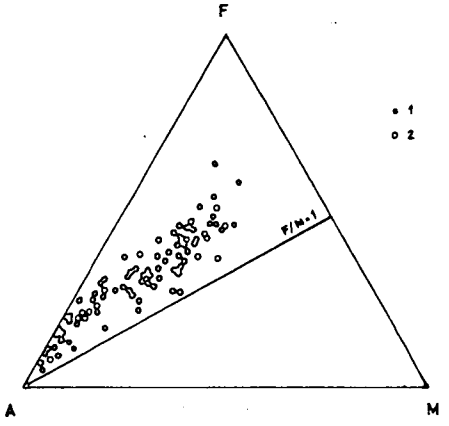

Fig. 6. AFM triangular diagram for the DBP- and QS-granitoids.

QS Complex. The data points of the QS granites fall also into the calc-alkaline field on the SiO_2 vs. alkali ratio diagram (*Fig. 4*) showing a continuous alkali-enrichment. The Na/K ratio and the F/M ratio always exceeds the unit which is similar to that of the DBP granites (*Fig. 5,6*), i.e. both granite complexes exhibit similar petrochemical evolutionary trend.

PETROGENESIS

Granitic rocks of the studied complexes show partly I-type and partly S-type affinity suggested by the ACF discrimination diagram (*Fig. 7*). The oxidation degree ($Fe_2O_3/(FeO+Fe_2O_3)$) of these rocks also indicates this two-fold character:

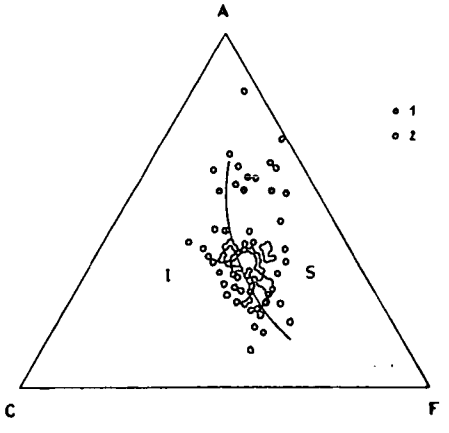

Fig. 7. ACF triangular diagram for the DBP- and QS-granitoids.

although, its values are varied strongly, the average of them is around 0.35 (*Fig. 8*) exhibiting both I-type and S-type feature. The Na/K ratio (1) and the high CaO-content indicate I-type nature, however, the peralumina index (Al/(Na+K+Ca/2)) is larger than 1.1 characterized the S-type granites (CHAPPEL and WHITE 1974). We can conclude from these data that both sedimentary and basic magmatic rocks had important roles in the ultrametamorphic granite petrogenesis.

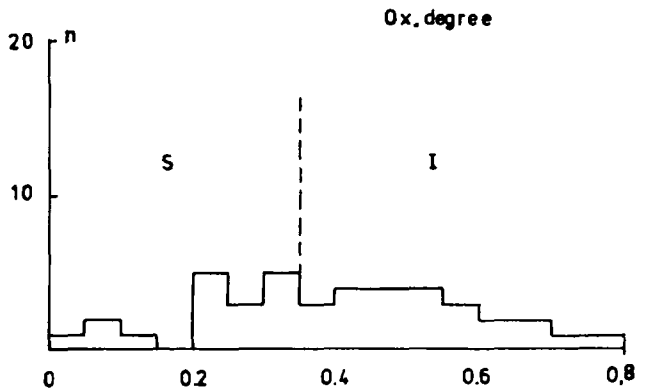

Fig. 8. Frequency distribution of the $Fe_2O_3/(Fe_2O_3+FeO)$ ratio in the studied granitoid series.

TECTONIC POSITION

The original tectonic position of the Late Palaeozoic-Early Mesozoic granitoid complexes in Vietnam was determined using the following parameters:

- — *Differentiation Index* (DI, THORNTON and TUTTLE, 1960), the normative An-content, the shape and the mode of the distribution curve on the histogram of these values.
- — The *F/M ratio* and the *differentiation trend* on the AFM triangular diagram.
- — The *calc-alkaline index* ($CaO/(Na_2O+K_2O)$), the alumina saturation, the total alkali- and the CaO-content, the oxidation degree.

DBP granite complex. The average of the DI-values is 70±25 indicating a strongly differentiated nature for this intrusive assemblage (*Fig. 9*). The distribution curve of DI has two maxima at the values of 60—70% and 90—95% respectively. The distribution of the normative An-content proved to be similar to that of the DI. The average of An is 17±15 (note the high standard deviation!), the maxima of the curve are at 14—16% and 20—22% respectively (*Fig. 10*). It can be explained as the DBP granitoids contain two-generation plagioclases. These features as well as the F/M ratio and the evolutionary trend on the AFM diagram all show compressional-type granitoid character for the DBP intrusive rocks. The position of data points on the SiO_2 vs. $CaO/(Na_2O+K_2O)$ diagram (*Fig. 11*) also supports this conclusion. Nevertheless, the high Na/K ratio and the total alkali-content indicate extensional-type granitoid character. Based on this two-fold behaviour of the DBP intrusive rocks they can be regarded transitional type (PETRO *et al.* 1979) granitoids.

The normative q-or-pl triangular diagram clearly displays the calc-alkaline granodiorite sequence (*Fig. 12*) characterized by a moderate potassium-content. This intrusive formation has transitional nature between the trondhjemites and the

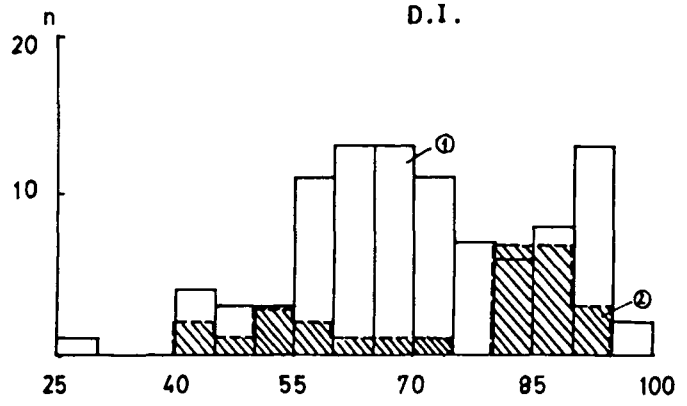

Fig. 9. Frequency distribution of the Differentiation Index in the studied granitoid series.

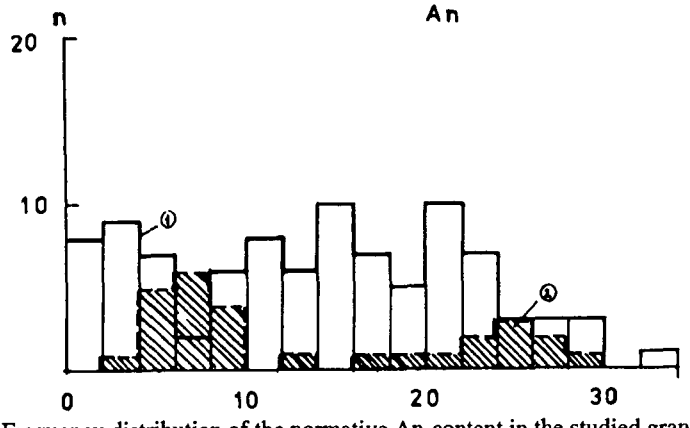

Fig. 10. Frequency distribution of the normative An-content in the studied granitoid series.

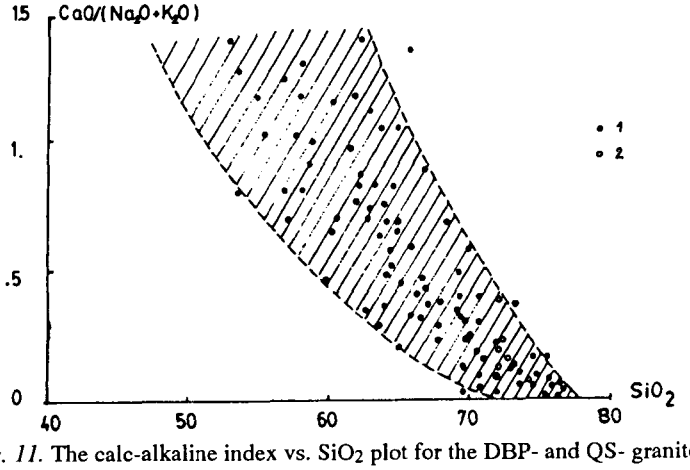

Fig. 11. The calc-alkaline index vs. SiO_2 plot for the DBP- and QS- granitoids.

monzonitic granites, i.e. they do not show direct relationship to the continental margin origin. They can be regarded as partly I-type and partly S-type (magnetite- or ilmenite-type; LAMEYRE *et al.* 1982) granitoids.

QS granite complex. It appears with a wide compositional variation (*Fig. 9*), the average of the DI-values is 70±25 indicating strongly differentiated behaviour. Two maxima can be observed on its frequency distribution curve at the values of 50—55% and 80—90% respectively. The normative An distribution is similar to that of the DI showing two maxima at the values of 6—8% and 24—26% respectively. The average of the An is 15±14 (note the high standard deviation!). These characters are typical to the extensional granitoids (PETRO *et al.* 1979), i.e. the QS granitoids differ from the DBS complex in this respect.

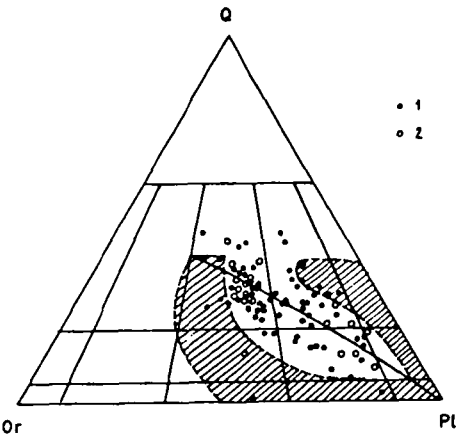

Fig. 12. Normative Q-Or-Pl triangular diagram for the DBP- and QS-granitoid series.

The F/M ratio (~1) on the AFM diagram (*Fig. 6*) is characteristic to the compressional plutonic rocks. The SiO_2 vs. $CaO/(Na_2O+K_2O)$ plot (*Fig. 11*), the peralumina ratio (1.1) as well as the calc-alkaline index also support the compressional nature of the QS granites like in the case of the DBP rocks.

On the normative q-or-pl plot (*Fig. 12*) data points of these rocks are situated along the line of the calc-alkaline granodiorite sequences. Summing up, the QS granitoids can be regarded as a transitional type plutonic assemblage showing both compressional and extensional feature.

CONCLUSIONS

Based on the major element chemistry the following characters have been recognized for the Late Palaezoic-Early Mesozoic Dienbienphu- and Queson granitoids (Vietnam):

— The Plutonic rocks of both complexes belong to a differentiation trend characterized by a petrochemical evolution from the calc-alkaline to the alkaline formations. Majority of these granitoids have calc-alkaline affinity, however, the evolved formations display higher alkaline-content. The Na/K ratio always exceeds the unit, the potassium-content increased slightly, whereas the sodium-content decreased during the fractional crystallization.

The first crystallization products were Fe-rich phases, the total iron content is higher than the MgO-content throughout the differentiation process.

— A part of the DBP- and QS-granitoids show S-type nature, while the others can be regarded as I-type granites. This means that not only sedimentary but magmatic rocks also had important roles in the ultrametamorphic process leading to the formation of the granitic magma.
— The DBS- and QS-granites are characterized by a transitional affinity, they show both compressional and extensional features. They belong to the calc-alkaline granodiorite sequences and they were formed in the inner part of the continental margin.
— The plutonic rocks of DBP- and QS-complexes exhibit similar petrological and geochemical characters indicating that they were formed in the same tectonic position. Therefore, despite the different spatial distribution and the slight differences in the K/Ar radiometric data of these complexes, they can be range into the same granitoid sequence formed during the Late Permian to the Early Triassic in the area of Vietnam.

ACKNOWLEDGEMENTS

B. M. T. is grateful to Professor I. KUBOVICS who supported his study at the Department of Petrology & Geochemistry, Eötvös University, Budapest, Hungary. Thanks are due to Dr. GY. BUDA and Dr. CS. SZABÓ for their critical comments on the manuscript.

REFERENCES

BUDA GY. (1985): Variszkuszi korú kollíziós granitoidok képződése (Magyarország, Ny-Kárpátok és Központi Cseh-Bohémiai masszívum granitoidjainak példáin). PhD. Theses. (in Hungarian)

CHAPPEL B. W. and WHITE A. J. R. (1979): Two contrasting granite type. Pacific Geology. **8**, 173—174.

DOPIJKOP E.A., *et al.* (1965): Geology of the Northern Vietnam. Moskau-Hanoi. (in Russian)

LAMEYRE I. and BONDOU P. (1982): Plutonic rock type series: discrimination of various granitoid series and related rocks. J. Volcan. Geoth. Res. **14**, 169—186.

PEACOCK M. A. (1931): Classification of igneous rock series. J. Geol. **39**, 54—67.

PETRO W. L., VOGEL, T. A. and WILBAND J. T. (1979): Major element chemistry of plutonic rock suites from compressional and extensional plate boundaries. Chem. Geol. **26**, 217—235.

STRECKEISEN, A. (1979): Classification and nomenclature of plutonic rocks. Geol. Rundschau. **63**, 773—786.

TRAU VAU TRI, *et al.* (1977): The geology of Vietnam. Hanoi (in Vietnam)

TRUNG H. (1980): Petrographic characters of the Queson-complex rocks. Geology. **47**, 76—80 (in Vietnam)

THORNTON C. P. and TUTTLE O. F. (1960): Chemistry of igneous rocks: I. Differentiation Index. Amer. J. Sci. **258**, 664—684.

WRIGHT, J. B. (1969): A simple alkalinity ratio and its application to questions of non-orogenic granite genesis. Geol. Mag. **106**, 370—384.

Manuscript received, 21 November, 1990

Acta Mineralogica-Petrographica, Szeged, XXXI, 77—87, 1990

STORMS AS AN ONSHORE DRIFT AGENT FOR COARSE SANDS, NILE DELTA COAST

NABIL M. EL-FISHAWI*

Geology Dept., Institute of Coastal Research,

ABSTRACT

Onshore movement of coarse sands during storms is one of the most characteristic features of the Nile Delta coastal sediments. At the western side of Burullus and Damietta beaches, it is indicated that a lot amount of sediments are derived to the beach after server storms. These storm sediments are deposited and covered the beach zone at some locations with a thickness not exceeding 70 cm. This sand accumulation differs from the native beach materials; the derived sediments being coarser, less sorted, more rounded and cleanly washed than the native beach sands. The related characteristics of the storm sands on the beach may simply reflect derivation from similar source area under special physical conditions. In fact, correlation of the grain size distribution and texture of new materials added to the beach and that of the adjacent offshore indicates that onshore movement has occurred. It is significant that coarse sand from offshore sources is added to some beaches by wave action on the bottom during winter severe storms.

INTRODUCTION

During performing fluorescent sand tracer experiments along the Nile Delta coast, it was observed that a lot amounnt of coarse sediments is lying on some beaches and derived from outside sources. These sediments include mainly corse sands with some clay balls, small beach pebbles and shell fragments. Their thickness do not exceed 70 cm over the original beach sand and covers the area between beach face slope and backshore. These new sediments are observed to occur during the stormy period form November 1991 to April 1992 at the western side Burullus and Damietta coasts (*Fig. 1*).

West of Burullus outlet, the coast is sandy and flat. The mean grain size of beach sands ranges between 1.5 and 2.4 Φ. The barrier between the sea and Burullus lake is mostly a backshore plain. The plain is flooded during stormy conditions but it is not below sa level. At the shore, the beach sand is 2—3 m thick overlying lagoonal clay. The beach sand is therefore a thin wedge which disappears lakewards.

The coast west of Damietta mouth (Ras El Bar) has a wide and flat beach with small cusps. Progressive widening, along with the increasing length of Ras El Bar tongue have been occurred from 1800 until 1909. The coast is subjected to retreat from 1909 to the present. The mean grain size of beach sands ranges between 2.1 and 2.5 Φ.

During the past three decades many studies have been carried out concerning the continental shelf sedimentation processes and onshore transport (SHEPARD

* 21514 Alexandria, 15 Faraana St., El-Shalallat. Egypt

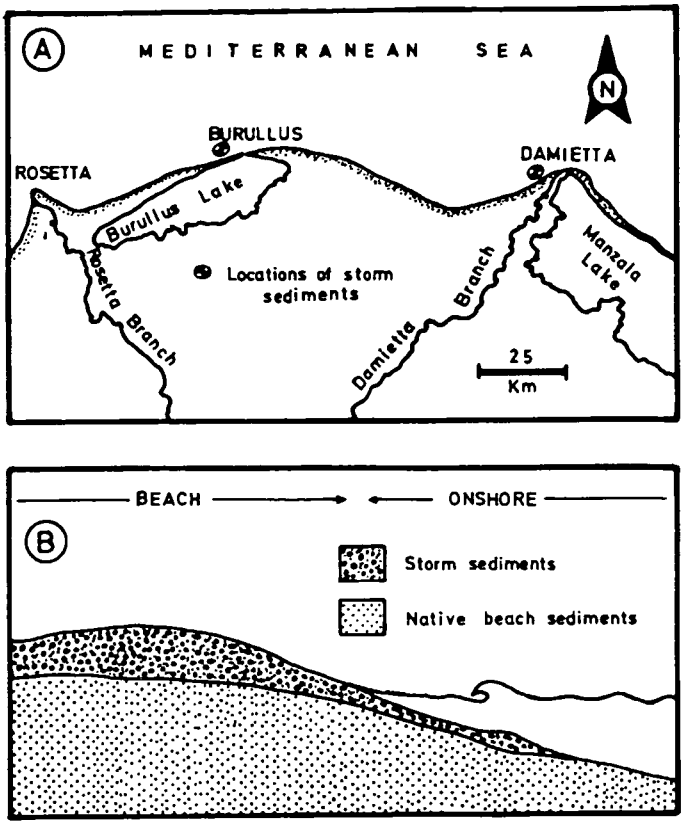

Fig. 1. A Location map showing the Nile Delta coast.
B Storm sediments on the beach.

1963; GUILCHER 1963; PEVEAR and PILKEY 1966; MEADE 1969; WINDOM *et al.* 1971; PILKEY and FIELD 1972 and EL-FISHAWI and MOLNAR 1981, 1983). PIERCE (1969) estimated that 44,000 cubic yards of sand were supplied annually to the shoreline from sources on the continental shelf to meet the requirement for beach and barrier island maintenance.

METHODS AND TECHNIQUES

The Nile Delta coast was surveyed during the winter season from Nov., 1991 to April, 1992. Samples were collected from the coarse sediments which derived to some beaches after storms. Samples were also collected from the original beach sediments. The characteristics of offshore sands were obtained from FRIHY *et al.* 1990.

All samples collected were washed, dried and split. Mechanical analysis was carried out by the conventional sieving method with screens placed at one-phi intervals. About 100 gm of materials was taken for grain size analysis, using a

mechanical shaker with a sieving time of 20 minutes. The data were plotted as cumulative curves on probability paper to ensure maximum accuracy in determining the grain size statistical parameters (FOLK and WARD 1957). The grain-roundness values for the collected samples were determined in each size fraction according to POWERS 1953.

STORMS AFFECTING THE NILE DELTA COAST

The Nile Delta coast, like the rest of the northern coasts, is subjecting to a number of quasi-periodic storms. These storms are mostly accompanied by heavy rains, high water level rise and high waves. Generally, these storms which are popular called "nawat", occur from October to April. The time and period of occurrence of the "navat" are summarized in Table 1.

TABLE 1.

Time and period of winter storms "Nawat" affecting the Nile Delta coast

Storm name	Time	period (days)
Saliba	Oct. 21	3
Kansa	Nov. 27	3
Kasem	Dec. 06	7
Faida Sugra	Dec. 20	2
Gatas	Jan. 11	3
Faida Kubra	Jan. 19	5

Storm name	Time	period (days)
Karam	Jan. 29	2
Shams Sugra	Feb. 08	5
Hosoum	Mar. 10	8
Shams Kubra	Mar. 20	2
Aowa	Mar. 25	6
Khamasin	Apr. 30	4

During Dec., 25—31, 1991, surveying was carried out along the eastern part of the Nile Delta coast. It was severe stormy conditions which caused a big rise in the sea level. Many costs were subjected to damage (i.e. east of Damietta) where the other are drowned (i.e. Ras El Bar resort at west of Damietta). At the western part of the Nile coast, many inhabitants were much threatened due to this storm and some coastal areas and cultivated lands were drowned (i.e. Nobaria and Idku). The characteristics of this storms were similar to Nawat Kasem which lead to the conclusion that it is Nawat Kasem but only came lately that year. In fact, it was worst storm that occurred during the last 15 years, at least as far as the rise in water level is concerned. Similar conditions were reported at Ras El Bar resort in Nov., 1964 (SUEZ CANAL AUTHORITY 1965). For such storm surges, the rise in the sea water level was about 50 cm. The predominant wind direction was from W and WNW with maximum speed of 14.5 m/sec. The maximum wave height attained in the storm was 5.0 m with frequency period of 9—11 sec.

A great deal of attention has been given to the erosion effect of waves on beaches, and not nearly so much to the constructive work that waves are doing continuously on some beaches. In fact, the waves play an effective role in moving sediments up or along the beaches and extend some beaches into the present accumulation forms (bars, berms and spits). KING (1972) mentioned that low, flat waves with low frequency will move sediments landwards and build up the beach.

For many years, textural analysis has been used to determine sedimentary environments. New approaches and insights into the nature and significance of grain size distributions have been investigated. There are many physical criteria available to identify specific depositional environments and textural studies can provide a separate line of evidence to aid in interpreting clastic deposits.

The present study aims to detect the source of storm sediments. Therefore, it is better to correlate between: 1 — Native beach sands, 2 — Onshore drift sands during storms, and 3 — Adjacent offshore sands. The following methods of treating the grain size distribution of sands were applied : 1 — Frequency distribution curves, 2 — Cumulative frequency curves, 3 — CM diagram, 4 — Statistical poarameters, and 5 — Grain roundness.

Discriminate between native beach and onshore drift sands

The grain size distribution of native beach sands appears to be fundamentally different from those added to the beach during heavy storms. *Figures 2, 3* and *4* show the main differences and characteristic features.

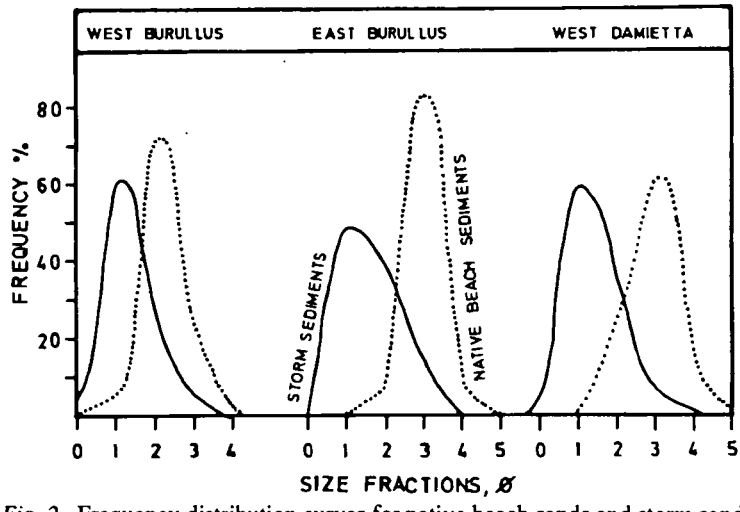

Fig. 2. Frequency distribution curves for native beach sands and storm sand.

The frequency distribution curves (*Fig. 2*) discriminate between these 2 types of sand. A visual inspection of the model classes and tails on the frequency curves can be used as a preliminary interpretation of the energy conditions within each type of sand. Native beach sands have a model class of 2 Φ unit at west of Burullus and 3 Φ unit at east of Burullus and west of Damietta. On the other hand, onshore drift sands (storm sediments) display a model in the 1Φ unit class. Thus, the storm sediments which added to the beach retain a higher percentage of coarser fractions than does the native beach sands. This indicates an increase in the energy level during onshore movement of coarse sands due to heavy storms.

Cumulative frequency curves drawn on probability paper were used to relate sedimentation dynamics to texture. Generally, there are 3 fundamental models of

transport; traction, saltation and suspension. For the curves, the truncation points between these 3 models of transport reflect the physical conditions at the time of deposition, and hence give the true limiting value of grain size for each model of transport. It is also important to recognize a separate lognormal populations which relate to the position of truncation points and the degree of mixing between these populations. Morover, it is valuable to depend upon the degree of sorting as indicated by the shape of each population. *Fig. 3* shows the cumulative curves for native beach sands and onshore drift ones. Of special significance is the fact that

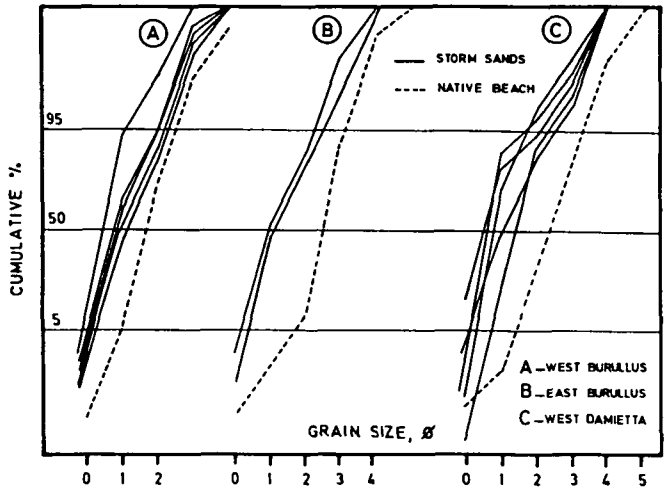

Fig. 3. Cumulative frequency curves for native beach and storm sands.

the onshore drift samples are characterized by high percentages of sediment in the coarse rolling population. Size distribution curves indicate the three models of transport with a high degree of mixing. The positions of the coarse trunction are highly variable and the range is between 0—1 Φ (2—93%) of the distribution. It is clearly observed that mixing occurs between rolling and saltation populations. The saltation population has a size range between 1—3 Φ (50—99%). A suspension population has been defined between 3—4 Φ, it represents less than 1% of the distribution. On the other hand, the three modes of transport in the native beach samples are more pronounced, without mixing, and have better sorted populations than that in the onshore drift samples.

CM diagram is constructed by plotting the one percentile particle diameter (C) versus the fifty percentile particle diameter (M) in μm on bilogarithmic paper. The texture of a clastic sediment represented in this way is characteristic of the depositionale agent. The transport mechanism that built up the deposit can be suggested on the basis of the shape and the arrangement of the pattern of the sample points in a CM diagram (*Fig. 4*). It is indicated that combinations of C and M permit distinction between native beach and onshore drift sands. Depending on the spreading C with relation to the M values, the native beach samples are formed essentially by particles with C values of 500—616 μm and M values of 177—308 μm. On the other hand, onshore drift samples are coarser, with C values of 732-1275 μm and M values of 366—707 μm. The change from a pattern parallel to the CM line (suspension) to a pattern parallel to the C axis (rolling) corresponds

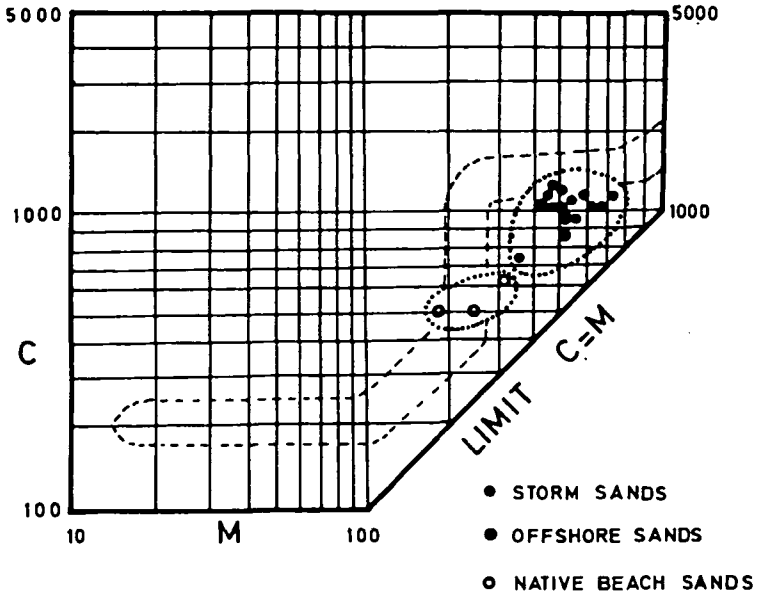

Fig. 4. C M diagram for native beach sands and storm sands (onshore drift)

to a difference in mode of deposition. Native beach points are distributed parallel to the limit of C=M, indicating an area of good sorting and transported by suspension. The majority of the onshore drift points are situated at a considerable distance from the limit C=M and can be related to the C axis. Therefore, they are poorly sorted and moved by means of rolling. The action of the tractive current caused by the waves during storms is responsible for onshore drift of coarse sands. The maximum value of C in the pattern is an indication of the maximum turbulance caused by waves during storms.

The mean grain size and the inclusive standard deviation (sorting) yielded an optimum discrimination (Table 2). Onshore drift sands are largely coarser and less sorted than the native beach ones. For example, the average mean grain size of onshore drift sands at west of Burullus was found to be 0.91Φ while it was 1.72 Φ for the native beach sands. The sorting values were 0.55 and 0.47 Φ for the onshore drift and native beach sands, respectively.

Grain roundness was used to investigate the depositional environment of sands in question. At first site, it will be seen that a difference in grain roundness was found between onshore drift storm sands and native beach ones (Table 3). The onshore drift grains are more rounded (0.52—0.58) than those of the native beach (0.41—0.43).

Correlation between onshore drift and offshore sands

The sands on most parts of the inner shelf are generally coarser than what the Nile mouths used to discharge in the present time (COASTAL EROSION STUDIES 1976). Terrigenous sands that make a patchy belt on the middle shelf are relict and can be related to some of the former Nile branches (*Fig. 5A*). The sands of western Abu Quir Bay occur north of the Canopic mouth. The sand patches of the west

TABLE 2.

Grain size fractions and parameters for native beach, storm (onshore drift) and offshore sands.

Stretch	Features	% of grain size fractions						Mz	σ I	C	M
		ø 0	ø 1	ø 2	ø 3	ø 4	ø 5	ø	ø	μm	μm
West of Burullus	Storm sands	3.99	60.08	29.47	6.31	0.09	—	0.91	0.55	1193	555
	Native beach	0.05	5.43	72.23	21.53	0.74	0.01	1.72	0.47	616	308
Just east of Burullus	Storm sands	1.61	48.17	37.20	12.37	0.64	0.02	1.18	0.65	1111	483
	Native beach	0.12	1.03	7.31	83.35	8.11	0.07	2.50	0.42	500	177
West of Damietta	Storm sands	2.97	58.82	31.21	6.10	0.90	—	0.94	0.47	993	545
	Native beach	0.19	0.97	25.92	61.36	11.31	0.25	2.35	0.57	500	196
Off Burulluss (offshore sands)	No. 9/2	0.38	54.60	43.60	1.37	0.02	—	0.95	0.39	871	500
	15/2	1.15	70.16	27.60	0.87	0.20	—	0.79	0.36	966	555
	25/1	0.40	46.56	52.74	0.30	—	—	1.03	0.38	1035	467
	Average	0.64	57.11	41.32	0.86	0.07	—	0.92	0.38	957	507

TABLE 3.

Roundness values for native beach, storm (onshore drift) and offshore sand grains.

Size fraction Φ	Burullus		Damietta		offshore sands
	Storm sands	Native beach	Storm sands	Native beach	
0	0.69	0.56	0.72	0.46	0.68
1	0.65	0.48	0.57	0.43	0.63
2	0.61	0.41	0.48	0.41	0.49
3	0.52	0.35	0.41	0.37	0.44
4	0.43	0.33	0.40	0.36	0.41
Total mean	0.58	0.43	0.52	0.41	0.53

Burullus inner shelf lie to the N and NW of the traces of the Saitic and associated branches. North of Burullus outlet, the N-S tongues of coarse sand are rather suggestive of an ancient stream, their location could be on the continuation of the Sebennytic branch. The sands that lie on Gamasa and Damietta terraces may have come from an old mouth at Gamasa. Some evidences for the old Atribic branch near Gamasa have been found by BARAKAT and IMAM (1976). these branches were probably more active in Pleistocene-Holocene times.

In 1989, exploration survey has been done for the area of Burullus using cores and vibrocores. The objects were to identify and evaluate the suitability of offshore borrow materials for beach nourishment. The survey covered the inner shelf zone off Burullus coast (*Fig. 5B*). The textural analysis of the sediment corings identified coarser sand at distance of 2—9 km from the coast and water depth between 8 and 15 m (FRIHY *et al.* 1990). Table 2 shows that the offshore sands has a mean size of 0.92 Φ and sorting of 0.38 Φ . The total volume of the identified borrow areas is estimated to be 22 million cubic meters within one meter subbottom layer.

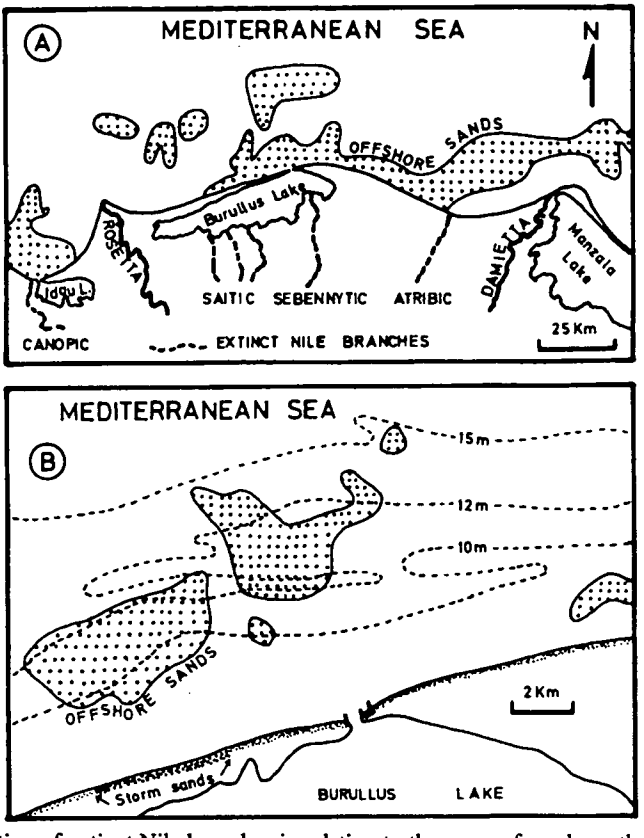

Fig. 5. A Position of extinct Nile branches in relation to the areas of sands on the offshore (after EL-FISHAWI *et al.* 1976).
B Offshore coarse sands in adjacent of Burullus coast (after FRIHY *et al.* 1990).

In fact, the similarities between the new material added to the beach during onshore drift and the offshore sands are indicated by textural analysis (*Fig. 6* and Table 2). The two types of sand are coarse, moderately well sorted and have nearly similar roundness values. Morover, the presence of index rosy quartz grains indicate close correlation between these two types of sands.

Thus, the evidences show that a reasonably close correlation exists between the nature of offshore sands and those added to the beach during onshore movement at some stretches of the Nile Delta coast. This similarity between the two types of sand is assumed to be due to the fact that the offshore area is acting as a source region for onshore movement of sand to some coastal areas during winter heavy storms. The evidence being that the only possible source of coarse, moderately well sorted sands with similar roundness values and rosy quartz grains which added to the beach is the offshore. The offshore and onshore drift sands are mostly free from heavy minerals and since the present mouths at Rosetta and Damietta are believed not to be contributing sand at present, the correlation may reflect onshore tranpsort of offshore sediments under special physical conditions.

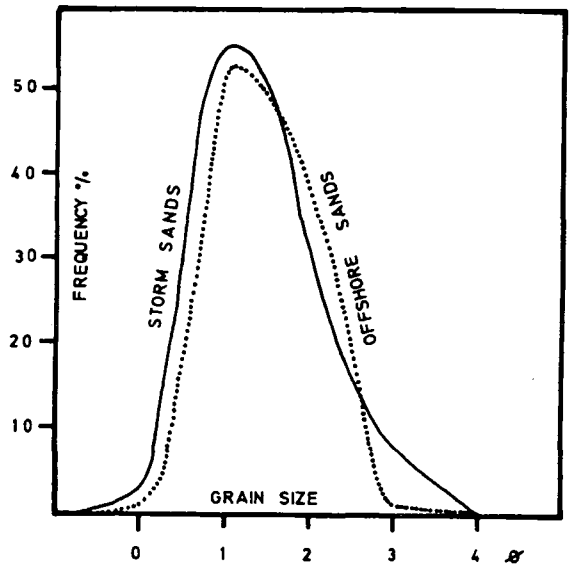

Fig. 6. Correlation between storm sands and adjacent offshore sands.

HYDRODYNAMIC FORCES AND ONSHORE MOVEMENT

The primary source of energy affecting the nearshore region is that of waves. According to MANOHAR (1976), two types of waves are predominant; the storm waves of the winter season (November — March) and the swells of the summer season (July — August). Records of the storm waves show that the waves rarely exceed 3.5 m in height, and the swells are generally 40—75 cm heigh. With average periods not exceeding 6-8 sec, the storm waves do not affect the bottom at depths more than 50 m. In general, the predominant direction of waves is NNW and NW. This means that all the time there is wave movement (75% of the time waves are over 75 cm), and the zone between 0 and 5 m depth is affected. During moderate storms (waves up to 1.5 m), the bottom is actively stirred to a depth of at least 12 m. The swells and the bigger waves during heavy storms can affect the bottom of continental shelf to a depth of 50 m by what is known as bottom current velocities (KORGN *et al.* 1970, KING 1972; MCCLENNEN 1973). This depth limit includes all the sand patches of the Nile Delta inner shelf (*Fig. 5*).

Therefore, during heavy storms the bottom currents are capable of moving coarse sediments from NW direction to feed the coast. Many evidences indicate the offshore-onshore transport of sediments (PILKEY and FIELD 1972; SUMMERHAYES and MARKS 1976; EL-FISHAWI and MOLNAR 1981). The distribution of the beach pebbles along Burullus coast is closely related to the position of the Rosetta and Burullus offshore banks. These pebbles reached storms (EL-FISHAWI and MOLNAR 1981). There is many evidence of large objects reaching the coast from known places even many km away from the shore (SHEPARD, 1963; BASCOM, 1964). In a similar way, as the beach pebbles have come from submarine ridges as far as 20—25 km to the NW of Burullus, could also have come the coarse sands from offshore sources to nourish some coasts. Time series analysis of mean grain size at Burullus area indicate that coarse sand is periodically added to the coast

(EL-FISHAWI and MOLNAR 1983). West of Burullus outlet, the barrier between sea and lake is narrow and the beach is a thin wedge (3—6 m thick) over lagoonal clays, so that the coarse sand found to nourish the coast should come from outside. On the other hand, for the beaches east of the outlet, the source of coarse sand is available in the land itself (backshore and dunes).

Although in the profiles of west Burullus the percentage of coarse sand decreases rapidly seaward and no more is found after 100 m from the shore (BADR 1990) it is indicated that during the storms a lot of offshore sediment is in suspension, and coarse sand is then derived shoreward.

RATE OF SAND DRIFT DURING STORMY CONDITIONS

Monthly field experiments, using fluorescent-dyed grains, were performed at the beaches located east and west of Damietta mouth. The experiments were carried out during the period from January to December, 1991 to trace the sand movement and to estimate the rate of drift. In fact, such period represented different sea conditions during summer and winter seasons. The field and lobarotory techniques were made according to INGLE (1966).

At the western side of Damietta coast, where the storm sediments are occurred, pattern of tracer sand dispersion indicated the tendency of a large percent of tracer sand to move eastwards. Most waves are approaching the coast from NW and consequently cause dominant eastward drift. During stormy conditions in November and December, the velocity of the eastward current may exceed 90 cm/sec.

The drift rate yielded a wide range of variety due to seasonal effect and surf conditions prevailing during tracer tests. The rate of drift at west Damietta ranges between 48,100 and 111,900 cubic meters per month. Generally, it is indicated that the rate of drift tends to be higher in winter season than that in summer one. At west of Burullus, it ranges between 76,000 and 100,000 cubic meters per month during stormy conditions.

CONCLUSION

A deposition of coarse sediments took place during storms, covering the beach and surf zone at the western side of Burullus and Damietta. Textural analysis indicates that these storm sands are coarse, less sorted and more rounded than the native beach sands. It is apparent that the storm sands added to the beach and adjacent offshore sands closely correspond to one another with regard to grain size distribution and texture. Therefore, the coarse sand accumulation which took place during storms are derived from the adjacent offshore sources. Possible mechanisms of onshore movement include the wave action on the bottom and strom-induced current.

The ivestigation has presented evidence indicating onshore movement of coarse sands from offshore sources at a distance of about 2—9 km and 8—15 m water depth. Rosetta and Damietta branches are not contributors of sand to the coast at present due to the construction of the Aswan High Dam. Furthermore, litoral current do not introduce new material to the beach but rather redistribute the quantities already present. Therefore, on a regional scale, only coastal erosion and onshore movement are the potential sources for generation of present day Nile Delta coastal sands.

REFERENCES

BADR, A.A. (1990): Sedimentological studies on the coastal zone between Rosetta and Burullus, Egypt. Ph. D. thesis, Alexandria Univ., 200 p.

BARAKAT, M. G. and IMAM, M. (1976): Preliminary note on the occurrence of old indurated sand dunes in the district of Gamasa, northern Nile Delta. In: Proc. Sem. Nile Delta sedimentology, UNESCO, Alexandria, pp. 33—39.

BASCOM, W. (1964): Waves and beaches. Anchor Books, Doubleday & Co., New York.

COASTAL EROSION STUDIES (1976): Detailed Technical Report on Coastal Geomorphology and Marine Geology, UNESCO, Alexandria, 175 p.

EL-FISHAWI, N. M. and MOLNAR, B. (1981): Nile Delta beach pebbles: 1-Grain size and origin. Act. Miner. Petro. **25/1**, 25—39.

EL-FISHAWI, N. M. and MOLNAR, B. (1983): Variations of beach sands with seasons, beach slpoe and shore dynamics on the Nile Delta coast. Act. Miner. Petro. **26/1**, 5—17.

EL-FISHAWI, N. M., SESTINI, G., FAHMY, M. and SHAWKI, A. (1976): Grain size of the Nile Delta beach sands. In: Proc. Sem. Nile Delta sedimentology, UNESCO, Alexandria, p. 79—94.

FOLK, R. L. and WARD, W. C. (1957): Brazos River bar, a study in the significance of the grain size parameters. Jour. Sed. Pet. **27**, 3—27.

FRIHY, O. E., KHAFAGY, A., EL-FISHAWY, N. M. and FANOS, A. (1990): Nile Delta coast: identification and evaluation of offshore sand sources for beach nourishment. Littoral 1990, Eurocoast, Marseille, P. 724-728.

GUILCHER, A. (1963): Estuaries, deltas, shelf, slope. In: The sea. M. N. HILL (Ed.) V. 3, Interscience, New York.

INGLE, J. C. (1966): The movement of beach sand. Developments in Sedimentology. Elsevier Pub. Comp. **5**, 221 p.

KING, C. A. M. (1972): Beaches and coasts. 2nd edition, Edward Arnold, 570 p.

KORGEN, B. J., BODVARSSON, G. and KULM, L. D. (1970): Current speeds near the ocean floor west of Oregon. Deep Sea Res. **17**, 353—357.

MANOHAR, M. (1976): Dynamic factors affecting the Nile Delta coast. In: Proc. Sem. Nile Delta Sedimentology. UNESCO, Alexandria, pp. 104—129.

MCCLENNEN, C. E. (1973): New Jersey continental shelf near bottom current meter records annd recent sediment activity. Jour. Sed. Pet. **43**, 371—380.

MEADE, R. H. (1969): Landward transport of bottom sediments in estuaries of the Atlantic coastal plain. Jour. Sed. Pet. **39**, 222—234.

PEVEAR, D. R. and PILKEY, O. H. (1966): Phosphorite in Georgia continental shelf sediments. Bull. Geol. Soc. Am. **77**, 849—858.

PIERCE, J. W. (1969): Sediment budget along a barrier Island Chain. Sed. Geol., **3**, 5—16.

PILKEY, O. H. and FIELD, M. E. (1972): Onshore transportation of continental shelf sediment: Atlantic southeastern United States. In: Self sediment transport: processes and pattern. SWIFT, D., DUANE, D. and PILKEY, O. (Eds), Dowden, Hutchinson and Ross, Inc. Stroudsburg, p. 429—446.

SHEPARD, F. P. (1963): Submarine geology. Harper & Row, New York, 557 p.

SUEZ CANAL AUTHORITY (1965): New harbour at Damietta. Report No. **32**, Research Center, 59 p.

SUMMERHAYES, C. P. and MARKS, N. (1976): Nile Delta: nature, evolution and collapse of continental shelf sediment system. In: Proc. Sem. Nile Delta Sedimentology, UNESCO, Alexandria, P. 162—190.

WINDOM, H. L., NEAL, W. and BECK, K. (1971): Mineralogy of sediments in three Georgia estuaries. Jour. Sed. Pet. **41**, 497—504.

Manuscript received, 8 August, 1990

Acta Mineralogica-Petrographica, Szeged, XXXI, 89—95, 1990

GRINDING OF MECSEK COALS IN PRESENCE OF ADDITIVES I.

É. SZÉKELY*, R. SZÉKELY*

Hungarian Hydrocarbon Industrial Research and Development Institute

ZS. GYÖNGYÖS-RADNAI**

Mecsek Coal Mining Co. Research Center

ABSTRACT

The authors have investigated the intensifying effect of surface active materials and water in series of laboratory tests by using energetic coals. They have stated that the quantity of fine fractions (the surplus output) increases when using water, but this effect can be increased further with additives.

INTRODUCTION

In our epoch striving against energy crises the using of coal as a traditional fuel has come into the limelight besides the investigation of the applicability of alternative energy resources. The role of thermoplants in the production of electricity is increasing and according to estimations the thermoplants will keep their importance for a long period due to their reliable operation. Despite the fact that the thermoplants functioning with coal have operated for over decades, however there are many tasks to be solved, just to mention the most important one, the elimination of the environment pollution. All, over the world researchers investigate the possibilities of the rationalization of costs in order to render more efficient the production of energy. Such a factor decreasing the costs could be the amelioration of the grinding of fuel by using additives in the power plants operating with pulverized coal.

During grinding in presence of additive (1)

— the performance of the mill can be increased with the same energy input
— with same performance of the mill and energy input the grinding is finer.

The using of materials facilitating the grinding has became widespread in the cement industry, where it is possible to produce dust with fine-grain structure only in presence of additives. Such additives are glycols, ethanolamins etc., (2, 3, 4). There is no reference data to our disposal regarding the grinding of coals with additives.

* H—2240 Százhalombatta, P.O. Box. 32, Hungary
**H—7629 Pécs, Keller J. u. 5, Hungary

EXPERIMENTAL PART

In our series of laboratory grinding tests we have tested the grinding capabilities of coals to be processed in the Pécs Thermal Plant — that is slurry, Pécs pulverized coal, coal with refuse, rice coal "B" from Komló —.

We investigated the relation between the type of coal to be grinded, the quality of the additives, the revolution number of the mill, the mass proportion of coal/grinding body in presence of additive or without additive. We considered as a basis for comparison the so-called standard grindings without grinding additive.

The characteristic ash, volatile and moisture content of the tested coals is resumed in Table 1.

TABLE 1.

Ash, volatile and water content of various coal types used in PTP.

Coal type	Ash (%)	Volatile (%)	Water (%)
Pécs mud	31.5—34.3	11.0—12.4	20.5—25.0
Pécs dust	53.0—64.0	10.0—13.0	0.8—1.5
Komló B breeze	52.3—62.2	13.7—15.1	5.5—7.0
Goaf with coal	66.0	10.0—11.0	5.3—6.2

In the furnace of the Pécs Thermal Plant an average fraction of 74 μm of mixtures of coal of a given calorific value are burned. The crushing is performed in ball crushers during grinding with a moisture content of coal mixtures of almost 0. We analyzed the components of the mixed materials due to the very different place of origin of the materials.

We have chosen as grinding additives the surface active materials sulfonate anion type:

— Évatriol (E) — sodium salt of dodecil-benzol sulfonic acid
— Evanat (T) — sodium salt of fatty alcohol sulfonic acid
— Persulfite alkaline dust — sodium salt of lignine sulfonic acid with carbohydrate content
— Petroleum sulfonate of type PS-948 with 18 % oil content.

We have characterized the surface active materials with the concentration dependence of the surface stress (*Fig. 1*).

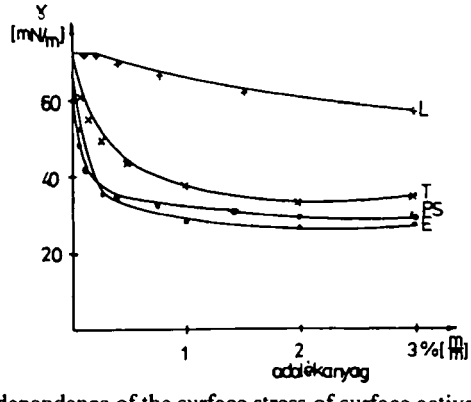

Fig. 1. Concentration dependence of the surface stress of surface active minerals. E—Evatriol, PS—Petroleum sulfonate, T—Evanat, L—alkaline dust of persulfit.

The original moisture content of coals varies considerably, therefore we have stocked the coals in a covered storage place for several weeks, so as to obtain an equilibrium moisture content (air dry coals) (Table 2).

TABLE 2.

Moisture of several air-dry coals

Type of coal	Moisture content %
slurry from Pécs	1.00
pulverized coal from Pécs	1.00
refuse with coal	1.20
rice coal from Komló	1.80

The raw coal samples were crushed in pre-crushers (VEB Special Maschinenbau 64 Typ 214) to obtain a grain size bellow 2.5 mm.

The distribution of the additive on the surface of the coal is carried out by means of spraying of water solution of the surface active material, so that the concentration of the surface active material is 0.05 % (m/m) and quantity of the distributed water was 1.5 % (m/m) regarding the air dry coals. The grinding experiments were carried out in a laboratory mill system with changeable revolution number.

Parameters of mill: Internal diameter: 12:0 mm, Volume: 950 cm^3, Height: 840 mm.

We have grinded parallel standard coals and coals containing additives with a mass proportion of coal:grinding body of 1:1 and 1:3, where the grinding bodies were steel balls of 11 and 15 mm.

The volumetric factor of the mill was 27 % (v/v).

By applying several additives we have investigated the effect of the revolution number of the mill on the grinding.

The revolution numbers were as follows: n_{opt} = 88 l/min., n_{opt} = 44 l/min., n_{opt} = 22 l/ min.

Furthermore, we have carried out a series of experiments regarding the effect of water to facilitate the grinding. We used the rice coal type "B" from Komló for grinding. We have increased the moisture content by 0.5 % (m/m); 1.5 % (m/m); 2.5 % (m/m) relating to air dry coal, then we have grinded with a mass proportion of coal:grinding body of 1:1 and 1:3, as well as with a varying revolution number.

RESULTS OF THE EXPERIMENTS

We have characterized the effect of the various additives and modified mill-parameters influencing the grinding by the amount of surplus output (K) comparing to the standard. After 60 minutes of grinding we have screened the grinding material and we have determined the (K) value of the quantity of fractions bellow 74 μm.

$$K = \frac{D_{60A} - D_{60E}}{D_{60E}} \cdot 100 \ (\%)$$

where: D_{60A} = % of the passing-through of material in 60 minutes of grinding with additive, D_{60E} = % of the passing-through of material of a standard grinding of 60

minutes. The diagrams plotted on the basis of our measuring results are shown in *Figures 2, 3, 4* and *5.*

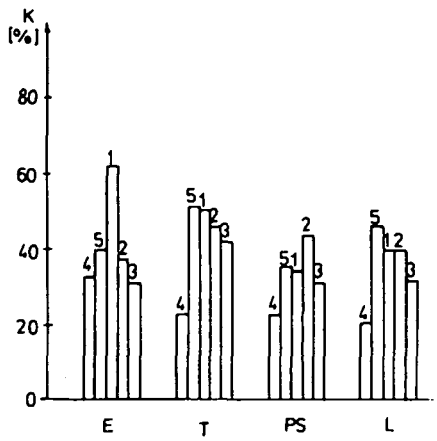

Fig. 2. Surplus output (K) during the grinding of slurry from Pécs with additives: Evatriol (E), Evanat (T), Petroleum sulfonate (PS) and lignine sulfonate (L). (1) Mass proportion 1:3 coal:ball, n_{opt}; (2) Mass proportion 1:3 coal:ball, $n_{opt}/2$; (3) Mass proportion 1:3 coal:ball, $n_{opt}/4$; (4) Mass proportion 1:1 coal:ball, n_{opt} ; (5) Mass proportion 1:1 coal:ball, $n_{opt}/2$

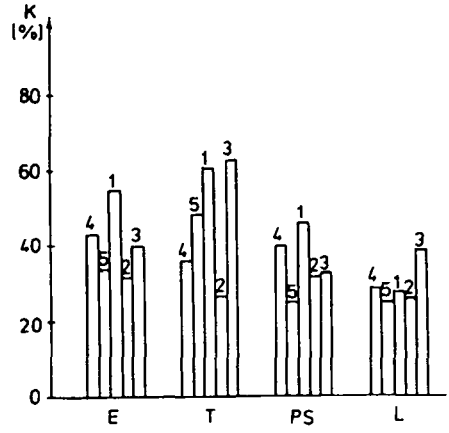

Fig. 3. Surplus output (K) during of the grinding of pulverized coal from Pécs (additives and mill parameters are shown in *Fig. 2*).

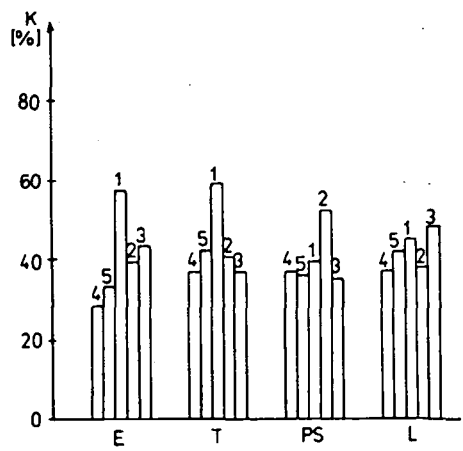

Fig. 4. Surplus output (K) during of the grinding of rice coal type "B" from Komló (additives and mill parameters are shown in *Fig. 2*).

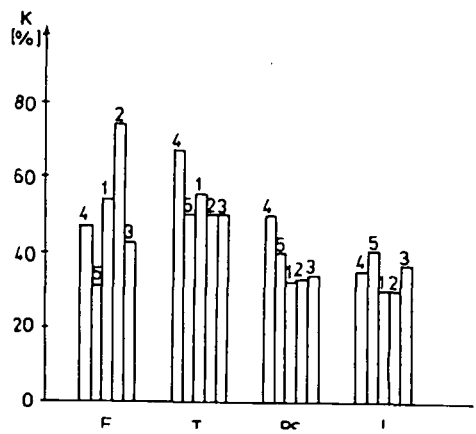

Fig. 5. Surplus output (K) during of the grinding of refuse with coal (additives and mill parameters are shown in *Fig. 2*).

Comparing the diagrams we can state the followings:

— the K factor varies from 20 to 50 %, irrespective of the concentration dependence of the surface stress of surface active material (*Fig. 1*).
— there is no significant effect of the mass proportion of coal:grinding body on the surplus output.
— the effect of the revolution number of the mill on the surplus output cannot be separated as well unambiguously, the K value is situated in one single band, that is between 20—60 % (*Figures 6, 7, 8, 9*).

During our study we have investigated the facilitating effect of the water regarding the grinding. *Fig. 10.* shows the dependence of the moisture content regarding the surplus output of fractions bellow 74 μm; the dependence of the surplus output on the revolution number is shown in *Figure 11.*

EVALUATION

In our series of study we have investigated the effect of various surface active materials on the grinding process of coals. We have determined the extent of the modification according to the place of origin of coals, mass proportion of coal:grinding body, the revolution number of the mill and the type of additive. We have characterized the grinding facilitating effect with the quantity of fraction size bellow 74 μm.

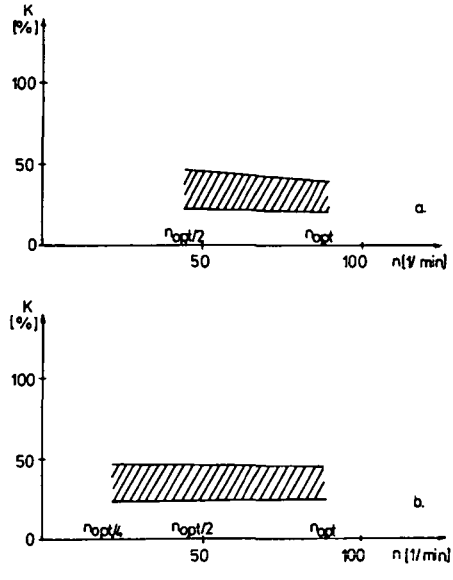

Fig. 6. Relation of the surplus output and revolution number in case of grinding rice coal type "B" from Komló, pulverized coal from Pécs, and slurry using lignine sulfonate (L) additive. (a) in case of mass proportion of coal:grinding body of 1:1; (b) in case of mass proportion of coal:grinding body of 1:3.

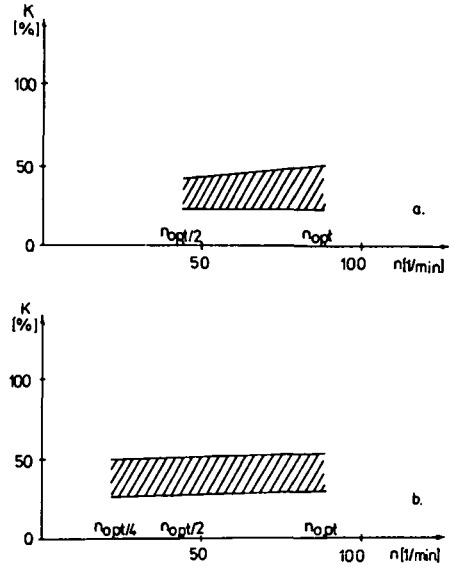

Fig. 7. Relation of the surplus output and revolution number in case of grinding slurry from Pécs and rice coal type "B" from Komló using petroleum sulfonate additive. (a) in case of mass proportion of coal:grinding body of 1:1; (b) in case of mass proportion of coal:grinding body of 1:3.

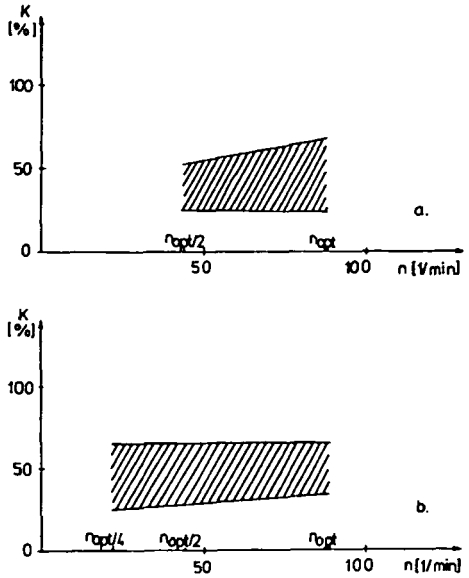

Fig. 8. Relation of the surplus output and revolution number in case of grinding rice coal type "B" from Komló, pulverized coal from Pécs, and slurry using Evanat (T) additive. (a) in case of mass proportion of coal:grinding body of 1:1; (b) in case of mass proportion of coal:grinding body of 1:3.

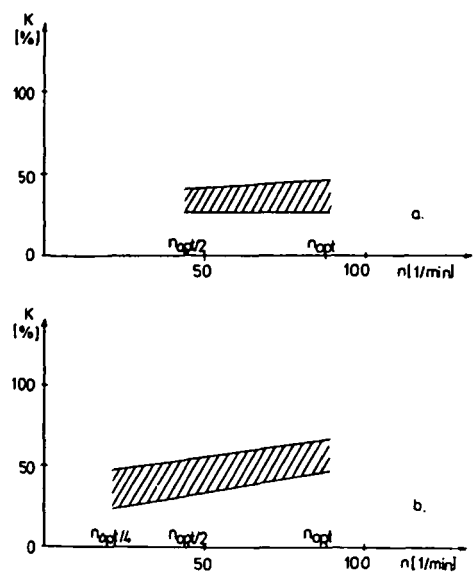

Fig. 9. Relation of the surplus output and revolution number in case of grinding rice coal type "B" from Komló, pulverized coal from Pécs, and slurry using Evatriol (E) additive. (a) in case of mass proportion of coal:grinding body of 1:1; (b) in case of mass proportion of coal:grinding body of 1:3.

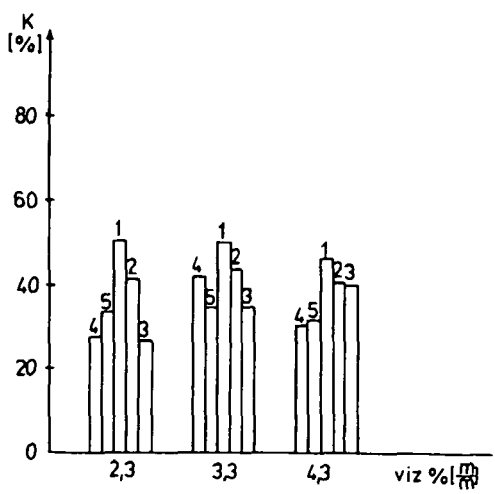

Fig. 10. Surplus of output (K) during the grinding of air dry rice coal type "B" from Komló increased with 0.5 %. 1.5 %, 2.5 % water. (1) mass proportion of coal:ball of 1:3 n_{opt}; (2) mass proportion of coal:ball of 1:3 $n_{opt}/2$; (3) mass proportion of coal:ball of 1:3 $n_{opt}/4$; (4) mass proportion of coal:ball of 1:1 n_{opt}; (5) mass proportion of coal:ball of 1:1 $n_{opt}/4$.

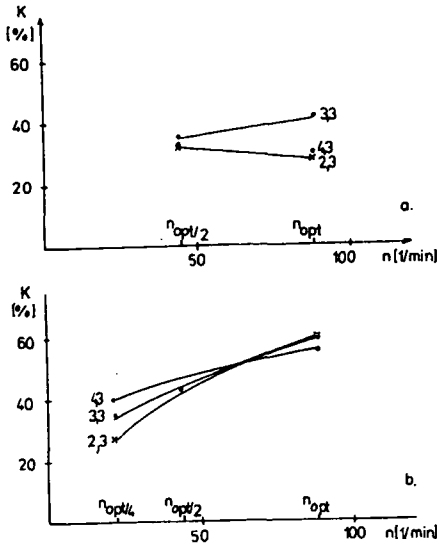

Fig. 11. Relation of surplus output during the grinding of rice coal type "B" from Komló in case of various moisture content. (a) mass proportion of coal:ball of 1:1; (b) mass proportion of coal:ball of 1:3

On the basis of our measurement results we can state that the anion surface active materials of sulfonate type have an effect of facilitating the grinding.

The value of the calculated surplus output factor (K) ranges from 20 to 60 %, which suggests that in case of grinding with additive the quantity of the finer fraction increases.

By using water as an auxilary material we have stated that the water in itself has an effect of facilitating the grinding. Our experiences acquired during the tests show that the intensifying of grinding is mainly a function of water content. This effect can be increased by means of surface active materials requires supplementary technological equipment.

Summing up our results we can state that in case of using of auxiliary materials for grinding, the revolution number of the mill can be decreased at a quarter of the optimal value; the mass proportion of coal:grinding body can be increased at 1:1 without any noticable change in the effect of intensifying the grinding.

REFERENCES

JUHÁSZ, A. Z., OPOCZKY L. (1982): Szilikátok Mechanikai Aktiválása finomőrléssel (Mechanical Activation of Silicates by fine-grinding. Akadémia Press, Budapest. (In Hungarian)
ROSIN, P., RAMLER, E., SPERLING, K. (1933): Bericht des Reichkohlenrats. Berlin, 1933.
BEKE, B. (1963): Aprításelmélet (Crushing-theory). Akadémia Press, Budapest. (In Hungarian)
US. PAT. Nr. 2. 141571.

Manuscript received, 1 August, 1990

Acta Mineralogica-Petrographica, Szeged, XXXI, 97—98, 1990

IS SITKE A NEW LOCALITY OF PERIDOTITE XENOLITHS IN HUNGARY? COMMENTS ON THE PAPER "TEXTURAL FEATURES AND MODES OF ULTRAMAFIC XENOLITHES FROM SITKE, LITTLE PLAIN (HUNGARY)" BY CS. SZABO AND O. VASELLI

A. EMBEY-ISZTIN*

Mineralogical and Petrological Department,
Hungarian Natural History Museum

In this paper, SZABÓ and VASELLI, (1989) describe the texture of a series of peridotite xenoliths from Sitke as being distinct from the xenoliths of Gérce studied or at least mentioned in a number of papers by EMBEY-ISZTIN, (1976, 1978, 1984), EMBEY-ISZTIN *et al.* (1989, 1990) and DOWNES *et al.* (1992). In the region there is *only one* locality yielding relatively fresh mantle xenoliths, and this is the tuff ring exposed by a large and several smaller quarries near the villages of Gérce and Sitke as correctly shown by SZABÓ and VASELLI (1989) in their *Fig.* 2. Since the large quarry inside the tuff ring, which is the best place to find xenoliths, is situated somewhat nearer to Gérce (2 km) than to Sitke (2.3 km), Gérce rather than Sitke was used to designate the locality with the exception of my first paper (EMBEY-ISZTIN 1976) where the name of Sitke, amd another paper (EMBEY-ISZTIN 1978) in which Gérce-Sitke (!) was used. Consequently, there can be no doubt that the locality of Sitke is identical with that of Gérce.

There is, however, another piece of evidence pointing to this conclusion. This is the result of the textural analysis of SZABÓ and VASELLI showing that porphyroclastic textures prevail in the Sitke (=Gérce) mantle xenoliths and they occasionally exhibit transtitional features towards equigranular texture. However, this is not new either and it is in perfect agreement with former results (EMBEY-ISZTIN 1978, 1984, 1989), even if SZABÓ and VASELLI (1989, page 73) surprisingly state that "EMBEY-ISZTIN (1978) described xenoliths have protogranular-porphyroclastic transitional texture, but we have not recognized this type yet." In fact, the last description was used to characterize xenoliths of Szentbékálla and Szigliget. As far as Gérce xenoliths are concerned, EMBEY-ISZTIN, (1984, page 31) unequivocally confirms that "The overwhelming majority (81%) of these peridotites have porphyroclastic texture (e.g. G—1002, *Fig. 2*)."

REFERENCES

DOWNER, H., EMBEY-ISZTIN, A. and THIRLWALL, M. F. in (1992): Petrology and geochemistry of spinel peridotite xenoliths from Hungary: evidence from an association between enrichment and deformation in the upper mantle. Contrib. Mineral. Petrol. **109**, 340—354.

* H—1088 Budapest, Múzeum krt. 14-16, Hungary